An Off-Lattice Model of the Sanchez-Lacombe Equation of State for Polymers with Finite Flexibility

by

Hassan Alam

A thesis
presented to the University of Waterloo
in fulfillment of the
thesis requirement for the degree of
Master of Science
in
Physics

Waterloo, Ontario, Canada, 2020

Author's Declaration

I hereby declare that I am the sole author of this thesis. This is a true copy of the thesis, including any required final revisions, as accepted by my examiners.

I understand that my thesis may be made electronically available to the public.

Abstract

An extension to the off-lattice Sanchez Lacombe equation of state is proposed by including internal degrees of freedom to account for the finite flexibility of polymer molecules. The extension allows polymer molecules to have two energy levels of flexing, a ground/unflexed state and a degenerate excited/flexed state. The finite flexibility of polymer molecules is characterized by two regression parameters, the energy of excited states and their degeneracy. The flexibility parameters are regressed by using two experimental values: the glass transition temperature of pure polymers at atmospheric pressure and the change in isobaric heat capacity of pure polymers across the glass transition at atmospheric pressure. A method has been outlined to regress these parameters from experimental data.

The glass transition temperature versus pressure and the isobaric heat capacity versus temperature predictions of the off-lattice model are compared with a lattice-based model from the literature. The lattice-based model is based on the Gibbs DiMarzio criterion which says that, at the glass transition, the configurational entropy of polymers becomes zero. However, the proposed off-lattice model shows that the Gibbs DiMarzio criterion is a consequence of the artificial lattice. Thus a new criterion is introduced which says that the glass transition occurs at a particular fraction of maximum polymer entropy that also minimizes the degeneracy of the excited state. Experimental data of several pure polymers are utilized to compare the predictions of both models. The proposed off-lattice model is found to be more accurate than the lattice-based model.

The model is also employed to predict the glass transition temperature versus pressure behaviour of binary polystyrene/CO_2, polycarbonate/CO_2 and poly(methyl methacrylate) mixtures. Experimental solubility data is used to regress the binary interaction parameters of the system. The model predicts that the binary polystyrene/CO_2 mixture shows depression in glass transition temperature with the increasing pressure of CO_2. The prediction is in agreement with the experimental observations and is superior to the lattice-based model. However, for binary polycarbonate/CO_2 and poly(methyl methacrylate)/CO_2 mixtures that undergo retrograde vitrification, predictions for the present theory are not correct because underlying inconsistencies in the model make regressed values of binary interaction parameters less accurate. Nonetheless, using hand-picked values of binary interaction parameters, retrograde vitrification trend can be obtained.

Acknowledgements

I would like to thank my research supervisors, Professor Russell B. Thompson and Professor Chul B. Park, for their overwhelming support and guidance throughout the research. Their ingenious insight on the topic assisted me a lot in performing this research.

I also want to thanks the Advisory Committee members, Professor Bae-Yeun Ha and Professor David Yevick, for critically examining my research performance, giving quality feedback and identifying improvement areas.

I am also extremely thankful to the Natural Sciences and Engineering Research Council of Canada (NSERC) for financially supporting this research.

Dedication

This is dedicated to my parents.

Table of Contents

List of Figures

List of Tables

List of Symbols

$\boldsymbol{F}$ Helmholtz free energy

$\boldsymbol{G}$ Gibbs free energy

$\boldsymbol{P}$ pressure

$\boldsymbol{T}$ temperature

$\boldsymbol{\rho}$ density

$\boldsymbol{P^*}$ characteristic pressure

$\boldsymbol{T^*}$ characteristic temperature

$\boldsymbol{\rho^*}$ characteristic density

$\boldsymbol{\tilde{F}}$ reduced Helmholtz free energy

$\boldsymbol{\tilde{G}}$ reduced Gibbs free energy

$\boldsymbol{\tilde{P}}$ reduced pressure

$\boldsymbol{\tilde{T}}$ reduced temperature

$\boldsymbol{\tilde{\rho}}$ reduced density

$\boldsymbol{\epsilon^*_{kk'}}$ interaction energy between segments of species k and k'

$\boldsymbol{\epsilon_{kk'}}$ characteristic interaction energy between segments of species k and k'

$\boldsymbol{\epsilon^*_{kk}}$ interaction energy between segments of species k

$\boldsymbol{\epsilon_{kk}}$ characteristic interaction energy between segments of species k

$\boldsymbol{Q_{conf}}$ configurational partition function

$\boldsymbol{Q}$ canonical partition function

$\boldsymbol{\alpha_{k,r}}$ ratio of volume of a molecule of species k to the reference volume

$\boldsymbol{\alpha_k}$ ratio of volume of a molecule of species k to the volume of one hole

$\boldsymbol{\phi_k}$ volume fraction of species k

$\boldsymbol{v^*}$ characteristic volume of one lattice site

$\boldsymbol{v_0}$ hole volume

$\boldsymbol{v_k}$ volume of one segment of species k

$\boldsymbol{v_r}$ reference volume

$\boldsymbol{\chi_s}$ solubility of solvent s in binary polymer-solvent mixture

$\boldsymbol{k_B}$ Boltzmann's constant

$\boldsymbol{\Lambda_k}$ de Broglie thermal wavelength of species k

Abbreviations

CO_2 Cardon Dioxide

EOS Equation of State

ESD Elliott, Suresh, Donohue

FH Flory-Huggins

FOV Flory-Orwoll-Vrij

HN Hong-Noolandi

HSC Hard-Sphere Chain

LCST Lower Critical Solution Temperature

LJ Lennard-Jones

MFT Mean Field Theory

PC Perturbed-Chain

PC Polycarbonate

PMMA Poly(Methyl-Methacrylate)

PR Peng–Robinson

PRSV Peng–Robinson-Stryjek-Vera

PS Polystyrene

PVAc Poly(Vinyl Acetate)

PVME Polyvinyl Methyl Ether

PVT Pressure-Volume-Temperature

RK Redlich-Kwong

SAFT Self-Associating Fluid Theory

SCFT Self-Consistent Field Theory

SL Sanchez-Lacombe

SRK Soave-Redlich-Kwong

SS Simha-Somcynsky

UCST Upper Critical Solution Temperature

WLF Williams, Landel and Ferry

Chapter 1

Introduction

1.1 Motivation

Numerous cutting-edge technologies require the use of advanced polymers for highly specialized applications. For example, smart polymers are used to produce artificial muscles, biodegradable plastics and bioengineered products [114]. Smart polymer hydrogels dramatically adjust their physical and electrical properties in response to changes in the environment such as pressure, pH, humidity, electric or magnetic field [193]. Functional and nano-cellular polymeric foams are used as super insulators and shock absorbers [10, 168]. Bioactive polymeric scaffolds are used in tissue engineering [30]. Thus, countless high-value products are made from polymers. On the other hand, polymers are also used in conventional products like plastic bags, PVC pipes, CD covers, paints, dishes, pan-coating as well as in the automotive and aviation industry [92]. Research to understand the underlying physics of these polymeric materials is very important because it will help to optimize their production processes. One area of active research in polymer physics is the phenomenon called gas retrograde vitrification that can be used to treat polymeric foams products at milder conditions [22, 23, 99]. In retrograde vitrification, glass transition temperatures of binary solvent-polymer mixtures decrease with the increase in pressure. The phenomenon is found to be driven by the changing solubility of solvent fluids in polymer matrices as a result of changing external pressure on solvents. Thus the phenomenon can be used to treat polymers at lower glass transition temperatures. Consequently, it can also aid engineers to control cell densities of polymeric foams [90,91]. However, to study retrograde vitrification, it is a prerequisite to first have precise knowledge of the glass transition temperature of pure polymer species at different pressures.

Many theories have been presented to understand the equation of state and glass transition behaviour of pure polymers as well as phase equilibrium and retrograde vitrification behaviour of binary polymer-solvent mixtures. Theories that can predict these behaviours with excellent accuracy but with the least complexity are considered to be most useful for industrial applications. Thus a robust theory should only include details that are essential to predict the equation of state and glass transition behaviour of polymers. Additional details, for instance, molecular features and internal degrees of freedom that do not affect these behaviours are undesirable [159]. By discarding such unfruitful details calculations can be greatly simplified. However, such simplicfications inevitably lead to a moderate compromise on the accuracy of predictions from the model [186]. For polymeric foams, the Sanchez-Lacombe equation of state (SL-EOS) [95,163–165] makes an excellent trade-off between these two competing factors. It is capable of predicting phase behaviour of polymeric foams with moderate accuracy. On the other hand, the model does not consider irrelevant details that can make calculations cumbersome. So, it is a very robust equation that provides excellent predictions of the thermodynamic properties of fluids. It is simple enough to be used to optimize processing conditions in the polymer industry. It requires only a few phenomenological parameters. However, it is very important to carefully calibrate the phenomenological parameters to obtain reliable results from the model [7,196]. Unfortunately, the model is not capable of predicting the glass transition behaviour of polymers. Other equations of state of polymers experience a variety of limitations [49,52]. For instance, the Simha Somcynsky equation of state (SS-EOS) [85,200] is very complex as it accounts for extra features that are not directly relevant to the PVT behaviour of polymers. Another theory, called Perturbed Chain Self Associating Fluid Theory (PC-SAFT) [66,67], requires 24 parameters to make predictions.

SL-EOS was first introduced in 1974 [163,164] to predict the thermodynamic behaviour of pure fluids. However, the model was subsequently generalized for multicomponent fluid mixtures [95]. The model is not limited to polymer fluids, it is equally applicable to small molecules in a gas or liquid phase. SL-EOS is based on *ab initio* principles of statistical mechanics. The theory divides molecules into small segments and allows each segment to occupy discrete positions on an artificial lattice. To account for the thermal expansion and compression of systems the theory allows vacant lattice sites called holes. These holes also accommodate secondary equation of state effects that are not directly considered in the model. Thus SL-EOS is classified as a semi-empirical lattice-fluid equation [95,164]. The SL-EOS is based on several assumptions that are substantiated by comparing predictions of the equation with experimental data [186]. The assumption of vacant lattice sites to accommodate finite compression of the system was novel. Theories preceding the SL model do not accommodate this feature [47,82]. Other assumptions of the SL model are the mean-

field approximation [71] and the assertion that internal and translational degrees of freedom do not affect the Pressure-Volume-Temperature (PVT) behaviour of the system [147].

Nevertheless, the lattice-based SL-EOS is not capable of accurately predicting solubility and swelling in binary polymer-solvent mixtures at high pressures [75, 105–108, 111]. Thus several alternate theories [75, 99, 101–103, 109, 110, 136, 201, 210] have also been adopted for situations where high pressure is necessary to manufacture polymeric foams. However, alternate theories are complex and require powerful computers to perform calculations. For instance, SS-EOS [85, 200] gives more accurate results but it requires more fitting parameters. PC-SAFT [66, 67] is very complex as it requires excessive molecular details that are not necessary for manufacturing processes.

Von Konigslow [197] argued that the poor agreement of SL-EOS with experimental solubility data is due to the poorly regressed pure-component parameters. Errors in pure-component parameters aggravate the subsequent regression of multicomponent parameters [7]. The poor regression practice includes applying the SL-EOS at conditions where the assumptions of the model tend to become invalid. For instance, if one includes the critical point of solvent while preforming regression then the regressed parameters will not be accurate because the mean-field approximation breaks down at critical conditions. SL-EOS also assumes that the solvent fluid is at low density. However, this assumption becomes invalid at high pressures, especially at supercritical conditions [166]. Yet, these assumptions are necessary to simplify the mathematics of the model [78, 93, 186] and thus should be removed from the model. Besides, the lattice-based multicomponent SL-EOS also contains severe inconsistencies as pointed out by Neau [124]. These inconsistencies cause a shift in the reference zero of chemical potential. Thus phase equilibrium calculations of SL-EOS for the binary polymer-solvent mixtures [124, 197] tend to be incorrect. Later, it has been shown that the SL-EOS is the homogeneous limit of Hong-Noolandi Self-Consistent Field Theory (HN-SCFT) [79] of inhomogeneous systems. HN-SCFT is a modern and more accurate theory. It is capable of predicting cell densities of polymeric foams qualitatively [89–91, 137, 184]. Since the HN-SCFT was derived by using functional integrals without using a lattice, this offered hope to derive the SL-EOS free from artificial lattice effects [79, 185].

In 2017, an off-lattice version of SL-EOS was introduced by von Konigslow *et al.* [195, 197]. The off-lattice approach is superior to the lattice-fluid approach because, for multicomponent mixtures, the lattice-fluid approach contains severe thermodynamic inconsistencies that are not as severe in the off-lattice approach [198]. However, for pure materials, there is no significant advantage of the off-lattice approach over the lattice-fluid approach [164, 197]. Moreover, von Konigslow *et al.* [195, 197] took additional care while regressing pure-component and binary interaction parameters by avoiding critical point

conditions. Thus they confirmed that their off-lattice SL-EOS accurately predicts solubility of binary polymers. However, swelling predictions remained unsatisfactory.

Apart from the above advantages, both the lattice-fluid approach and the off-lattice approach have a common limitation. Both models ignore internal degrees of freedom of molecules especially their finite flexing energy. Thus both models are incapable of predicting properties such as glass transition temperature, retrograde vitrification, and heat capacity of fluid polymers since these properties depend on internal degrees of freedom of molecules. These properties are also important for designing manufacturing processes of polymers. By using alternate models and experiments, several authors have identified that the glass transition temperature of polymers changes with the change in pressure of solvents depending on their solubility in polymer matrices. For instance, Wang *et al.* [202] showed that a minimum in glass transition temperature can occur in solvent-polymer mixtures, while Assink *et al.* [4] showed that for binary mixtures with low solubility solvents, pressurizing the system causes an increase in the glass transition temperature. However, for highly soluble solvents, increasing pressure decreases the glass transition temperature of the system.

Several theoretical attempts have been made in the past to predict the glass transition temperature behaviour of pure polymer and binary solvent-polymer mixtures. However, there is a significant debate in the physics community on the thermodynamic nature of the glass transition. Several authors argue that the glass transition is purely a kinetic phenomenon [64,77,88,183]. However, several studies also revealed that the glass transition involves a discontinuity in heat capacity [16] of systems indicating that the glass transition is perhaps a second-order thermodynamic transition. In 1948, Walter Kauzmann [88] showed that extrapolation of thermodynamic properties of glass-forming materials from a supercooled liquid state to finite low temperatures result in values that are less than the values of crystalline solids of those materials. So, he argued that the glass transition is not a thermodynamic transition. Thus, resolving the Kauzmann paradox [88] by using thermodynamic arguments is the central mystery to justify the thermodynamic nature of glass transitions.

One model that offers a resolution to the Kauzmann paradox is presented by Gibbs and DiMarzio [35,61,62]. As discussed, the finite flexibility of polymer molecules plays a significant role in the glass transition. Thus, Gibbs and DiMarzio considered a lattice-based model in which they assigned two energy levels to account for the finite flexibility of molecules. Consequently, the model revealed that the glass transition occurs with a second-order thermodynamic transition where the configurational entropy of the system also becomes zero. Their model showed that the expression of entropy has a discontinuity and thus extrapolation of thermodynamic properties to low temperatures is not allowed. Consequently, the

theory was found to be moderately successful in predicting glass transition temperatures of polymeric systems [143].

In 1992, Condo *et al.* [23] developed the idea further by combining the SL model [50, 134, 135, 164, 165] and the Gibbs DiMarzio criterion [36, 62] into a single more powerful theory. They offered an extension of the SL model that assigns two energy levels to account for the finite flexibility of polymer molecules. Their model also revealed that at sufficiently low temperature the entropy of the system becomes negative. Thus, following the Gibbs-DiMarzio criterion, they argued that the negative value indicates the onset of the glass transition. Consequently, they identified four possible types of glass transition temperature versus pressure behaviours of binary solvent-polymer mixtures. They predicted the phenomenon of retrograde vitrification for the first time and later experimentally verified their predictions [21, 22].

However, the Condo model has some severe problems because it is a lattice-fluid model. First, the model uses the Gibbs DiMarzio criterion [36, 62] to predict glass transition temperature. However, it has been found that as the coordination number of lattice increases the entropy of the system ceases to become zero. Thus the Gibss DiMarzio criterion is perhaps incorrect [6, 206, 207]. Second, the expression of entropy from the Condo model [23] depends on the coordination number of the lattice. However, entropy is a thermodynamic property that should be independent of artificial parameters. Other authors [31, 41, 72, 85, 113, 172] have also developed lattice-fluid models to predict the glass transition temperature versus pressure behaviour of polymers so their models are not capable of solving this problem. Thus, a new lattice-free theory is required.

Fortunately, in 2017 von Konigslow *et al.* [197] have presented an off-lattice derivation of SL-EOS. But their model ignores the finite flexibility of polymer molecules so it cannot predict the onset of glass transitions in polymers. However, their model offers a hope to formulate a lattice-free theory for the glass transition temperature predictions.

The above discussion provides a way to generalize the off-lattice SL model [197] in a fashion similar to how Condo *et al.* generalized the lattice-fluid SL model [23]. So, to improve the off-lattice SL model one can assign two internal energy states (the ground state and the excited state) to polymer molecules following Condo *et al.* Consequently, the resulting off-lattice model for polymers with finite flexibility should be successful in predicting glass transition temperatures at different pressures.

1.2 Objectives

The primary aim of this research is to devise a mathematical model, free from the artificial lattice, that should be able to predict the glass transition temperature of polymers at different pressures. To achieve this goal the off-lattice Sanchez-Lacombe model [197] is extended similar to the extension of lattice-based SL-EOS by the Condo *et al.* [23].

Second, since the extended model will be lattice-free so it should be able to conclude the long-lasting debate against the validity of Gibbs DiMarzio criterion.

Third, we aim to check the effectiveness of the model by applying it to several pure polymers. For this purpose, the chosen pure polymers are poly(methyl-methacrylate) (PMMA), polystyrene (PS), poly(vinyl acetate) (PVAc), polyvinyl methyl ether (PVME), and polycarbonate (PC). To judge the accuracy of the model the predictions of the model need to be compared with the experimental data available in literature as well as with the Condo model. The model is also aimed to predict the isobaric heat capacity versus temperature behaviour of polymers. Moreover, while designing the model a special focus is to be made to minimize the need for experimental data for making predictions.

Fourth, we also aim to apply the model on binary polymer-solvent mixtures. The model should be able to predict all four types of glass transition temperature versus pressure behaviours identified by the Condo *et al.* [23], especially the retrograde vitrification. Such predictions are very important for assessing the conditions necessary to manufacture polymeric foam products at milder temperatures. For this purpose, the binary polystyrene/CO_2, polycarbonate/CO_2 and poly(methyl-methacrylate)/CO_2 mixtures are chosen for the study.

As discussed, this research will provide a basis to predict retrograde vitrification phenomenon in polymeric foams. Precise knowledge of the retrograde vitrification temperature versus pressure curve will allow the manufacturing of nano-cellular polymeric foams at a reduced cost.

The purpose of the research is to predict the glass transition temperature versus pressure behaviour of pure polymeric systems and binary polymer-solvent mixtures. This research is not an attempt to expand the understanding of the underlying physics and nature of the glass transition phenomenon.

1.3 Foreword

The thesis is divided into six chapters. Chapter 2 contains a detailed literature review that is necessary to understand this research. This chapter contains eight sections. In sections

2.1 and 2.2, an overview of thermodynamics and statistical mechanics is presented that is relevant to this research. Sections 2.3 and 2.4 discuss different types of mixtures and polymeric foams. Section 2.5 discusses a basic overview of equations of state of different physical systems whereas section 2.6 discusses models of equations of state specifically designed for polymeric systems. Sections 2.7 and 2.8 are the most important sections of the literature review. Section 2.7 discusses the on-lattice and off-lattice Sanchez-Lacombe equation of state whereas section 2.8 discusses models designed to predict the glass transition in polymers.

In chapter 3 the mathematical foundation of the present research is discussed. This chapter contains eight sections. Section 3.1 is an introduction on this chapter. Sections 3.2, 3.3 and 3.4 describe specific details of the proposed model with the derivation of the partition function of a general multicomponent system. In section 3.5 equations of thermodynamic properties are derived for the multicomponent system. In sections 3.6 and 3.7, the equations of general multicomponent system are re-written for single-component systems and for binary solvent-polymer mixtures, respectively. The last section 3.8 discusses the limitations and possible extensions of the present model.

Chapter 4 is the central chapter of this thesis. In this chapter pure polymeric systems are discussed in five sections. This chapter starts by discussing two methods to regress the characteristic parameters of the model. In section 4.1, the first method is discussed which is basically an adaptation of a method from preceding literature. Later in the section limitations of the method are discussed. In section 4.2 a new method to regress characteristic parameters of the model is devised in a hope to overcome limitations of the first method. In this section, detailed arguments and plots are presented that inspired the development of this method. In section 4.3, characteristic parameters of the model are regressed for five different pure polymeric systems based on the second method. In section 4.4 corresponding characteristic parameters of a previous model from the literature review are regressed. Finally, in section 4.5 plots are presented to compare predictions of the present model with the previous model.

In chapter 5 binary solvent-polymer mixtures are discussed. In section 5.1, a summary of a method to regress characteristic parameters of binary mixtures is discussed. In section 5.2 the success of the present model is evaluated by comparing predictions of the model with experimental data of a binary solvent-polymer system. Finally, in section 5.3, limitations of the present model are identified.

Lastly, in chapter 6 complete research with its major findings is summarized.

Chapter 2

Background

Reliable theoretical or experimental data are often required to design and optimize industrial processes. However, only limited experimental data on polymeric systems are available in the literature because performing experiments is not always easy. Moreover, experiments involve time and cost constraints. So, an alternative is to develop theoretical models to be used for process designing. Such models also help experimentalists by identifying potential areas that require further experimental exploration.

Polymers were first synthesized in 1869 by John Wesley Hyatt. The development was revolutionary because it enabled engineers to make new materials free from economic constraints that arise due to the lack of natural resources. Subsequently, in 1907, the first synthetic plastic, Bakelite, was invented by Leo Baekeland. Bakelite substituted for Shellac, a natural plastic used for electric insulation because Bakelite was durable, heat resistant and could be produced in large amounts. Bakelite was used to meet the growing demand for electric insulators due to the growing use of electricity. In the 1930's demand for plastics significantly increased to preserve natural resources. In 1935, Nylon was invented by Wallace Carothers. It was used to make ropes, helmets, parachutes, etc. With the increasing demand for polymer products, the demand to improve their manufacturing processes by using theoretical models grew rapidly. Previous theoretical models that were designed to describe the thermodynamics of small molecules were incapable of predicting the behaviour of polymers [86]. More and more deviation from ideal behaviour had been observed with the increasing molecular mass of polymer molecules [86]. Thus, the inevitable need for developing new equations of state for pure and mixed polymer solutions caught the attention of scientists and several theoretical models were developed.

Models to predict thermodynamics of polymers can be based on simple empirical ap-

proaches or rigorous ab initio approaches. Empirical approaches can only predict thermodynamic relations of polymeric systems but do not reveal details of underlying physics. On the other hand, models based on statistical mechanics take account of details at the molecular level and predict average macroscopic thermodynamic behaviour of polymers based on microscopic interactions [186]. Thus, several models were developed based on ab initio approaches of statistical mechanics.

With the above perspective, this research is an attempt to develop a rigorous model that can describe the behaviour of pure and mixed polymeric systems. The proposed model is based on the principles of statistical mechanics. The model is designed to describe pressure-volume-temperature (PVT) and the glass transition behaviour of polymers. Thus, before going into the details of the model it is a good idea to first have a look at theoretical models and equations of state that are present in literature. The discussion will also provide justification for designing a new theoretical model. The present research deals with the glass transition temperature behaviour of pure polymers and binary polymer-solvent mixtures. Moreover, the proposed and previous models for predicting glass transition behaviour are based on equations of state so it is also necessary to include a discussion on equations of state of polymers. Consequently, this chapter is divided into eight sections. In the first four sections, the context to understand literature has been developed whereas in the last four sections a detailed review of existing literature is presented. All these sections together establish the background necessary to understand this research.

2.1 An Overview of Thermodynamics

The word *Thermodynamics* is composed of two words: *therm* means heat and dynamics means *to flow*. It is a branch of physics that describes the relationship between heat and other forms of energy on the macroscopic scale. On the other hand, *Statistical Mechanics*, a more fundamental theory, is the microscopic description of macroscopic thermodynamic relations. Consequently, contrary to thermodynamics, statistical mechanics can describe the underlying physics of thermodynamic systems [186]. In thermodynamics, the state of a system is described by macroscopic properties called state variables and its direction of evolution towards equilibrium is defined by thermodynamic potentials. Thermodynamic potentials also determine relationships between different thermodynamic properties. Some famous thermodynamic potentials are internal energy U, Gibbs free energy G, Helmholtz free energy F, and Grand potential Φ_G.

In thermodynamics, there are two kinds of state variables: extensive and intensive. Extensive variables depend on the extent (mass) of thermodynamic systems whereas intensive

variables do not depend on the extent of thermodynamic systems. For instance, the number of particles $\{n_k\}$, entropy S, volume V are extensive variables because they depend on the mass of the thermodynamic system. Several thermodynamic potentials are also extensive variables including Gibbs free energy G, Helmholtz free energy F, internal energy U and grand potential Φ_G. On the other hand, intensive variables include pressure P, temperature T, chemical potential $\{\mu_k\}$, etc. Extensive variables divided by the mass of the system are called specific variables. Consequently, specific variables no longer depend on the extent of the system. A set consisting of a minimum number of state variables that are necessary to completely define the state of a thermodynamic system is termed as thermodynamic coordinates. Consequently, thermodynamic potentials are defined in terms of appropriate thermodynamic coordinates. Another famous terminology in thermodynamics is *equation of state*. Equations of state are equilibrium relations between thermodynamic coordinates [93]. Equations of state are usually derived by taking appropriate partial derivatives of thermodynamic potentials.

For a given thermodynamic system all choices of thermodynamics potentials are equivalent. But, depending on the expected evolution behaviour of a given thermodynamic system some potentials are easier to work with [187–189]. Mathematical definitions of some common thermodynamic potentials are given below,

Helmholtz free energy: $F = U - TS = -PV + \sum_k \mu_k n_k,$

Gibbs free energy: $G = U + PV - TS = \sum_k \mu_k n_k,$

Grand potential: $\Phi_G = U - TS - \sum_k \mu_k n_k = -PV.$

State variables are first-order partial derivatives of thermodynamic potentials. However, there is another category of variables called response functions that are second-order partial derivatives of thermodynamic potentials. Sometimes state variables cannot be measured through experiments, for instance, entropy. In that case, state variables can be calculated by using experimentally measurable response functions [87, 155]. Common response functions are given below,

Isobaric heat capacity: $C_P = T\frac{\partial S}{\partial T}\Big|_P = -T\frac{\partial^2 F}{\partial T^2}\Big|_P,$

Isochoric heat capacity: $C_V = T\frac{\partial S}{\partial T}\Big|_V = -T\frac{\partial^2 F}{\partial T^2}\Big|_V$,

Thermal expansivity: $\alpha_V = \frac{1}{V}\frac{\partial V}{\partial T}\Big|_P = \frac{1}{V}\frac{\partial^2 G}{\partial P \partial T}$,

Adiabatic compressibility: $\beta_S = -\frac{1}{V}\frac{\partial V}{\partial P}\Big|_S = -\frac{1}{V}\frac{\partial^2 F}{\partial P^2}$,

Isothermal compressibility: $\beta_T = -\frac{1}{V}\frac{\partial V}{\partial P}\Big|_T = -\frac{1}{V}\frac{\partial^2 G}{\partial P^2}$.

Apart from the above, there exist two major types of thermodynamics phase transitions that are classified in two different ways. The first classification of phase transitions was presented by Ehrenfest [42]. But, the Ehrenfest classification is no longer in use and it has been replaced by a modern more appropriate classification. A discussion on these transitions is necessary to understand the present research.

2.1.1 Ehrenfest Classification:

First-Order Transition:

A first-order transition is the discontinuity in first order partial derivatives of *continuous* Gibbs free energy $G = G(P, T, V)$ with respect to thermodynamic variables. For instance, $(\partial G/\partial P)_T$ and $(\partial G/\partial T)_P$. Consider the following thermodynamic relations [87],

$$V = \frac{\partial G}{\partial P}\Big|_T, \tag{2.1}$$

$$S = -\frac{\partial G}{\partial T}\Big|_P, \tag{2.2}$$

$$H = \frac{\partial (G/T)}{\partial (1/T)}\Big|_P, \tag{2.3}$$

where, S is entropy and H is enthalpy of the system. This implies that during the first-order transition volume, entropy and enthalpy show discontinuous trends. Two examples of first-order transitions are vaporization and fusion. This definition of first-order transition was first mentioned by Ehrenfest [42].

Second-Order Transition:

A second-order transition is the discontinuity in second order partial derivatives of *continuous* Gibbs free energy $G = G(P, T, V)$ with respect to thermodynamic variables whereas first order partial derivatives remain continuous. For instance, $(\partial^2 G/\partial P^2)_T$ and $(\partial^2 G/\partial T^2)_P$. Consider the following thermodynamic relations [87],

$$kV = -\frac{\partial V}{\partial P}\bigg|_T = -\frac{\partial^2 G}{\partial P^2}\bigg|_T, \tag{2.4}$$

$$C_P = T\frac{\partial S}{\partial T}\bigg|_P = -T\frac{\partial^2 G}{\partial T^2}\bigg|_P, \tag{2.5}$$

$$\alpha V = \frac{\partial V}{\partial T}\bigg|_P = \frac{\partial}{\partial T}\left[\frac{\partial G}{\partial P}\right]_T\bigg|_P, \tag{2.6}$$

where, k is compressibility, α is thermal expansion coefficient, and C_P is heat capacity of the system. Thus, entropy S, enthalpy H and volume V of the system do not show discontinuity at second-order transition, however, compressibility k, thermal expansion α and heat capacity C_P show discontinuous trends. Few examples of second-order transitions are onset of superconductivity, ferroelectricity, ferromagnetism, and order-disorder transtion of metal alloys [152, 154, 170].

2.1.2 Modern Classification:

Ehrenfest's classification is an incomplete scheme to classify phase transitions because it cannot explain cases where derivatives of free energy diverge. For example, during ferromagnetic transitions, the heat capacity of systems becomes infinity. Thus, a new scheme to classify phase transitions have been proposed [84].

First-Order Transition:

Under the modern scheme, first-order phase transitions are classified as transitions that involve absorption or rejection of a fixed amount of latent heat per unit volume while the temperature of systems remains constant. For instance, boiling of water or melting of ice. During these transitions, the system exists in a mixed-phase *i.e.* a portion of the system completes the transition while the other portion of the system remains in the transition.

Second-Order Transition or Continuous Phase Transition:

The modern scheme classifies the second-order transition as a transition that involves an infinite correlation length, divergent susceptibility and power-law decay of correlations in

the vicinity of critical conditions. During a second-order phase transition heat capacity and thermal expansion of amorphous substances changes suddenly at glass transition temperatures [127].

2.2 An Overview of Statistical Mechanics

As discussed, thermodynamics is a macroscopic study of systems and thus cannot be used to explore the underlying physics of microscopic particles. Fortunately, statistical mechanics offers a procedure to study the macroscopic behaviour of systems by using arguments at the microscopic level [87]. Thermodynamics only provides relations between thermodynamic properties, however, statistical mechanics provides a procedure to calculate thermodynamic properties independent from each other. Real thermodynamic systems are usually very complicated, their behaviour depends on shape, size, and interactions of constituting particles. Thus, idealized statistical mechanical models are used to simplify analytical and numerical calculations. However, idealized models should consider the necessary details to predict a variety of observed phenomenon at different physical conditions under study [186]. In statistical mechanics, the state of a system is defined by using microscopic variables *i.e.* positions, velocities, state of excitation, etc. of all particles constituting the system. Observed macroscopic thermodynamic variables are considered to be the average response from microscopic variables. Thus, the state of a system when defined by using microscopic variables is called a *microstate* and the average behaviour of microstates results in a *macrostate* [87]. At a given thermodynamic state (macrostate) there can exist a tremendous number of microstates since systems usually have a very high number of particles. The probability of finding a system in a given macrostate is proportional to the number of possible configurations (microstates) that result in the same macrostate. Statistical mechanics assumes that at equilibrium the system should be in its most probable macrostate *i.e.* the macrostate having the highest number of microstates. Small probabilities of not finding a system in its most probable macrostate are called thermal fluctuations.

In statistical mechanics, the first step is to count the number of allowed microstates of a system at an arbitrary macrostate. While counting the number of allowed microstates quantum mechanical effects cannot be ignored [87]. A quantity called the partition function Q is evaluated by using,

$$Q \equiv \sum_{k} e^{-E_k/k_B T}, \tag{2.7}$$

where E_k is the energy of the system in k^{th} microstate, k_B is Boltzmann's constant and

T is the temperature of the system [87]. The sum is over all possible microstates at an arbitrary macrostate. Then, from the partition function, the Helmholtz free energy F is calculated by using,

$$F = -k_B T \ln Q. \tag{2.8}$$

All other thermodynamic properties can be evaluated by taking appropriate partial derivatives of the free energy and/or partition function. Also, the average of any thermodynamic property O can be evaluated by using,

$$\langle O \rangle = \sum_k \frac{O_k e^{-E_k/k_B T}}{Q}. \tag{2.9}$$

The sum is over all possible microstates of the system.

2.2.1 Common Assumptions

Two common assumptions of statistical mechanical models that are relevant to the present topic are highlighted below.

Mean Field Approximation:

For systems involving a large number of particles, the mean-field approximation is often utilized to replace discrete interactions from surrounding particles with an averaged field. This is true because in the case of a large number of particles fluctuations can be ignored [15]. The mean-field approximation also ignores correlations between particles by assuming them to be short-ranged [13]. However, near critical points correlations are not short-ranged [12, 13, 15, 139] and thus the mean-field approximation cannot be applied near a critical condition.

Under the mean-field approximation, the logarithm of the summation over microstates is replaced by the logarithm of the largest term in the summation [87, 186, 211]. This approximation is correct because for large numbers of particles the highest term in the summation is found to be significantly greater than all other terms [115].

Additive Property:

In statistical mechanical models that are based on the mean-field approximation, the energy of a system can be written as the sum of energies from different degrees of freedom because the mean-field approximation ignores correlations between different degrees of freedom.

Thus, the system can be decomposed into independent subsystems and the total energy of the system becomes equal to the sum of energies of independent subsystems [147, 186]. For instance, in systems where the external configuration of molecules is independent of the internal state of molecules, the energy of the system can be split into configurational energy $E_{conf.}$ and internal energy $E_{int.}$. Consequently, the partition function Q in Eq. 2.7 becomes equal to the product of the partition function Q_{conf} of configurational states and the partition function Q_{int} of internal states. Subsequently, the free energy F in Eq. 2.8 becomes equal to the sum of free energy F_{conf} of configurational states and free energy F_{int} of internal states [87]. As a result, thermodynamic properties from internal degrees of freedom only depend on the temperature of the systems. Since the pressure of a system is equal to the partial derivative of free energy with respect to the volume so these internal degrees of freedom do not contribute to PVT properties of polymers [157].

2.3 Types and Properties of Mixtures

2.3.1 Types of Mixtures:

Ideal mixtures assume no coupling/interaction between different species in multicomponent mixtures. Thus, molecules of each species remain unaware of the presence of other species [93]. Consequently, when an ideal mixture is formed by mixing pure components the enthalpy of mixing is assumed to be zero. However, the entropy of mixing is assumed to be greater than zero [93].

Real mixtures can be divided into three types: Regular, Athermal and General. Real mixtures are characterized by comparing their thermodynamic behaviour with ideal mixtures [186]. Regular mixtures assume *weak* interactions between different species of multicomponent mixtures. Thus, the enthalpy of mixing is assumed to be non-zero. However, saying that interactions are *weak* implies that the interactions do not contribute to the non-zero mixing entropy. Thus, the entropy of mixing is the same as that of ideal mixtures [93]. On the other hand, in athermal mixtures, the entropy of mixing is different from the mixing entropy of ideal mixtures, however, the enthalpy of mixing is assumed to be zero. Lastly, in general mixtures both, enthalpy and entropy of mixing, are assumed to be different from ideal mixtures.

2.3.2 Properties of Mixtures:

For multicomponent mixtures, several new phenomena and properties can be defined. However, the two most important phenomena are mentioned below that account for the stability of homogeneous mixtures.

Upper Critical Solution Temperature (UCST):

UCST is defined as a temperature above which all components of the mixture remain miscible at all compositions. So, it is the upper bound of temperature interval above which the mixture will certainly be miscible at all compositions [162].

Lower Critical Solution Temperature (LCST):

LCST is defined as a temperature below which components of the mixture remain miscible at all compositions. So, it is the lower bound of temperature interval below which the mixture will certainly be miscible at all compositions [162].

2.4 Polymeric Foams

Polymeric foams are used in every aspect of life. They are used in toys, packaging, heat insulators, sports goods, etc. [3, 9, 96, 99, 161] because of their unique mechanical, thermal and chemical properties and economical production cost. They are lightweight but strong, durable, and chemically inert [3, 9, 96, 161].

Polymeric foams are solid polymers with macroscopic voids or cells that are produced by blowing solvent gases through liquid polymers. The size and geometry of cells play a very important role in determining the properties of foams [99]. Substances used to create voids in polymeric materials are called blowing agents (BAs). Blowing agents can be classified into two categories, physical blowing agents (PBAs) and chemical blowing agents (CBAs). Chemical blowing agents emit gas due to thermal decomposition or chemical reaction at processing conditions. On the other hand, physical blowing agents are stable or inert gases like carbon dioxide, nitrogen, hydrochlorofluorocarbons, propane, pentane, and argon [3, 9, 96, 98, 99, 126, 161]. The process for the production of polymeric foams is carried out in following steps [99, 104]:

1. A polymeric material is placed in a solvent rich environment. The pressure of the solvent in the environment is increased with a simultaneous increase in the temperature of the system.

2. Due to the increased pressure, the solvent gas diffuses inside the liquid polymer to achieve saturation.
3. The pressure of the environment is rapidly decreased which results in the formation of bubbles of the solvent (blowing agent). The bubbles of the blowing agent nucleate and grow.
4. The temperature of the system is decreased to obtain a solid or glassy state and this freezes the bubbles before they collapse.
5. The closed solvent rich environment is then removed. Consequently, the blowing agent evacuates from the voids of the resulting polymeric foam.

Since solvent gases create voids in polymeric foams so gases with higher solubility result in polymeric foams of lesser weight to volume ratios. Solvent gas diffuses into the polymer until a chemical equilibrium is achieved between solvent gas in the polymer and solvent gas in the environment. The polymer-solvent phase is called polymer-solvent mixture (or mixed-phase) and the solvent in the environment is called the pure solvent phase. The equilibrium between the mixed-phase and the pure solvent phase is determined by the equation of state behaviour of the system. Note that the present research only discusses stable polymeric systems without voids.

2.4.1 Properties of Polymeric Foams:

For multicomponent polymeric foams, two more quantities are found to be useful *i.e.* solubility and swelling. These quantities are defined below.

Solubility:

Solubility is defined as the weight fraction of a solvent dissolved in a polymer matrix at saturation. It is denoted by χ_s.

$$\chi_s = \frac{\sum_k^s n_k M_k}{\sum_k^s n_k M_k + \sum_k^p n_k M_k}, \tag{2.10}$$

where, superscript s denotes that the sum over solvent species only, superscript p denotes that the sum over polymer species only, n_k is number of moles of species k, and M_k is molar mass of species k.

Swelling:

Swelling is defined as the ratio of the volume of a polymer matrix in the presence of a blowing agent to the volume of the polymer matrix in the absence of the blowing agent. It is denoted by S_W.

2.5 Equations of State

Equations of states (EOS) are equations that relate thermodynamics variables describing the state of physical systems [43]. The thermodynamics variables may include pressure, temperature, volume, internal energy, entropy, specific heat, thermal expansion etc. Equations of state cannot be derived by using thermodynamics principles. Thus, simplified models are used to capture the underlying physics especially interactions in the system. Consequently, a single equation of state cannot be used for all physical systems because idealized models are based on assumptions that may be valid for one particular group of systems at given physical conditions but completely absurd for another group of systems or conditions. For instance, the ideal gas equation of state can only be used to describe real gases at high temperatures and low pressures since intermolecular forces can be neglected. However, at high pressures and/or low temperatures, the behaviour of real gases deviates from the ideal gas equation of state and consequently, the ideal gas model requires modification. Since physical systems are very diverse thus a large number of equations of state are designed for different physical systems. Consequently, equations of state for systems composed of small molecules in gas, liquid or solid phase belong to one small group of equations of state in a large pool of possible equations of state. There are equations of state used to describe systems as alien as neutron stars, white dwarf, supernova, quark-gluon plasma, Bose-Einstein condensate, and radiation fields. Given that a system is in thermodynamic equilibrium, EOS provides a universal treatment to consider nature at different conditions. EOS often leads to the development of various branches of physics. For instance, the ideal gas equation of state is considered to be the major factor in the development of thermodynamics. Thus, equations of state have fundamental importance in physics, chemistry, material science and engineering. Equations of state are also important in interdisciplinary fields including polymer physics, geophysics, and astrophysics. In general, EOS can be used to relate any thermodynamic variables, however, most equations of state relate pressure, volume and temperature of physical systems.

As discussed, simplified models (called the analytical approach) can be used to derive equations of state, however, there are at least two other approaches, namely, the empirical approach and the semi-empirical approach, that can also be used to describe the

behaviour of thermodynamic systems. Empirical relations utilize extensive experimental data whereas semi-empirical relations utilize both, the models and the experimental data, to make predictions. Empirical equations of state cannot provide insight into the underlying physics of systems, however, they can be used to accurately calculate thermodynamic properties within the given range of experimental data. On the other hand, equations of state based on analytical methods can provide significant insight into the underlying physics of systems. However, since they rely on simplified/idealized models so their predictions of thermodynamics properties are not always satisfactory. Finally, the accuracy of predictions from semi-empirical equations of the state lies in between the other two approaches.

2.5.1 Tait Equation (Empirical)

The Tait equation [181] is an empirical relation that is used to represent PVT data of polymeric systems. The Tait equation is a pressure-volume relation at given temperature (isotherm) and is given by,

$$V(P,T) = V(0,T)\Big[1 - C\ln\{1 + P/B(T)\}\Big], \tag{2.11}$$

where, $C = 0.0894$ is a universal constant [123], $B(T)$ is called the Tait parameter and $V(0,T)$ is the isotherm at zero pressure. $B(T)$ is given as,

$$B(T) = B_0 \exp(-B_1 T), \tag{2.12}$$

where, B_0 and B_1 are constants. The isotherm $V(0,T)$ is given as,

$$V(0,T) = V_0 \exp(\alpha T), \tag{2.13}$$

where α is the thermal expansion coefficient. So there are four fitting parameters (B_0, B_1, V_0, α) that are used to fit Tait equation on PVT data.

2.5.2 Cubic Equations of State (Semi-Empirical)

Equations that can be written as a cubic function of molar volume of a given system are called cubic equations of state. These empirical/semi-empirical equations of state are based on observations and experiments. So, they are not derived from first principles.

Van der Waals Equation of State

The ideal gas EOS fails at low temperature and/or high pressure because it neglects the finite size of molecules and attractive forces between molecules composing the system. Consequently, it cannot predict the condensation of gases. Thus, in 1873, the van der Waals equation of state was introduced by J. D. van der Waals. The van der Waals equation of state is a semi-empirical equation that contains two constants, a and b, to account for the attraction and repulsion (finite molecular volume) between molecules, respectively [194]. The values of attraction parameter a and repulsion parameter b are determined from experimental data. These constants were necessary because, in real gases, the presence of attractive forces leads to a decrease in pressure of the system whereas the presence of repulsive forces prevents condensation of gases to infinitesimal volumes. The van der Waals EOS was the first EOS that predicted the condensation and gas-liquid phase diagrams of real gases, however, the agreement with experimental data was not satisfactory. The van der Waals EOS is given as,

$$\left(P + \frac{a}{V^2}\right)(V - b) = RT, \tag{2.14}$$

where, $a = 3P_cV_c^2$ and $b = V_c/3$. Here P_c and V_c are critical pressure and critical volume, respectively.

The Law of Corresponding States:

The van der Waals equation shows that during the vapour-liquid phase transition the difference between the vapour phase and the liquid phase disappears at critical point (P_c, V_c, T_c). If one writes van der Waals equation of state in terms of dimensionless reduced variables $P_r = \frac{P}{P_c}$, $T_r = \frac{T}{T_c}$ and $V_r = \frac{V}{V_c}$ then the same equation remains valid for a broad set of simple substances over a wide range of temperature and pressure, reasonably close to the critical point. This is called the *law of corresponding states*. In other words, the law of corresponding states asserts that for a given substance at some constant temperature the van der Waals EOS gives a P-V relation. But, if one changes the substance the P-V relation also changes since the new substance can have different values of constants a and b. However, if one rewrites the relation in terms of dimensionless reduced variables P_r, T_r and V_r by dividing each state variable P, T and V with corresponding critical values P_c, T_c and V_c the resulting relationship is considered to be universal *i.e.* at given reduced temperature and reduced volume all substances have equal reduced pressures. [53, 145, 146, 178]. The

corresponding van der Waals EOS is,

$$\left(P_r + \frac{3}{V_r^2}\right)(3V_r - 1) = 8T_r. \tag{2.15}$$

In the above expression, if $P_r < 1$ and $T_r < 1$ the system is at vapour-liquid phase equilibrium. The reduced van der Waals EOS is a cubic equation so this equation has three solutions of the reduced volume V_r. The largest value of reduced volume corresponds to the vapour phase whereas the lowest value of reduced volume corresponds to the liquid phase.

Besides, the law of corresponding states is not limited to the van der Waals EOS. It is a universal principle and is followed by several equations of state [49,52,95,100,164] with the exception that, instead of critical point values, thermodynamic state variables are reduced by some other appropriate characteristic parameters. So, this law is not only valid for real gases but is also applicable to liquid, fluids with non-polar molecules, polymers etc. This law has been experimentally verified for several real gases including nitrogen, methane and carbon dioxide [63].

Redlich-Kwong Equation of State

Redlich-Kwong EOS (RK-EOS) was proposed in 1949 to improve the van der Waals EOS. However, RK-EOS is likewise not accurate for the liquid phase but it works well for the gaseous phase under conditions where reduced pressure (the ratio of system pressure to critical pressure) is less than one-half of reduced temperature (the ratio of system temperature to critical temperature). In 1972, an improvement to RK-EOS has been proposed by G. Soave [174] by allowing a substance-specific constant in RK-EOS to be a function of temperature and acentric factor. The modified equation is called the Soave-Redlich-Kwong EOS (SRK-EOS). SRK-EOS is especially used for hydrocarbons. However, it is still not accurate for liquid phases because of its incapability to accurately predict the molar volume of the liquid phase. Thus, in 1982, Peneloux *et al.* modified SKR-EOS by introducing a new parameter to slightly offset the molar volume and thus corrected the error in the molar volume of the liquid phase. Thus, this modification significantly improved predictions of the molar volume in the liquid phase while maintaining good predictions of the molar volume in the gaseous phase — thanks to the fact that the pressure of liquid phase is very sensitive to small changes in molar volume, however, pressure of gaseous phase is not sensitive to such small changes in molar volume.

Peng–Robinson Equation of State

Peng–Robinson equation of state (PR EOS) was introduced in 1976 [142]. It is also based on van der Waals EOS but proved to be more accurate than SKR EOS for predicting liquid densities. It is also accurate near the critical points of materials. For mixtures, PR EOS considers a binary interaction parameter that is assumed to be constant. As with the van der Waals EOS, the theory has two fitting parameters to characterize excluded volume effects (repulsive forces) and attractive intermolecular forces [142]. Excluded volume is assumed to be constant whereas intermolecular forces are assumed to be dependent on the temperature of the system. In addition, if one needs to apply the model on polymeric fluids, then instead of critical parameters some other appropriate characteristic parameters are required to reduced thermodynamic state variables [69]. Moreover, to extend the PR EOS to multicomponent polymeric systems appropriate mixing rules are also required to calculate values of fitting parameters [142].

Later, Stryjek and Vera [179] introduced two pure component parameters in attraction terms of PR EOS to get better predictions from the model. The resulting equation called Peng–Robinson-Stryjek-Vera equations of state (PRSV-EOS) is accurate for vapour-liquid phase equilibrium calculations. However, PRSV-EOS has a limitation that it only works for temperatures below the critical temperature of the given material.

Advantages:

1. PR EOS is very simple to do calculations.
2. PR EOS can be used to calculate PVT behaviour of pure and multicomponent systems.

Limitations:

1. The simplicity of PR EOS implies that it is less accurate as compared to more sophisticated EOS [69].
2. PR EOS is even less accurate for large molecules.

Elliott, Suresh, Donohue Equation of State

In 1990, Elliott, Suresh, Donohue equation of state (ESD-EOS) was introduced to improve PR EOS by making corrections in the repulsive term of PR EOS [44]. ESD-EOS was developed by using computer simulations. It takes into account the shape, size, and hydrogen bonds of molecules.

2.5.3 Virial Equation of State (Analytical)

Virial equation of state is based on statistical mechanics [87] and utilizes an expansion (perturbations) having constants called virial coefficients. With an appropriate mathematical form of intermolecular forces, these virial coefficients can be evaluated. However, the first virial coefficient is always 1 which corresponds to the fact that for a very large volume the fluid behaves as an ideal gas. The second virial coefficient accounts for pairwise interactions between molecules and similarly higher virial coefficients correspond to three-particle interactions, four-particle interactions and so on. These virial coefficients are considered to be functions of temperature. Accuracy of the virial equation of state can be increased indefinitely by accounting for more and more expansion terms. However, higher-order virial coefficients are difficult to manage because of multiple integrals. Moreover, the convergence of virial expansion deteriorates at higher densities.

2.5.4 Debye-Huckel Model for Electrolytes

In 1923, Debye and Huckel presented a theory to explain thermodynamics, especially osmotic pressure, of electrolyte solutions in the dilute limit. In this model, it was assumed that strong electrolytes behave as isolated ions in continuous dielectric medium *i.e.* solvent (for instance, water). Contrary to an ideal gas, in an electrolyte solution, there are significant Coulomb interactions between charged ions. However, the model assumes that these interactions are small as compared to the thermal energy of charged particles k_BT. Moreover, ions are considered to be randomly distributed due to the presence of repulsive electrostatic forces between the ions of the same charge. Ions are assumed to be spherical in shape and the degree of ionization was assumed to be constant. Other assumptions of the model are:

1. Strong electrolyte assumption *solute dissociates completely*.
2. Ions do not polarize due to neighbouring charges.
3. The solvent only acts as a uniform medium of appropriate dielectric constant with no feature and structure.
4. The model assumes that a charge of a given polarity (positive or negative) is mainly surrounded by charges of opposite polarity. Moreover, the surrounding charges act as a continuous spherically symmetric cloud with some appropriate charge density.
5. Ion-solvent interactions are assumed to be negligible and thus ignored.
6. Size of ions is assumed to be negligible.

Limitations:

1. This model gives reasonable results only for electrolyte solutions at low concentrations.
2. The model does not perform satisfactorily for unsymmetrical electrolytes.
3. The assumption of ion dissociation may also become invalid at higher charge concentrations.
4. Polyatomic ions polarize easily so the model cannot describe the behaviour of polyatomic ions.
5. The solvent is considered to be uniform with no structure. However, in aqueous solutions, water molecules can polarize.
6. At a high concentration of charges, the size of ions becomes comparable to the size of the ion cloud. This renders the assumption of small size ions invalid.

2.5.5 Models for Solid State

In crystalline solids, a new degree of freedom emerges *i.e.* oscillation of atoms in the crystal lattice. One famous model for solids is the Debye model. In this model, the solid crystal lattice is considered to have quasi-harmonic oscillators to account for the oscillation of atoms. Moreover, the solid system is assumed to be isotropic and homogeneous. Thermal excitation in the crystal is assumed to be sound waves called phonons. Moreover, in solids, electrons also play a vital role in determining the thermodynamics of the system. To calculate the effect of electrons it was assumed that electrons move in a periodic potential. With these assumptions, the Debye model successfully predicts the thermodynamic behaviour of crystalline solids.

2.5.6 Hard-Sphere and Soft-Sphere Models

In liquids, the main contributing forces are repulsive while attractive forces only account for minor corrections. Thus, two types of potentials are commonly used to represent repulsive forces: hard-sphere model and soft-sphere model. The hard-sphere model is given as,

$$V(r) = \begin{cases} \infty, & \text{if } r \leq a \\ 0, & \text{if } r > a, \end{cases}$$

where, a is the radius of hard-sphere. This model represents highly-compressed liquids. It is also used in integral equations.

The soft-sphere model that is given as,

$$V(r) = \begin{cases} \epsilon(\frac{a}{r})^n, & \text{if } r \leq a \\ 0, & \text{if } r > a, \end{cases}$$

This model is used in the Monte-Carlo method. The soft-sphere model, when used to modify the van der Waals equation of state, can drastically improve predictions of thermodynamic properties of dense gaseous phase and liquid phase. The modified van der Waals EOS approaches the ideal gas EOS in high temperature and low-pressure limit. Thus, the resulting EOS can be used over a wide range of temperatures and pressures with successful predictions of critical points and vapour-liquid transitions.

2.6 Advanced Equations of State for Polymers

Equations of state for polymer fluids are very important for designing manufacturing processes. It is very important for an EOS to predict correct PVT behaviour over a wide range of temperatures and pressures. Thus, several theoretical equations have been proposed for polymers [32, 73, 100, 125, 132, 140, 147, 171, 177] to accurately predict PVT data.

The development history of equations of state for polymer liquids can be traced back to van der Waals' work [178]. Initial attempts were based on extending the models of real gases and crystalline solids. This is because the liquid state can be assumed as an equilibrium state between the gaseous phase and the solid phase, especially near melting points the density of liquids is found to be very close to the density of solids.

Equations of state can be divided into three categories: theoretical, empirical and semi-empirical equations of state. However, in this section, only theoretical and semi-empirical equations of state are discussed. These equations of state are based on the principles of statistical mechanics thus use microscopic details to predict the macroscopic response of the system. Theoretically, models based on quantum mechanics may give more accurate predictions but such models require a detailed description of potentials that are often unknown.

Most sophisticated equations of state of polymers are inspired by two preliminary theories of polymer fluids, namely, Flory-Huggins theory and free volume theory. Thus, to understand advanced equations of state of polymers it is necessary to learn Flory-Huggins theory and free volume theory. Consequently, I have first discussed these two theories and then other advanced equations of state of polymers.

Flory-Huggins Theory:

Flory-Huggins (FH) theory deals with the thermodynamics of binary polymer-solvent solutions. Considering that polymer molecules are very large as compared to solvent molecules the theory divides polymers molecules into smaller segments. Then, the segments of polymers and solvent molecules are only allowed to take discrete positions on an artificial lattice of coordination number z. Since solvent molecules are small so each solvent molecule is allowed to occupy only one lattice site. Thus, the volume of one lattice site is assumed to be equal to the volume of one solvent molecule. Consequently, this assumption also prescribes the size of coarse-gaining of polymer molecules [78]. Moreover, interactions are considered to be short-ranged and polymer segments are assumed to occupy lattice sites by following statistics of random walk [78].

The model initially assumes two separate pure systems: the pure solvent system and the pure polymer system. Let the pure solvent system have N_s number of solvent molecules, whereas, the pure polymer system has N_p number of polymer molecules with each polymer molecule divided into x segments. Thus, when the two systems are mixed the total number of lattice sites should be $N = N_s + xN_p$. By following the statics of random walk, the change in entropy occurs due to mixing is found to be,

$$\Delta S_m = -k_B \Big[N_s \ln \phi_s + N_p \ln \phi_p \Big], \tag{2.16}$$

where, $\phi_s = N_s/N$ is the volume fraction of solvent, $\phi_p = xN_p/N$ is the volume fraction of polymer. Moreover, due to mixing, the enthalpy of the system should also change. The mixed system has three types of interactions: solvent-solvent interaction of energy ϵ_{ss}, polymer-polymer interaction of energy ϵ_{pp}, and solvent-polymer interaction of energy ϵ_{sp}. The increase in solvent-polymer interactions is accompanied by an average decrease in solvent-solvent and polymer-polymer interactions. Thus, we can define energy increment due to solvent-polymer interaction as,

$$\epsilon = \epsilon_{sp} - \frac{1}{2}(\epsilon_{ss} + \epsilon_{pp}). \tag{2.17}$$

Moreover, solvent-polymer interaction parameter χ_{sp} is defined as,

$$\chi_{sp} \equiv \frac{z\epsilon}{k_B T}. \tag{2.18}$$

Solvent-polymer interaction parameter χ_{sp} is the only factor in the model that depends on the nature of materials of polymer and solvent. In addition, the model ignores correlations based on mean-field approximation discussed in section 2.2.1. Moreover, solvent molecules and polymer segments are assumed to be randomly distributed on the lattice by allowing each segment to move independently in a random manner. By using these assumptions, Flory [47] and Huggins [82] obtained the following expression of the change in Gibbs free energy as a result of the mixing of solvent in the polymer.

$$\Delta G_m = RT(n_s \ln \phi_s + n_p \ln \phi_p + n_s \ln \phi_p \chi_{sp}), \tag{2.19}$$

where, R is the universal gas constant, n_s is the number of moles of solvent, and n_p is the number of moles of the polymer. In FH theory solvent-polymer interaction parameter χ_{sp} plays a central role in defining the nature of the mixture. For the case of mixture where $\epsilon_{ss} + \epsilon_{pp} = 2\epsilon_{sp}$ the solvent-polymer interaction parameter becomes zero and the solution behaves as an ideal mixture discussed in section 2.3.1. If $0 < \chi_{sp} < 1/2$ the polymer-solvent interactions are repulsive but weak. Thus solvent-polymer phase separation does not occur. However, if $\chi_{sp} > 1/2$ the phase separation occurs into polymer-rich and solvent-rich phases [162].

Flory-Huggins theory can predict the stability of mixture, upper critical solution temperature and lower critical solution temperature. However, predictions from the theory are mostly qualitative. The model is based on an incompressible lattice so the volume and the total number of molecules in the system are not independent parameters. Thus, the model cannot predict the swelling of polymeric foams [99].

Free Volume Theory:

In usual mixtures, molecules are free to move under the influence of thermal vibration due to interstitial spaces, called free volume, between molecules [59]. However, Flory-Huggins theory, as well as other lattice theories, do not allow such motion of segments. Thus, to account for the existence of free volume, vacant sites are allowed on lattice models. These vacant sites are termed as *holes* [59].

Several models have been introduced based on a free volume assumption [56, 58, 199]. The free volume assumption has proven to be very useful for calculating diffusion in liquids [58, 59, 199]. Moreover, in polymers, free volume improves calculations of glass transition temperatures [20, 56, 192].

Equations of state for polymer fluids that are based on free volume theory and their models can be categorized into four main groups:

1. Cell Models
2. Lattice-Fluid Models
3. Hole Models
4. Tangent-Sphere Models

The above models, except tangent-sphere models, are based on a common assumption that molecules of the system are acted on by an averaged field from neighbouring molecules. The averaged field confines molecules of the system in a relatively small area thus offering hope to treat the system as if it has a lattice. So these models work best for highly compressed liquids where total energy of the system is significantly greater than the kinetic energies of that system. These models have been designed to account for the finite compressibility and thermal expansion of polymer systems. They can be used to describe the behaviour of pure polymers fluids, polymer blends, and multicomponent polymer solutions. However, they are only valid above the glass transition temperature of amorphous polymers and above the melting point of crystalline polymers.

Equations of state from all models work reasonably well at low pressure. However, to fit PVT data over a wide range of pressure some equations of state outperform others. Moreover, all discussed equations of state require PVT data to determine characteristic parameters P^*, T^* and ρ^* (or v^*) and can be represented in terms of reduced variables. Thus they obey the law of corresponding states.

2.6.1 Cell Models

As discussed in these models, polymer molecules are divided into small discrete segments. The space around each segment is considered as cells and the volume of cells is assumed to be a variable to allow compression and expansion of the polymeric system. Each segment is considered to have $3c$ degrees of freedom, where constant c is called the segmental parameter. It is introduced to account for constraints that are present between segments. Polymer molecules are assumed to have two distinct modes: internal and external. Internal modes account for the motions present within molecules whereas external modes account for interactions present between molecules. It is assumed that internal modes play no role in defining the PVT behaviour of the system. This distinction of two modes was introduced by Prigogine *et al.* [147, 149].

Several cell theories have been developed based on the choice of intermolecular potential and cell geometry. An overview of important cell models is discussed below.

Prigogine Square-Well Equation of State

Prigogine *et al.* [148] developed two different cell models by using Lennard-Jones (LJ) potential [100] and hexagonal close packing for the geometry of cells. The major difference between two models is that one model is based on square-well approximation of LJ potential [147] whereas the other model is based on harmonic oscillator approximation of LJ potential. [149]. However, the square-well model is mostly used so it is discussed here. The EOS from square-well approximation is,

$$\frac{\tilde{P}\tilde{v}}{\tilde{T}} = \frac{\tilde{v}^{1/3}}{\tilde{v}^{1/3} - 0.8909} - \frac{2}{\tilde{T}}\left(\frac{1.2045}{\tilde{v}^2} - \frac{1.011}{\tilde{v}^4}\right), \tag{2.20}$$

where, $\tilde{P} = P/P^*, \tilde{T} = T/T^*$, and $\tilde{v} = v/v^*$ are reduced variables and P^*, T^* and v^* are characteristic parameters given as,

$$P^* = \frac{ck_BT^*}{v^*}, \tag{2.21}$$

$$T^* = \frac{s\eta}{ck_B}, \tag{2.22}$$

$$v^* = \sigma^3, \tag{2.23}$$

where, σ is the radius of hard-sphere, η is the interaction energy between segments, s represents number of contacts per segment, c accounts for intermolecular constraints on segments and k_B is Boltzmann's constant.

A brief outline of the model is as follows. This model is also based on a lattice in which polymer molecules are divided into small segments (r-mers) and each segment is allowed to occupy one lattice site. Given the position of one segment of a polymer molecule, the next connected segment on the molecule is allowed to occupy only the adjacent neighbouring sites. The segments are allowed to have thermal fluctuations due to the finite temperature of the system. However, since segments are connected so segments tend to vibrate about their equilibrium positions under the influence of forces from neighbouring sites. In short, the segments are assumed to be confined in cells of some finite volume. The value of constraint parameter c is assumed to be in between 1 and r. This assumption is based on the fact that for rigid molecules there are only three degrees of freedom to allow translation of molecule whereas for infinitely flexible molecules of r-mers (segments) there should be $3r$ degrees of freedom. Thus, for semi-flexible molecules, degrees of freedom must be in between these two extremes *i.e.* $3c$. The resulting equation of state is found to maintain excellent PVT data fittings over a wide range of pressure [157].

Flory, Orwoll, Vrij Equation of State

The most famous and extensively used cell model is Flory, Orwoll, and Vrij (FOV). Flory, Orwoll, and Vrij developed a new theory [49, 51, 52] for polymer-solvent mixtures to accurately predict the lower critical solution temperature (LCST) of polymer-solvent mixtures. In this model the lattice sites are assumed to be occupied by either segments of polymer molecules or small solvent molecules. The geometry of cell is assumed to be simple cubic [49, 52, 157]. Moreover, in this model two types of potentials were considered. For repulsive forces hard-sphere potential was assumed whereas for attractive forces an arbitrary soft potential was assumed. FOV cell model results in the following EOS,

$$\frac{\tilde{P}\tilde{v}}{\tilde{T}} = \frac{\tilde{v}^{1/3}}{\tilde{v}^{1/3} - 1} - \frac{1}{\tilde{T}\tilde{v}}, \tag{2.24}$$

where, $\tilde{P} = P/P^*, \tilde{T} = T/T^*$, and $\tilde{v} = v/v^*$ are reduced variables and P^*, T^* and v^* are characteristic parameters having the same definitions as mentioned before in Prigogine Square-Well EOS.

Equations of state from FOV and Prigogine square-well models have a similar first term with the exception that in FOV-EOS the factor 0.8909 is replaced by 1. This difference is because in the FOV model simple cubic cells are assumed whereas in the Prigogine model hexagonal close-packed cells are assumed.

Limitations:

1. FOV EOS fails to fit PVT data over a wide range of pressure [157].
2. The model underestimates entropy of the system because it assumes artificial lattice for fluid phase [172].

Dee and Walsh Equation of State

This model is a modification of the Prigogine square-well cell model. In this model Dee and Walsh have decoupled potential from geometry of cell by introducing a universal constant factor $q = 1.07$ [28]. EOS from this model is given as,

$$\frac{\tilde{P}\tilde{v}}{\tilde{T}} = \frac{\tilde{v}^{1/3}}{\tilde{v}^{1/3} - 0.8909q} - \frac{2}{\tilde{T}}\left(\frac{1.2045}{\tilde{v}^2} - \frac{1.011}{\tilde{v}^4}\right), \tag{2.25}$$

where, all variables and parameters have the same definitions as mentioned before for Prigogine square-well cell model.

2.6.2 Lattice-Fluid Models

Lattice-fluid models are similar to cell models as these models also divide polymer molecules into small segments and are based on the artificial lattice. However, contrary to cell models, lattice-fluid models assume the volume of cells to be constant. Thus, to account for finite compressibility of the system, lattice vacancies (empty sites or holes) are allowed on the lattice. So, the volume of the system can be changed by changing the number of empty sites on the lattice. The presence of artificial holes significantly increases the entropy of the system. Consequently, the partition function of the system is found by using the principles of statistical mechanics by treating holes as a species. There are several important lattice-fluid models including the Panayiotou-Vera model [130, 131, 133, 135] and others [25–27]. However, the lattice-fluid model by Sanchez and Lacombe [95, 164] is the most widely used lattice-fluid model so it is discussed below.

Sanchez Lacombe Equation of State

The Sanchez Lacombe Equation of State (SL-EOS) is the most successful lattice-fluid model for classical fluids (polymers or solvent). This equation was first introduced in 1976 by Sanchez and Lacombe Refs. [95, 164].

As discussed in lattice-fluid models the compressibility is introduced by allowing empty sites (holes) on the lattice. The change in volume is obtained by changing the number of holes whereas lattice itself is assumed to be incompressible. As in other models, the polymer molecules are divided into r-mers (or segments) and each segment occupies one site on the lattice. The interaction energies between segments are assumed to be short-ranged and thus independent of the volume of the lattice. Since holes are artificial so it is assumed that holes do not interact. Moreover, holes and segments are assumed to be randomly mixed throughout the lattice. By using this model, the SL-EOS was found to be,

$$\tilde{\rho}^2 + \tilde{P} + \tilde{T}\left[\left(1 - \frac{1}{r}\right)\tilde{\rho} + \ln\left(1 - \tilde{\rho}\right)\right] = 0. \tag{2.26}$$

In the above equation $\tilde{\rho}, \tilde{P}$ and $\tilde{T}$ are reduced density, pressure and temperature of the fluid system, respectively. They are given as follows,

$$\tilde{\rho} = \frac{\rho}{\rho^*}, \tag{2.27}$$

$$\tilde{P} = \frac{P}{P^*}, \tag{2.28}$$

$$\tilde{T} = \frac{T}{T^*}, \tag{2.29}$$

where, ρ^*, P^* and T^* are called the characteristic parameters of the fluid system. These parameters are found by fitting the Eq. 2.26 on PVT data. Finally, r is the number of lattice sites occupied by polymer segments (or r-mers). It is given as,

$$r = \frac{MP^*}{R\rho^* T^*}, \tag{2.30}$$

where R is the universal gas constant (8.314 J/mol K). In general, SL-EOS does not follow the law of corresponding states because of the presence of r in the equation 2.26. However, for long polymer molecules $r \to \infty$. This means the term involving r vanishes and thus the law of corresponding states is satisfied. Moreover, for polymers, the SL-EOS becomes independent of the molecular weight of polymer. Physically, the characteristic temperature T^* represents the interaction energy and the characteristic pressure P^* represents the cohesive energy of the system.

This is a limited overview of SL-EOS. However, since it is central to the current research additional details on the Sanchez Lacombe model are explained later in section 2.7.

2.6.3 Hole Models

Hole models were introduced to improve cell models. Hole models are a mixture of cell models and lattice-fluid models since finite compressibility of the polymeric system is achieved by varying the cell volume as well as the number of holes (empty sites). The varying cell volume is necessary to describe the thermodynamic behaviour of the system whereas the varying number of holes plays a vital role in thermal expansion.

Simha-Somcynsky Equation of State

Simha-Somcynsky hole model [85,171,172,209] uses square-well approximation of Lennard-Jones (LJ) 6-12 potential to account for interactions between segments and face-centered

cubic for lattice geometry. Furthermore, the interactions are considered to be long-ranged [157]. Calculations from this model are based on two equations. The first equation is the Simha-Somcynsky equation of state (SS-EOS) whereas the second equation is obtained by minimizing the partition function of the model with respect to the fraction of occupied sites. These two equations are solved simultaneously to obtain PVT behaviour of the system [85, 141, 157]. For pure fluids, this model requires four fitting parameters to characterize the length of polymer molecules, external degrees of freedom, the attractive energy and the repulsive potential (excluded volume) of the model. On the other hand, for mixed polymeric systems, SS-EOS utilizes a mixing rule that is based on the average of pure component parameters weighted as per their composition in the mixture [85].

Advantages:

1. SS-EOS maintains excellent PVT data fittings over a wide range of pressure compared to other models [157].

Limitations:

1. SS-EOS requires cumbersome calculations. This is because interactions are assumed to be long-ranged, it allows variable cell volume as well as artificial vacancies. So, these factors significantly increase the required manipulation.

2.6.4 Tangent-Sphere Models

These models have been developed to present an alternative treatment of pure and mixed polymeric systems free from the artificial lattice. These models are also based on statistical mechanics. Since polymeric systems involve a large number of degrees of freedom thus simplifications are also necessary. Thus, in these models, polymer molecules are assumed like a chain of freely jointed hard spheres [17, 19, 80, 176]. Consequently, this model guarantees the presence of chain connectivity and excluded volume effects. The resulting equation is called the hard-sphere chain equation of state (HSC-EOS). In HSC EOS properties of polymer molecules are represented in terms of properties of smaller molecules *i.e.* hard-spheres.

HSC EOS is amenable to improvements by allowing the addition of perturbation terms. The perturbation terms account for the attractive forces of the system. If we assume that the attractive forces are weak and do not significantly alter the system then the perturbation terms can be approximated to van der Waals EOS *i.e.* $P = P_{HSC} + P_{pert}$. Two famous tangent sphere models are discussed below.

Statistical Associated Fluid Theory

The statistical associating fluid theory (SAFT) was proposed by Chapman *et al.* [18] based on statistical mechanics. SAFT utilizes perturbation theory to account for interactions between molecules. SAFT models use the perturbation theory of polymerization proposed by Wertheim [203]. Wertheim perturbation theory is based on the expansion of the Helmholtz free energy of the system in terms of integrals of suitable potentials and distribution functions of molecules. After the first proposal of SAFT in 1989, many versions of SAFT have been introduced.

Advantages:

1. SAFT is more accurate as compared to cubic equations of state [68].
2. SAFT EOS can be used for pure polymers as well as binary polymer-solvent mixtures [81, 213].
3. Fitting parameters of SAFT are independent of the molecular mass of polymers.

Perturbed-Chain Statistical Associated Fluid Theory

One version of SAFT is called Perturbed Chain SAFT (PC-SAFT) [67]. This model assumes polymer molecules as freely jointed spheres having a modified radial square-well potential [67] given by,

$$V(r) = \begin{cases} \infty, & \text{if } r < (\sigma - s_1) \\ 3\epsilon, & \text{if } (\sigma - s_1) \leq r < \sigma \\ -\epsilon, & \text{if } \sigma \leq r < \lambda\sigma \\ 0, & \text{if } r \geq \lambda\sigma, \end{cases}$$

where, ϵ is the attractive interaction energy, σ is the diameter of segments, and s_1 is the hardcore repulsion length. The hardcore repulsion length and diameter are related by $s_1/\sigma = 0.12$. The model requires significant computational power because the model considers accurate molecular details. The model is based on an idea that the Helmholtz free energy of the system can be expanded in terms of inverse temperature around the free energy of a reference system [66] that assumes polymer segments to be hard-spheres. Higher-order corrections are based on square-well potential to account for softcore repulsive forces of real systems. The model requires four characteristic parameters for pure fluid systems. Moreover, to extend the theory to multicomponent systems appropriate mixing rules are also required.

Advantages:

1. PC SAFT offers good predictions of phase equilibrium.
2. The model can be used for pure as well as multicomponent polymeric systems.
3. It is found to be more accurate as compared to SL-EOS [69].
4. It has excellent predictive power [67, 68, 190, 191].

Limitations:

1. Solubility predictions in binary mixtures from PC SAFT are not widely available.
2. PC-SAFT requires extensive numerical calculations and thus more powerful computers.
3. PC-SAFT requires to simultaneously solve several nonlinear equations.
4. PC-SAFT model use 24 parameters for fitting apart from three pure component characteristic parameters. However, once calculated from experimental data, those 24 parameters are considered to be universal.

2.7 Sanchez Lacombe Equation of State

2.7.1 On-Lattice SL-EOS

A brief discussion on SL-EOS is presented before in section 2.6.2 so specific details are highlighted in this section. SL-EOS was introduced by Sanchez and Lacombe in 1976 [95, 164]. Sanchez and Lacombe first developed the model for pure fluids [164] then later extended the model to multicomponent fluids [95]. Since the model is based on principles of statistical mechanics so the key step is to calculate the number of possible configurations of the system. The description of the model is as follows.

Consider a pure polymer fluid having n molecules that are divided into r segments. Since SL-EOS is a lattice-fluid theory so consider a lattice of coordination number z. Assume that each lattice site has constant volume v^* independent of temperature and pressure of the system. The lattice is considered to be rigid. Finite compression of the system is achieved via empty lattice sites. The empty lattice sites are considered to be another species that are called holes. An increase or decrease in the number of holes n_0 dictates the expansion or compression of the system. Since the lattice is rigid with a fixed site volume v^* so the volume of any species (holes or polymer segments) occupying a lattice site is also v^*. This means that the volume occupied by one polymer molecule is rv^*.

Moreover, assume that the segments of the same polymer molecule are connected. Thus, each inner segment of molecules should have $z-2$ neighbour segments of other molecules and only two neighbour segments of the same molecule. However, segments located at the ends of molecules should have $z-1$ neighbour segments of other molecules and only one neighbour segment of the same molecule. The number of possible configurations of this lattice problem had already been found by Guggenheim [70, 71] before Sanchez and Lacombe. Thus, the configuration partition function, Gibbs free energy and subsequently other thermodynamic properties can be found by using the Guggenheim's approach.

In the SL model, the interaction energy ϵ between segments of different molecules is considered to be short-ranged and constant, whereas, the interaction energy between segments of the same chain is neglected. Finally, holes are artificial so they do not offer any interaction. Thus the total interaction energy ϵ^* per segment is found to be $\epsilon^* = z\epsilon/2$. Note that the same energy, ϵ^*, is also required to create one hole in the system. Thus the model has three characteristic parameters v^*, r, and ϵ^* that completely define a pure polymeric system. These characteristic parameters are called molecular parameters since they depend on microscopic details of molecules. However, the same information can be presented in terms of macroscopic (thermodynamic) parameters P^*, T^*, and ρ^*(or V^*) by using the following definitions,

$$P^* \equiv \frac{\epsilon^*}{v^*}, \tag{2.31}$$

$$T^* \equiv \frac{\epsilon^*}{k_B}, \tag{2.32}$$

$$\rho^* \equiv \frac{M}{rv^*} \qquad or \qquad V^* \equiv rnv^*, \tag{2.33}$$

where M is the molecular mass of the polymer.

Extension of the model to the multicomponent system is straightforward [95] except for one problem. For instance, if we have two pure fluids A and B with corresponding hole volumes v_A^* and v_B^*. Suppose these two pure fluids are then mixed to have a binary mixture. Now the problem is that there is no *ab initio* method to determine the hole volume v^* of the resulting mixture. To deal with this problem Sanchez and Lacombe proposed a mixing rule [95] to calculate mixture hole volumes from pure component hole volumes. The mixing rule was based on the conservation of the lattice volume of each pure system and the conservation of the number of pair interactions in each pure system. The assumption of conserved lattice volume ensures that the number of lattice sites occupied by molecules of

each species remains the same before and after mixing. The resulting expression of mixture hole volume was found to be the composition-weighted-average of holes volumes of pure systems. The weighted average also ensures that the mixture hole volume limits correctly to corresponding hole volumes of pure fluids in the limit of vanishing composition of all other components. There are other mixing rules mentioned in the literature, for instance, Ref. [1, 144].

Regression:

For pure fluids, SL-EOS requires three fitting parameters P^*, T^* and ρ^* (or equivalently, ϵ^*, v^* and r) that are obtained by fitting SL-EOS 2.26 on PVT data [164]. Alternatively, for solvents (small molecules) in the gaseous phase, molecular parameters (*i.e.* ϵ^*, v^* and r) can be determined by using vapour pressure data. However, for multicomponent mixtures, binary interaction energies $\epsilon^*_{ij}(i \neq j)$ are also required. These binary interactions energies are usually determined by using solubility and/or swelling data of binary mixtures [95].

Advantages:

1. SL-EOS works reasonably well to predict the PVT behaviour of fluids.
2. SL model can make accurate predictions of thermal expansivity and isothermal compressibility.
3. SL-EOS can predict binodal and spinodal curves as well as upper and lower critical solution temperatures [165].
4. It can be used for supercritical fluids [197].
5. SL-EOS also offers reasonable predictions for ternary mixtures.
6. SL-EOS gives excellent predictions of solubility of solvent fluids in polymer liquids [158, 166]
7. SL model can also be used to predict other thermodynamic properties besides PVT properties.
8. Only three characteristic parameters P^*, T^* and ρ^* are required to make predictions.
9. SL model can predict the phase behaviour of multicomponent fluids [163].

Limitations:

1. SL-EOS is a lattice-fluid model so it cannot be used for solid and glassy polymers.

2. SL model avoids internal degrees of freedom of molecules especially vibrational and rotational degrees of freedom. Thus, SL-EOS cannot predict heat capacities of fluid because the neglected degrees of freedom absorb significant heat [129]. These degrees of freedom only depend on the temperature of the system and thus do not affect the PVT behaviour of the system.
3. SL model cannot predict glass transition and retrograde vitrification behaviour of binary mixtures because the model ignores the finite flexing energy of molecules [23].
4. SL-EOS is not able to make accurate predictions near the critical point of fluids. This is because the mean-field approximation does not remain valid near second-order phase transitions. Thus, Sanchez and Lacombe avoided fittings on PVT data near the critical point of fluids by about $15 - 20^0$ C [95].
5. SL-EOS is not accurate to describe PVT data over a wide range of pressure [157].
6. SL-EOS requires arbitrary mixing rules for multicomponent mixtures. Thus it has troublesome inconsistencies stemming from the change in reference values [124]. Moreover, these thermodynamic inconsistencies cannot be fixed [197].
7. SL-EOS is not accurate to predict the behaviour of binary polymer-solvent mixtures.

Inconsistencies and Corrections:

As discussed, for multicomponent mixtures, arbitrary mixing rules are unavoidable due to differing hole volumes of pure phases. These mixing rules are not derived from *ab initio* principles of statistical mechanics because significant molecular details are required to achieve this task. On the other hand, the use of arbitrary mixing rules makes the SL model inconsistent because of changes in reference values. In 2002, these inconsistencies were first highlighted by Neau [124] by arguing that the reference zero of chemical potential tends to change due to variable mixture hole volume and thus phase equilibrium calculations from SL-EOS are not correct. She proposed that the phase equilibrium should be calculated by using fugacities (a thermodynamic property that measures the tendency of a component in liquid mixture to escape from the mixture) instead of chemical potentials. Her proposal was based on the argument that the partition function of the SL model is, in fact, a configurational partition function that is different from the canonical partition function. Thus, to make the model correct an additional partition function $Q_{int}(T, n_0, \{n_i\})$ that depends only on internal degrees of freedom should be multiplied with the configurational partition function.

In 2017, von Konigslow *et al.* [197] showed that the correction proposed by Neau contains a problem that makes her correction implausible. The Neau correction was based on a critical assumption that the number of holes n_0 in the system is independent of the volume of the system. However, due to the incompressibility of lattice, the number of holes must depend on the volume of system *i.e.* $n_0 = n_0(V)$ because the number of holes dictates expansion of the system. Consequently, the partition function proposed by Neau should result in a different equation of state.

Assumptions:

The model proposed by Sanchez and Lacombe has two major simplifications.

1. It is based on an artificial lattice *i.e.* molecular segments are only allowed to take specific positions in the system.
2. Molecules are considered to be infinitely flexible *i.e.* there is no energy plenty associated with the flexing of molecular segments.

The first assumption had been addressed in 2017 when SL-EOS was re-derived by using an off-lattice model Ref. [197]. Thus, the off-lattice SL model is discussed below.

2.7.2 Off-Lattice SL-EOS

Since the original SL-EOS is based on artificial lattice so von Konigslow *et al.* proposed an off-lattice treatment to derive SL-EOS [197]. The present research is an extension of this off-lattice SL model so the specific details of the model are outlined with the proposed model in chapter 3. Thus here only a rudimentary outline is presented. The main features of the off-lattice SL-EOS are the same as on-lattice SL-EOS. The off-lattice model also divides polymer molecules into small segments having finite constant volume, segment-segment interactions are assumed to be short-ranged and constant, artificial holes are also included to account for finite thermal expansion of the system. The holes are assumed to be a distinct chemical species that offer no interactions. The volume of holes is also assumed to be constant so the volume of the system is controlled by the number of holes in the system. Following the original SL model, this model also ignores the rotational and vibrational degrees of freedom. Moreover, the model does not focus on structural details of molecules and their finite flexibility. Apart from the model, there are also novel peripheral technical arguments made by von Konigslow *et al.* [197]. For instance, to avoid inconsistencies in the multicomponent mixtures von Konigslow *et al.* assumed mixture hole volume to be constant at all compositions while the original SL model assumes that the mixture hole volume is a function of the composition of constituting species.

Advantages:

The advantages of this model are the same as that of the on-lattice model. However, advantages particularly important for the present work are re-mentioned below,

1. The model is successful in predicting the phase behaviour of binary polymer-solvent mixtures.
2. Holes volumes are assumed to be constant and arbitrary mixing rules are discarded.
3. The model successfully predicts solubility of binary and ternary polymer-solvent mixtures.
4. The off-lattice SL model fits swelling data with moderate accuracy.
5. The model is equally applicable to polymers as well as solvents in the fluid phase.

Limitations:

The limitations of this model are the same as that of the on-lattice model. However, limitations particularly important for the present work are re-mentioned below,

1. SL model avoids internal degrees of freedom of molecules, especially vibrational and rotational degrees of freedom of polymer segments. Thus, SL-EOS cannot predict heat capacities of fluids because the neglected degrees of freedom absorb significant heat [129]. These degrees of freedom only depend on the temperature of the system and thus do not affect the PVT behaviour of the system.
2. SL model cannot predict glass transition and retrograde vitrification behaviour of polymers because the model ignores the finite flexing energy of polymer molecules [23].

Since the off-lattice model was not generalized to incorporate finite flexibility of polymer molecules so the primary focus of the present research is to accomplish this generalization. The flexibility of molecules plays a significant role in the determination of glass transition and retrograde vitrification behaviour of polymers. Thus, the success of the proposed model is examined by predicting the glass transition temperature versus pressure behaviour of pure polymeric systems and the retrograde vitrification behaviour of binary solvent-polymer mixtures. The infinitely flexible off-lattice SL model [197] is incapable of predicting these behaviours.

The literature discussed above covers only one aspect of the present work. Since the goal of the research is to predict the glass transition temperature versus pressure behaviour of polymeric systems thus an overview of glass transition theories is also necessary.

2.8 The Glass Transition

The true nature of the glassy state and the physics of glass formation are still unknown so it is an active area of research. Researchers usually define glass transition based on two competing perspectives. One perspective assumes that the glass transition is a thermodynamic second-order transition while the other perspective assumes that the glass transition is a kinetic phenomenon [64, 77, 183]. The glass transition temperature is usually denoted by T_g.

It is observed that for polymeric systems the behaviour of V-T curves at constant pressure departs from equilibrium line at a temperature where the characteristic time of molecular motion becomes greater than the time scale of experiments [116]. This change in the behaviour of systems from liquid to glassy also affects the thermodynamics of systems, especially, heat capacities of systems show a discontinuous behaviour at their glass transition temperatures [16]. The values of heat capacities suddenly drop across glass transitions and the changes in heat capacities are *not* found to be a function of the time-scale of experiments. Consequently, along with kinetic reasons glass transitions should also involve thermodynamic transitions. When a glassy state is obtained by cooling a polymer liquid the non-equilibrium glassy state slowly evolves towards an equilibrium volume of the system. This also accompanies changes in the mechanical properties (for instance creep compliance) of the system [97]. This phenomenon is called physical ageing. The kinetics of glass transitions is beyond the scope of this study. Thus, only the thermodynamics of glass transitions is discussed below.

2.8.1 The Kauzmann Paradox

Kauzmann paradox [88] is central to study the thermodynamics of glassy states. In 1948, Kauzmann showed that for glass-forming substances extrapolation of thermodynamic properties of supercooled liquids to low temperatures (but above 0K) result in values less than the corresponding values of their thermodynamically stable crystalline solids [88]. This trend was not specific to entropy but other thermodynamic properties like volume, enthalpy, etc. also revealed this anomalous behaviour. Consequently, he argued that the glass transition cannot be thermodynamic. Thus, he presented an alternative explanation of the glass transition by extending the liquid model of Mott and Gurney [122]. The model assumes liquid states as being composed of small crystallites. The orientation of crystallites is assumed to be the driving force of the entropy of the system that in turn drives the glass formation of the system. As a result, the model revealed that at a certain temperature the rate of crystallization of supercooled liquids decreases to an extent at which the time required for crystallization exceeds experimental time scales *i.e.* glassy

state is achieved. Thus, the temperature was termed as the pseudo-critical temperature. The model was successful to explain the experimental observation that thermodynamic properties of liquid state when extrapolated to low temperatures become smaller than corresponding crystalline state values. Despite the Kauzmann argument that glass transition is a purely kinetic phenomenon there is still significant debate in the physics community over the thermodynamic interpretation of glass formation.

2.8.2 Glass Transition Versus Second-Order Transition:

The behaviour of thermodynamic properties at glass transition temperatures shows a discontinuity in heat capacity while volume, entropy and enthalpy remain continuous [154]. Thus, glass transitions can be characterized as second-order transitions with an exception that true second-order transition temperatures do not depend on the time scale of experiments, however, glass transition temperatures decrease with the increasing time scale of experiments.

Prigogine-Defay [29] derived a ratio to check the validity of the claim that the glass transition is a second-order thermodynamic transition. It is given as,

$$R = \frac{\Delta k \Delta C_P}{TV(\Delta\alpha)^2} = 1, \tag{2.34}$$

where $R = 1$ corresponds to the second-order transition. It is observed that if thermodynamic data of glasses having the same glass formation histories is utilized then the ratio is indeed equal to be 1. However, if thermodynamic data of glasses having different glass formation histories is utilized then the ratio does not become equal to 1 [60, 117, 138]. Besides, the glass transition temperature also depends on the path of glass formation (*i.e.* heating or cooling) [116]. In short, even though the glass transition is a kinetic phenomenon there are possibilities to work on the glass transition as if it is a pure thermodynamic second-order transition.

2.8.3 Gibbs DiMarzio Theory

Gibbs-DiMarzio theory [35, 61, 62] offers a solution to the Kauzmann paradox [88]. It is based on the Flory-Huggins lattice theory of polymer mixtures [48, 83]. The theory takes several factors into consideration including chain connectivity, chain stiffness and degree of polymerization (chain length). The model considers n number of polymer chains of a degree of polymerization x on a lattice with coordination number z. The lattice has n_0

holes (or vacant sites). The energy required to create a hole is assumed to be proportional to the bond energy because it is assumed that the creation of holes results in broken intermolecular bonds. Two energy states, flexed and unflexed, are also considered to account for the shape of molecules. The unflexed state is assumed to have energy ϵ_1 and the flexed state is assumed to have energy ϵ_2. Thus, the required energy to flex a bond from its lowest state is $\Delta\epsilon = \epsilon_2 - \epsilon_1$. The fraction of bonds in the flexed state is assumed to be f. The fraction of flexed bonds f and the number of holes n_0 are assumed to be functions of energies [33]. The partition function of the model was calculated by using the Flory-Huggins method [118].

Consequently, the model revealed that [35, 61, 62] the configurational entropy of the system becomes zero at a second-order thermodynamic transition temperature T_2. This implies that extrapolation of thermodynamics variables from temperatures above the glass transition to temperatures below the glass transition is not allowed because the second-order transition at temperature T_2 causes a discontinuity in the corresponding thermodynamic variables (*i.e.* $S-T$ curve). This provides a solution to Kauzmann paradox [88] because it explains the Kauzmann observations by using thermodynamic arguments instead of kinetic arguments.

The decrease in configurational entropy of the model with the decreasing temperature is due to two reasons. First, as temperature decreases the volume of the system decreases. This implies that the number of holes in the system should decrease thus entropy should also decrease. Second, decreasing temperature results in the decreasing number of flexed bonds thus entropy of the system should decrease.

Gibbs and DiMarzio argued that the temperature T_2 corresponds to the glass transition temperature T_g [35, 61, 62]. In other words, the Gibbs DiMarzio theory asserts that glassy state is a state of matter for the case of non-crystallizing materials, just like solid, liquid or gas state. Thus kinetically measured glass transition temperature T_g corresponds to thermodynamic second-order transition temperature T_2 where configurational entropy of the system becomes zero. This is called the *Gibbs-DiMarzio criterion*. Gibbs-DiMarzio theory is found to be in excellent agreement with experimental data [143]. Besides, predictions of the change in heat capacities across glass transitions from Gibbs DiMarzio theory are also compared with experimental data by several authors Refs. [11, 76]. Moreover, since the model does not incorporate lattice vibration so DiMarzio and Dowell [34] later added a term to accommodate lattice vibration effects.

2.8.4 Free Volume Theory and Simha-Somcynsky Hole Model

Free volume theory was initially proposed to explain the dependence of viscosity of liquids on temperature [8, 38]. Later, the theory was then extended to discuss polymer melts [54, 55, 57, 204]. Williams, Landel and Ferry [204] developed an empirical relation, called the WLF equation, by allowing the free volume to have a linear dependence on temperature. WLF equation was capable of predicting changes in viscoelastic properties of polymers above glass transition temperatures. WLF equation predicts a steep increase in viscosity of polymers near glass transition temperatures. This indicates that free volume influences the mobility of liquids that in return defines the glass transition behaviour of polymers [116]. Later, WLF model has been further extended to account for pressure dependence of glass transition [46, 119–121]. WLF equation was found to have excellent predictions over a wide range of temperatures and pressures but there are still some exceptions [94]. Therefore, the significance of free volume in glass transitions is not well-established. The criticism on free volume theory is based on the fact that there is no clear definition of free volume in the WLF equation and the free volume is also treated as a fitting parameter in the equation [38–40, 116]. However, equations similar to the free volume theory can also be derived by using the Gibbs-DiMarzio model of configurational entropy.

Kauzmann paradox can also be resolved by using the argument that molecular mobility depends on the free volume of the system as follows. Suppose the free volume of a system is decreased by decreasing the temperature of the system. Since decreasing free volume also decrease molecular mobility, thus at some point, the time for molecular rearrangement should exceed the time scale of experiments. Consequently, equilibrium cannot be achieved [116]. Moreover, since the viscosity of the system dictates the time required for rearrangement of molecules, therefore, the free volume model correctly predicts infinite viscosity at zero free volume. Thus, the free volume concept offers a solution to the Kauzmann paradox based on the kinetic explanation.

Several ideas have been developed to quantitatively explain free volume on a molecular basis [64, 77, 183]. For instance, Simha-Somcynsky hole model [172, 175] as already discussed in section 2.6.3 offers a quantitative definition of free volume. In that section, the emphasis was given on the PVT behaviour of fluids. However, SS-EOS has a much broader application as it can be used for the glassy state and describes glass transition as a kinetic phenomenon. Unfortunately, the SS model cannot accurately predict entropy and energy of the system. Consequently, predictions of the heat capacity of liquid and glassy polymers from the SS model are also poor [64, 116].

2.8.5 The Condo Model

In 1992, Condo *et al.* [23] presented a model to predict glass transition temperature versus pressure behaviour of pure polymers and binary mixtures. The model combines lattice-fluid model [50,134,135,164,165] and Gibbs DiMarzio criterion [36,62] into a single theory to predict glass transition temperatures. In the Condo model, the entropy of polymeric systems also becomes negative at sufficiently low but finite temperatures. Thus, following Gibbs DiMarzio, Condo *et al.* also argued that the negative entropy indicates the onset of glass transitions in polymeric systems. Consequently, by using the Gibbs DiMarzio criterion they predicted the glass transition temperature versus pressure behaviour of polymeric systems. Moreover, several authors including Condo *et al.* [23] have argued that theoretical models predict *ideal* glass transition temperatures that can only match with infinitely slow cooling experiments, however, in reality, experiments are performed at finite cooling rates. Thus, ideal/theoretical glass transition temperatures tend to be lower than experimental glass transition temperatures [37]. To ignore this problem, Condo assumed that the relation between entropy and theoretical glass transition temperature is the same as the relation between entropy and experimental glass transition temperature. A broad overview of the Condo model is discussed below.

In section 2.7 it was highlighted that the lattice-based SL model is based on two assumptions. The second assumption, *i.e.* polymer molecules are infinitely flexible, is not present in the Condo model. However, the first assumption of artificial lattice still persists in the Condo model. In fact, the Condo model [23] also yields SL-EOS, so it can be regarded as an extension of lattice-fluid SL model that considers polymer molecules to be finitely flexible. To account for finite flexibility of polymer molecules, the Condo model assigns two energy states, a ground unflexed state of zero energy and an excited flexed state of energy ϵ_k of molecules of species k. In the model only two species were assumed with $k = 1, 2$. Designate the number of molecules of species k by n_k and divide each molecule of species k into N_k segments (or mers). The lattice coordination number is z and the number of holes (empty sites) in the lattice are n_0. By using the mean-field approximation and assuming a large coordination number limit, Condo *et al.* calculated the number of configurations and thus the Gibbs free energy G of the system. A new parameter f_k was also introduced in the model to represent the fraction of segments in the excited/flexed state. Since molecules have $r_k - 2$ bonds so the number of bonds in the excited state are $f_k(r_k - 2)$ and the number of bonds in the ground state are $(1 - f_k)(r_k - 2)$. The model defines reduced density (*i.e.* fraction of occupied states) as,

$$\tilde{\rho} = \frac{N_1 n_1 + N_2 n_2}{n_0 + N_1 n_1 + N_2 n_2} \equiv \frac{nN}{n_0 + nN}, \tag{2.35}$$

where,

$$n = n_1 + n_2, \tag{2.36}$$
$$x_k = \frac{n_k}{n}, \tag{2.37}$$
$$N = x_1 N_1 + x_2 N_2. \tag{2.38}$$

The model also defines composition fraction ϕ_k as,

$$\phi_k = \frac{N_k n_k}{Nn}, \tag{2.39}$$
$$\frac{1}{N} = \frac{\phi_1}{N_1} + \frac{\phi_2}{N_2}. \tag{2.40}$$

Since, the lattice has coordination number z so the flexed state can have $z-2$ degenerated states of the same energy ϵ_k whereas the unflexed state is non-degenerate. In pure systems, the energy required to generate a vacancy is assumed to be ϵ^*_{kk}. For binary mixtures, binary interaction parameters are also introduced as,

$$\epsilon^*_{12} = \zeta_{12}(\epsilon^*_{11}\epsilon^*_{22})^{1/2}, \tag{2.41}$$
$$X_{12} = \frac{\epsilon^*_{11} + \epsilon^*_{22} - 2\epsilon^*_{12}}{k_B T}. \tag{2.42}$$

Thus, the energy required to create a vacancy in binary mixtures under the mean-field approximation is,

$$\epsilon^* = \phi_1 \epsilon^*_{11} + \phi_2 \epsilon^*_{22} - \phi_1 \phi_2 k_B T X_{12}. \tag{2.43}$$

At equilibrium, the fraction of excited bonds are,

$$f_k = \frac{(z-2)e^{-\epsilon_k/k_BT}}{1+(z-2)e^{-\epsilon_k/k_BT}}. \tag{2.44}$$

The volume of each lattice site of pure systems of species $k = 1, 2$ is assumed to be v_k^*. In addition, following mixing rule is also assumed to give the volume v^* of lattice site of binary mixture,

$$v^* = \phi_1 v_1^* + \phi_2 v_2^*. \tag{2.45}$$

Thus the volume of binary mixture is,

$$V = (n_0 + Nn)v^*. \tag{2.46}$$

With these assertions the energy of binary mixture is found to be,

$$E = -Nn\tilde{\rho}\epsilon^* + n_1(N_1-2)f_1\epsilon_1 + n_2(N_2-2)f_2\epsilon_2. \tag{2.47}$$

The entropy of binary mixture is found to be,

$$\begin{aligned} -\frac{S}{k_B} = Nn\Bigg[&(\tilde{v}-1)\ln(1-\tilde{\rho}) + \frac{\ln\tilde{\rho}}{N} + \left(\frac{\phi_1}{N_1}\right)\ln\left(\frac{\phi_1}{N_1}\right) + \left(\frac{\phi_2}{N_2}\right)\ln\left(\frac{\phi_2}{N_2}\right) + 1 + \frac{\ln(2/z)-1}{N} \\ &+ \left(\frac{\phi_1}{N_1}\right)(N_1-2)\left\{\ln(1-f_1) - f_1\frac{\epsilon_1}{k_BT}\right\} + \left(\frac{\phi_2}{N_2}\right)(N_2-2)\left\{\ln(1-f_2) - f_2\frac{\epsilon_2}{k_BT}\right\}\Bigg]. \end{aligned} \tag{2.48}$$

For binary solvent-polymer mixture with solvent (small molecules) denoted as species $k = 1$, the chemical potential of solvent μ_1 in mixed-phase is [23, 165],

$$\frac{\mu_1}{k_BT} = \ln\phi_1 + \left(1-\frac{N_1}{N_2}\right)\phi_2 + N_1\tilde{\rho}X_{12}\phi_2^2 + N_1\left[\frac{(-\tilde{\rho}+\tilde{P}_1\tilde{v})}{\tilde{T}_1} + (\tilde{v}-1)\ln(1-\tilde{\rho}) + \frac{\ln\tilde{\rho}}{N_1}\right], \tag{2.49}$$

where, $\tilde{v} = 1/\tilde{\rho}$, $\tilde{P}_1 = P/P_1^*$, and $\tilde{T}_1 = T/T_1^*$. To obtain the chemical potential of solvent in the pure solvent phase set $\phi_2 = 0$,

$$\frac{\mu_1^0}{k_B T} = N_1 \left[\frac{(-\tilde{\rho}_1 + \tilde{P}_1 \tilde{v}_1)}{\tilde{T}_1} + (\tilde{v}_1 - 1) \ln (1 - \tilde{\rho}_1) + \frac{\ln \tilde{\rho}_1}{N_1} \right], \tag{2.50}$$

where, $\tilde{\rho}_1 = \rho/\rho_1^*$, and $\tilde{v}_1 = 1/\tilde{\rho}_1$. The condition of chemical equilibrium implies $\mu_1 = \mu_1^0$. The Condo model assumes solvent molecules to be infinitely flexible *i.e.* $\epsilon_1 = 0$. Moreover, for binary mixtures, Condo *et al.* argued that mixture entropy becomes zero at the glass transition temperature by following the Gibbs DiMarzio model [36]. However, some authors tend to assume that for binary mixtures the pure polymer entropy will be zero [24] at the glass transition temperature.

The pure-component characteristic parameters P_k^*, T_k^* and ρ_k^* can be determined by using PVT data of pure systems. For polymer species ($k = 2$) the value of z and ϵ_2 are regressed by using two experimental values, *i.e.* the glass transition temperature T_g at atmospheric pressure and the slope of $T_g(P)$ curve (*i.e.* dT_g/dP). By using these two values a straight line can be plotted in the $T_g(P)$ domain. On the other hand, the theoretical $T_g(P)$ relation can be obtained by setting $S(T_g) = 0$ in Eq. 2.48. Thus, regression for z and ϵ_2 can be carried out by fitting the $T_g(P)$ relation on the straight line in $T_g(P)$ domain. Finally, to obtain ζ_{12} solubility data is used by Condo *et al.* [23]. Theoretical solubility is calculated by simultaneously solving the condition of chemical equilibrium $\mu_1 = \mu_1^0$, the SL-EOS in pure solvent phase and the SL-EOS in mixed-phase.

Thus, Condo *et al.* identified four fundamental $T_g(P)$ behaviours in binary solvent-polymer mixtures as a function of the solubility of solvents in mixed-phase, the flexibility of polymer molecules, and the critical temperature of solvents. They also argued that the $T_g(P)$ behaviours of binary mixtures mainly depend on the binary interaction energy coefficient ζ_{12} and the critical temperature of solvents.

Advantages:

1. The model successfully describes thermodynamic properties and phase equilibrium of binary solvent-polymer mixtures.
2. The model correctly predicts depression of the glass transition temperature of polymers as a function of the pressure of solvents in the liquid, gas or supercritical phase [22].

3. Model predicts four different types of $T_g(P)$ behaviours of binary mixtures including retrograde vitrification phenomenon.
4. The retrograde vitrification phenomenon has been proved through experiments on the binary PMMA/CO_2 mixture [21].
5. The Condo model correctly predicts the dependence of glass transition temperature on the sorption of solvent in polymers.
6. To regress unknown parameters for pure polymeric systems the model requires only two experimental values, *i.e.* T_g at atmospheric pressure and dT_g/dP.

Limitations:

1. It is based on an artificial lattice.
2. The equation of entropy of the Condo model depends on the lattice coordination number. Since the lattice is artificial so the model is exposed to serious criticism from the physics community.
3. It was found that at high coordination numbers entropy ceases to become negative. This violates the Gibbs DiMarzio criterion [6, 206, 207].
4. The model can only be used for polymers having linear $T_g(P)$ behaviour.
5. Significant $T_g(P)$ data is required to evaluate the correct value of dT_g/dP.

The Condo model inspires to extend the off-lattice SL model by von Konigslow *et al.* [197] in a similar fashion. In this manner, the resulting model will be free from the assumptions of artificial lattice and infinitely flexible molecules. The proposed model should be capable of predicting the glass transition temperature versus pressure and retrograde vitrification behaviour of polymeric systems. Consequently, in this work, a detailed comparison has been presented between the proposed model and the Condo model.

Moreover, since several authors [6, 206, 207] have argued that the Gibbs DiMarzio criterion is a consequence of using artificial lattice because at sufficiently high lattice numbers the entropy of the system ceases to become negative thus with the proposed model the validity of this claim can be examined.

Chapter 3

Theory

3.1 Introduction

To derive thermodynamic properties of polymeric systems based on principles of statistical mechanics the first step is to hypothesize a simplified model of the real system. To accurately describe real polymeric systems a huge number of parameters are usually required. However, many features of the system tend to produce only a minor effect on thermodynamic properties so they can be neglected. Furthermore, if one is only interested to predict the properties within a certain range of conditions then several additional details of the system can be approximated to further simplify the model. The knowledge of what factors significantly influence the properties of the system and what factors do not contribute and thus can be neglected comes from experiments, by studying prior models in the literature, and even a result of educated guesses. Such simplifications are necessary to simplify analytical, computational manipulations, to reduce the amount of experimental data needed to regress fitting parameters of the model, to provide straight insight on the physics of the system, and to easily guess the response of the system. Once an appropriate model is identified, the next step is to derive an expression of the partition function of the system by using combinatorics. Then, from the partition function, other thermodynamic properties can be derived by using appropriate partial derivatives of the partition function [186].

To calculate partition functions of models, the number of possible states of systems needs to be evaluated. Even with a simplified model, more approximations are usually required based on standard combinatorics rules. This task is especially difficult for amorphous systems. However, if one assumes that the polymeric fluids have crystalline structures the calculation greatly simplifies but at the cost of the accuracy of predictions from the

model because the number of possible states in amorphous fluids is significantly higher than the number of possible states in lattice fluids [112]. Finally, the assumptions of the model can be verified by analyzing the accuracy of predictions from the model as well as by critically examining that the results obey all fundamental principles of thermodynamics. From past literature, it is obvious that lattice fluid models are indeed reasonably accurate and powerful enough to capture the physics of some systems. However, in 2017, von Konigslow [197] proposed an off-lattice treatment of polymer fluids. The model was successful in re-deriving the Sanchez Lacombe equation of state by using a continuum statistical model. Thus, the present research is inspired by the off-lattice model. For SL models, it is a usual practice to separately discuss pure polymeric systems and multicomponent systems because multicomponent systems require mixing rules that are responsible for thermodynamic inconsistencies in multicomponent models, however, pure fluid models are free from any inconsistency [95, 164, 165, 195, 197]. Thus, the same practice is followed in the present work.

In addition, the aim of the present work is to predict the glass transition temperature versus pressure behaviour of pure polymeric systems and binary polymer-solvent mixtures as discussed in chapter 2. Thus, the present model proposes to extend the off-lattice SL-EOS [197] to the case of semi-flexible molecules. This extension is inspired by the lattice-fluid model of Condo *et al.* [23]. In the off-lattice SL-EOS, it was assumed that molecules can take any configuration without any constraint on their shapes. Thus, molecules had no stiffness. However, now, in this model, it is assumed that each segment of molecules can be in two states of stiffness, the ground state having zero energy and the excited state having a finite value of energy. The excited state is also considered to be degenerate *i.e.* multiple states with equal energies. Moreover, to take account of finite compressibility of the fluid system it is assumed that the fluid system also contains artificial holes (or vacancies) that offer no interactions.

3.2 Description of Model for Multicomponent Fluid Mixtures

Consider a multicomponent system at pressure P, volume V and temperature T. Let n_0 be the number of vacancies (or holes) in the system and n_k be the total number of molecules of species k. Each molecule of species k is divided into N_k segments with each segment having volume v_k. Since holes cannot be divided so for holes $N_0 = 1$ while v_0 is the volume of each hole. To account for the finite flexibility of molecules assign internal degrees of freedom (called flexing states) to each segment of all molecules of the system. Let $\Omega_{s,i}$ be

the flexing state of the i^{th} segment of a molecule of species k. Also, denote the set of all the flexing states of all segments of all molecules of all species k excluding holes by $\{\Omega_{s,k\neq 0}\}$. Moreover, let $\mathbf{r}_{s,i}$ be the position of the i^{th} segment of a molecule of species k and denote the set of all the positions of all segments of all molecules of all species k excluding holes by $\{\mathbf{r}_{s,k\neq 0}\}$. Consequently, the potential energy $U(\{\mathbf{r}_{s,k\neq 0}\},\{\Omega_{s,k\neq 0}\})$ will be a function of the positions of all segments $\{\mathbf{r}_{s,k\neq 0}\}$ and the flexing states of all segments $\{\Omega_{s,k\neq 0}\}$. Finally, let $\mathbf{p}_{i,k}$ be the momentum the center of mass of the i^{th} molecule of species k and denote the set of all the momentums of the centers of mass of all molecules of all species k excluding holes by $\{\mathbf{p}_{k\neq 0}\}$.

3.3 Hamiltonian of Multicomponent Model

The Hamiltonian $H \equiv H(\{\mathbf{p}_{k\neq 0}\},\{\mathbf{r}_{s,k\neq 0}\},\{\Omega_{s,k\neq 0}\})$ of the system discussed in section 3.2 will be,

$$H = \sum_{k}\sum_{i=1}^{n_k} \frac{\mathbf{p}_{i,k}^2}{2m_k} + U(\{\mathbf{r}_{s,k\neq 0}\},\{\Omega_{s,k\neq 0}\}). \tag{3.1}$$

The first term in the above expression is the kinetic energy of molecules and the second term is the potential energy of the system that arises due to interactions and stiffness of molecules, m_k is the molecular mass of k^{th} species and $\mathbf{p}_{i,k}$ is the momentum of center of mass of the i^{th} molecule of species k, while the sum is over all n_k molecules of species k.

The instantaneous volume fraction operator $\hat{\phi}_k(\mathbf{r})$ of species k will depend on positions of segments $\{\mathbf{r}_s\}$ and flexing state of segments $\{\Omega_s\}$ of molecules.

$$\hat{\phi}_k(\mathbf{r},\Omega) \equiv v_k \sum_{i=1}^{N_k n_k} \delta(\mathbf{r}-\mathbf{r}_{s,i})\delta(\Omega-\Omega_{s,i}), \tag{3.2}$$

where $\mathbf{r}_{s,i}$ is the position and $\Omega_{s,i}$ is the flexing state of the i^{th} segment of a molecule of species k and sum is over all $N_k n_k$ segments of that species. v_k is the volume of one segment of species k. Assume that holes and molecules completely fill the volume of the system, therefore,

$$\sum_{k}^{0} \hat{\phi}_k(\mathbf{r},\Omega) = 1, \tag{3.3}$$

where the superscript 0 over the sum indicates that holes are included in the summation. Assume that the potential $U(\{\mathbf{r}_{s,k\neq 0}\},\{\Omega_{s,k\neq 0}\})$ can be split into two parts, one part is the

potential due to position of segments $U_1(\{\mathbf{r}_{s,k\neq 0}\})$ while other part is the potential due to flexing of segments $U_2(\{\Omega_{s,k\neq 0}\})$,

$$U(\{\mathbf{r}_{s,k\neq 0}\},\{\Omega_{s,k\neq 0}\}) = U_1(\{\mathbf{r}_{s,k\neq 0}\}) + U_2(\{\Omega_{s,k\neq 0}\}). \tag{3.4}$$

Lets expand these potentials in the following manner,

$$U_1(\{\mathbf{r}_{s,k\neq 0}\}) = \frac{1}{2}\sum_{k''k'}\sum_{i=1}^{N_{k'}n_{k'}}\sum_{j=1}^{N_{k''}n_{k''}} u_{1,k''k'}(|\mathbf{r}_{s,i}-\mathbf{r}_{s,j}|), \tag{3.5}$$

$$U_2(\{\Omega_{s,k\neq 0}\}) = \sum_k f_k \sum_{i=1}^{N_k n_k} u_{2,k}(\Omega_{s,i}), \tag{3.6}$$

In above expression of $U_2(\{\Omega_{s,k\neq 0}\})$ we have multiplied the summation over the k^{th} species with the fraction of flexed segments f_k of that species because only excited segments will contribute to $U_2(\{\Omega_{s,k\neq 0}\})$. Thus, Eq. 3.4 becomes,

$$U(\{\mathbf{r}_{s,k\neq 0}\},\{\Omega_{s,k\neq 0}\}) = \frac{1}{2}\sum_{k''k'}\sum_{i=1}^{N_{k'}n_{k'}}\sum_{j=1}^{N_{k''}n_{k''}} u_{1,k''k'}(|\mathbf{r}_{s,i}-\mathbf{r}_{s,j}|) + \sum_k f_k \sum_{i=1}^{N_k n_k} u_{2,k}(\Omega_{s,i}). \tag{3.7}$$

Following von Konigslow *et al.*, $U_1(\{\mathbf{r}_{s,k\neq 0}\})$ can be written in terms of volume fraction operators as,

$$U_1(\{\mathbf{r}_{s,k\neq 0}\}) = \frac{1}{2}\sum_{k''k'}\frac{1}{v_{k''}v_{k'}}\int d\Omega d\Omega' d\mathbf{r} d\mathbf{r}' \hat{\phi}_{k''}(\mathbf{r},\Omega) u_{1,k''k'}(|\mathbf{r}-\mathbf{r}'|)\hat{\phi}_{k'}(\mathbf{r}',\Omega'). \tag{3.8}$$

In addition, expand $U_2(\{\Omega_{s,k\neq 0}\})$ in terms of volume fraction operators as,

$$U_2(\{\Omega_{s,k\neq 0}\}) = \sum_k \frac{f_k}{v_k}\int d\Omega d\mathbf{r}\hat{\phi}_k(\mathbf{r},\Omega)u_{2,k}(\Omega). \tag{3.9}$$

Before moving forward, we can first verify Eqs. 3.8 and 3.9. Consider $U_1(\{\mathbf{r}_{s,k\neq 0}\})$ in equation 3.8 and substitute the expression of volume fraction operator $\hat{\phi}_k(\mathbf{r},\Omega)$ from Eq. 3.2,

$$\begin{aligned} U_1(\{\mathbf{r}_{s,k\neq 0}\}) = \frac{1}{2}\sum_{k''k'}\frac{\cancel{v_{k''}}\cancel{v_{k'}}}{\cancel{v_{k''}}\cancel{v_{k'}}}\sum_{i=1}^{N_{k'}n_{k'}}\sum_{j=1}^{N_{k''}n_{k''}}\int d\Omega d\Omega' d\mathbf{r} d\mathbf{r}' \delta(\mathbf{r}-\mathbf{r}_{s,i})\delta(\Omega-\Omega_{s,i}) \qquad (3.10)\\ \times u_{1,k''k'}(|\mathbf{r}-\mathbf{r}'|)\delta(\mathbf{r}'-\mathbf{r}_{s,j})\delta(\Omega'-\Omega_{s,j}) \\ = \frac{1}{2}\sum_{k''k'}\sum_{i=1}^{N_{k'}n_{k'}}\sum_{j=1}^{N_{k''}n_{k''}} u_{1,k''k'}(|\mathbf{r}_{s,i}-\mathbf{r}_{s,j}|), \qquad (3.11) \end{aligned}$$

which is same as Eq. 3.5. Now, consider $U_2(\{\Omega_{s,k\neq 0}\})$ in equation 3.9 and substitute the expression of volume fraction operator $\hat{\phi}_k(\mathbf{r},\Omega)$ from Eq. 3.2,

$$U_2(\{\Omega_{s,k\neq 0}\}) = \sum_k \frac{f_k \cancel{v_k}}{\cancel{v_k}} \sum_{i=1}^{N_k n_k} \int d\Omega d\mathbf{r} \delta(\mathbf{r}-\mathbf{r}_{s,i})\delta(\Omega-\Omega_{s,i}) u_{2,k}(\Omega) \tag{3.12}$$

$$= \sum_k f_k \sum_{i=1}^{N_k n_k} u_{2,k}(\Omega_{s,i}), \tag{3.13}$$

which is same as Eq. 3.6. If we assume that each segment can move independently in a random manner *i.e.* random mixing then we can replace instantaneous volume fraction operators $\hat{\phi}_k(\mathbf{r},\Omega)$ in Eqs. 3.8 and 3.9 with random mixing mean-field volume fractions ϕ_k,

$$\phi_k \equiv \frac{1}{V}\int d\mathbf{r} \langle \hat{\phi}_k(\mathbf{r})\rangle, \tag{3.14}$$

where $\langle \hat{\phi}(\mathbf{r})\rangle$ are ensemble average volume fractions and V is the volume of the multicomponent system. Under this random mixing mean-field assumption Eq. 3.3 becomes,

$$\sum_k^0 \phi_k = 1, \tag{3.15}$$

where

$$\phi_0 = \frac{n_0 v_0}{V}, \tag{3.16}$$

$$\phi_k = \frac{N_k n_k v_k}{V}. \tag{3.17}$$

Thus, Eq. 3.1 becomes,

$$H = \sum_k \sum_{i=1}^{n_k} \frac{\mathbf{p}_i^2}{2m_k} + \frac{1}{2}\sum_{k''k'} \frac{\phi_{k''}\phi_{k'}}{v_{k''}v_{k'}} \int d\Omega d\Omega' d\mathbf{r} d\mathbf{r}' u_{1,k''k'}(|\mathbf{r}-\mathbf{r}'|) \tag{3.18}$$

$$+ \sum_k \frac{f_k \phi_k}{v_k} \int d\Omega d\mathbf{r} u_{2,k}(\Omega). \tag{3.19}$$

Following von Konigslow *et al.* [197] we introduce average interaction parameters $\epsilon_{1,kk'}$ as follows,

$$\epsilon_{1,kk'} = -\frac{v_r}{V}\frac{1}{2v_k v_{k'}} \int d\Omega d\Omega' d\mathbf{r} d\mathbf{r}' u_{1,kk'}(|\mathbf{r}-\mathbf{r}'|). \tag{3.20}$$

In addition, define average flexing parameters $\epsilon_{2,k}$ as follows,

$$\epsilon_{2,k} \equiv \frac{v_r}{V}\frac{1}{v_k}\int d\Omega d\mathbf{r} u_{2,k}(\Omega), \tag{3.21}$$

where, v_r is an arbitrary reference volume. Also, assume that average interaction energies and average flexing energies are constant with respect to volume V because these interactions are short-ranged. By using these definitions Eq. 3.19 becomes,

$$H = \sum_k \sum_{i=1}^{n_k} \frac{\mathbf{p}_i^2}{2m_k} - \frac{V}{v_r}\sum_{kk'} \phi_k \phi_{k'} \epsilon_{1,kk'} + \frac{V}{v_r}\sum_k f_k \phi_k \epsilon_{2,k}. \tag{3.22}$$

The above expression for the Hamiltonian can be written in a more elaborate form as,

$$H = \underbrace{\sum_k \sum_{i=1}^{n_k} \frac{\mathbf{p}_i^2}{2m_k} - \frac{V}{v_r}\sum_{kk'} \phi_k \phi_{k'} \epsilon_{1,kk'}}_{H_p} + \underbrace{\frac{V}{v_r}\sum_k f_k \phi_k \epsilon_{2,k}}_{H_{ex}} + \underbrace{\frac{V}{v_r}\sum_k (1-f_k)\phi_k \cancelto{0}{\epsilon_{3,k}}}_{H_g} + \underbrace{\frac{V}{v_r}\phi_0^2 \cancelto{0}{\epsilon_0}}_{H_h}, \tag{3.23}$$

where, H_p is the energy of motion of centers of mass of molecules plus the energy of molecular interactions, H_{ex} is the energy of excited state segments, H_g is the energy of ground state segments and H_h is the energy of holes in the system. Since holes are artificial and have no interactions, ϵ_0 is zero. In addition, flexing energies of ground state (unflexed) segments $\epsilon_{3,k}$ are assumed zero following convention. The above expression shows that the Hamiltonian H of the complete system is the sum of Hamiltonians of the above four independent sub-systems. This decoupling into sub-systems is the consequence of the mean-field approximation.

3.4 Partition Function

The general expression for the partition function is,

$$Q = \sum_{\{\mu\}} e^{-\frac{H}{k_B T}}, \tag{3.24}$$

where $\{\mu\}$ represents the set of all possible microstates that are allowed within system constraints, k_B is Boltzmann's constant and T is the temperature of the system. Since H

can be written as sum Hamiltonians of sub-system, we can split the exponential and write Eq. 3.24 as,

$$Q = Q_p \cdot Q_h \cdot Q_{ex} \cdot Q_g. \tag{3.25}$$

Lets focus on the details of these sub-systems and find their corresponding partition functions.

3.4.1 Partition Function for Interactions and Motions of Molecules Q_p

The partition function of interactions and motions of molecules should be,

$$Q_p = \int \frac{d\{\mathbf{p_k}\}d\{\mathbf{r_k}\}}{\prod_k (n_k!\, h^{3n_k})} e^{-\frac{H_p}{k_B T}}, \tag{3.26}$$

where,

$$H_p = \sum_k \sum_{i=1}^{n_k} \frac{\mathbf{p}_i^2}{2m_k} - \frac{V}{v_r} \sum_{kk'} \phi_k \phi_{k'} \epsilon_{1,kk'}. \tag{3.27}$$

Since molecules can have continuous microstates so the discrete summation is replaced by an integral over all possible microstates i.e. the set of position vectors $\{\mathbf{r}_k\}$ and the set of momentum vectors $\{\mathbf{p}_k\}$ of centers of mass of each molecule. Moreover, molecules of same species are indistinguishable thus factors $n_k!$ are introduced to avoid over counting. Finally, h is Planck's constant that is introduced $3n_k$ times for each species to keep the partition function dimensionless.

We can now integrate Eq. 3.26 by splitting the exponential into kinetic energies and potential energies and by noting that $\frac{V}{v_r} \sum_{kk'} \phi_k \phi_{k'} \epsilon_{1,kk'}$ is constant because of the mean-field and random mixing approximations. Integration over position $\{\mathbf{r}_k\}$ of centers of mass of each molecule will give volume V because each molecule can explore the complete volume of the system. Since there are n_k molecules of species k so the system's volume V is multiplied n_k times. Thus,

$$Q_p = \prod_k \left(\frac{V^{n_k}}{n_k!\, \Lambda_k^{3n_k}} \right) e^{\frac{V}{v_r} \sum_{kk'} \frac{\phi_k \phi_{k'} \epsilon_{1,kk'}}{k_B T}}, \tag{3.28}$$

where Λ_k are the de Broglie thermal wavelengths that come from the integration over momentum $\int d\{\mathbf{p}_k\}$ of all molecules of species k. It is given by,

$$\Lambda_k(T) = \frac{h}{\sqrt{2\pi m_k k_B T}}. \tag{3.29}$$

3.4.2 Partition Function for Holes Q_h

Partition function for holes is,

$$Q_h = \int \frac{d\{\mathbf{p_0}\} d\{\mathbf{r_0}\}}{n_0!\, h^{3n_0}} e^{-\frac{H_h}{k_B T}}, \tag{3.30}$$

where,

$$H_h = \frac{V}{v_r}\phi_0^2 \cancel{\epsilon_0}^{0} = 0. \tag{3.31}$$

In the above expression, $\int d\{\mathbf{p}_0\}$ are not integrals over the momenta of holes. Holes are artificial and have no mass or momentum. These integrals are introduced to keep the partition function dimensionless.

We integrate Eq. 3.30 by putting $H_h = 0$ and as before and notice that integration over position $\{\mathbf{r_0}\}$ of each hole should give the volume V of the system. Since there are n_0 holes so volume V is multiplied n_0 times. Thus,

$$Q_h = \frac{V^{n_0}}{n_0!\, \Lambda_0^{3n_0}}, \tag{3.32}$$

where Λ_0 is the normalization constant that comes from integrals $\int\{\mathbf{p}_0\}$, keeping the partition function dimensionless. The above partition function can abstractly be considered as the partition function for an ideal gas of holes (although Λ_0 is not a thermal wavelength) [79].

3.4.3 Partition Function for Flexed/Excited State Segments Q_{ex}

Microstates of excited segments of the system should be discrete. So the partition function of this sub-system will have a summation over microstates instead of integrations. Also note that due to the mean-field approximation, the Hamiltonian of excited segments of the

complete system $H_{ex} = \frac{V}{v_r}\sum_k f_k\phi_k\epsilon_{2,k}$ can be considered as the sum of Hamiltonians of excited segments of individual species H_k^{ex}.

$$H_{ex} = \sum_k H_k^{ex}, \tag{3.33}$$

where

$$H_k^{ex} = \frac{V}{v_r} f_k\phi_k\epsilon_{2,k}. \tag{3.34}$$

Moreover, individual molecules of species k are also independent from other molecules. Thus Hamiltonians $H_k^{ex,m}$ of excited segments of individual molecules of species k are,

$$H_k^{ex,m} = \frac{V}{v_r}\frac{f_k\phi_k\epsilon_{2,k}}{n_k}. \tag{3.35}$$

The above expression has been written by dividing the energy H_k^{ex} of excited state segments of species k equally into n_k molecules of that species. Moreover, within each molecule there are f_kN_k excited segments so the energy packet $H_k^{ex,s}$ that is available to each excited segment within a molecule of species k is given by,

$$H_k^{ex,s} = \frac{H_k^{ex,m}}{f_kN_k} \tag{3.36}$$

$$= \frac{V}{v_r}\frac{\phi_k\epsilon_{2,k}}{N_kn_k}. \tag{3.37}$$

Assume that each excited segment of species k has g_k different configurations (degeneracy). Thus, partition functions $Q_k^{ex,s}$ of such excited segments within molecules are,

$$Q_k^{ex,s} = \sum_{\{\mu\}} e^{-\frac{H_k^{ex,s}}{k_BT}} = g_ke^{-\frac{H_k^{ex,s}}{k_BT}}. \tag{3.38}$$

Thus, partition functions $Q_k^{ex,m}$ of excited segments of individual molecules of species k will be the product of partition functions of excited segments within that molecule of that species. Therefore,

$$Q_k^{ex,m} = \frac{1}{(f_kN_k)!}\prod_{j=1}^{f_kN_k} g_ke^{-\frac{H_k^{ex,s}}{k_BT}} \tag{3.39}$$

$$= \frac{1}{(f_kN_k)!}g_k^{f_kN_k}e^{-\frac{\sum_{f_kN_k}H_k^{ex,s}}{k_BT}} \tag{3.40}$$

$$= \frac{1}{(f_kN_k)!}g_k^{f_kN_k}e^{-\frac{H_k^{ex,m}}{k_BT}}, \tag{3.41}$$

where,

$$H_k^{ex,m} = \frac{V}{v_r}\frac{f_k\phi_k\epsilon_{2,k}}{n_k}. \tag{3.42}$$

The factor $(f_kN_k)!$ is included to prevent over counting because the excited segments within a given molecule are identical. Thus,

$$Q_k^{ex,m} = \frac{1}{(f_kN_k)!}g_k^{f_kN_k}e^{-\frac{V}{v_r}\frac{f_k\phi_k}{n_k}\frac{\epsilon_{2,k}}{k_BT}}. \tag{3.43}$$

Next, the partition function Q_k^{ex} of excited segments of species k should be the product of partition functions of excited segments of individual molecules of that species. Therefore,

$$Q_k^{ex} = [Q_k^{ex,m}]^{n_k} \tag{3.44}$$

$$= \frac{g_k^{f_kN_kn_k}}{[(f_kN_k)!\,]^{n_k}}e^{-\frac{V}{v_r}\frac{f_k\phi_k\epsilon_{2,k}}{k_BT}}. \tag{3.45}$$

Finally, the partition function Q_{ex} of excited state segments of the complete system is the product of partition functions of excited segments of individual species.

$$Q_{ex} = \prod_k Q_k^{ex} \tag{3.46}$$

$$= \prod_k \left(\frac{g_k^{f_kN_kn_k}}{[(f_kN_k)!\,]^{n_k}}e^{-\frac{V}{v_r}\frac{f_k\phi_k\epsilon_{2,k}}{k_BT}}\right) \tag{3.47}$$

$$= \left(\prod_k \frac{g_k^{f_kN_kn_k}}{\{(f_kN_k)!\,\}^{n_k}}\right)e^{-\frac{V}{v_r}\sum_k\frac{f_k\phi_k\epsilon_{2,k}}{k_BT}}. \tag{3.48}$$

3.4.4 Partition Function for Unflexed/Ground State Segments Q_g

Let's follow the similar reasoning as mentioned for the flexed/excited state segments. Since microstates of ground state segments are discrete so the partition function will have summation over microstates instead of integration. Moreover, due to the mean-field approximation, ground state segments of individual molecules of species constitute independent subsystems having Hamiltonian $H_k^{g,m} = 0$. Moreover, within individual molecules of species k there are $(1-f_k)N_k$ ground state segments and thus the energy packet $H_k^{g,s}$ that is available to each ground state segment within individual molecules of species k is also zero. In

addition, assume that each ground state segment has only one configuration (no degeneracy) and thus partition functions of each ground state segment $Q_k^{g,s}$ within molecules of species k are,

$$Q_k^{g,s} = \sum_{\{\mu\}} e^{-\frac{\cancelto{0}{H_k^{g,s}}}{k_B T}} = 1. \tag{3.49}$$

Thus, partition functions $Q_k^{g,m}$ of ground state segments of individual molecules of k^{th} species will be the product of partition functions of ground state segments within that molecule.

$$Q_k^{g,m} = \frac{1}{\{(1-f_k)N_k\}!} \prod_{j=1}^{(1-f_k)N_k} (1) \tag{3.50}$$

$$= \frac{1}{\{(1-f_k)N_k\}!}, \tag{3.51}$$

whereas, the factor $\{(1-f_k)N_k\}!$ is included to prevent over counting because ground segments within a molecule are identical. Finally, the partition function Q_k^g of ground state segments of species k is equal to the product of all partition functions of ground state segments of individual molecules of that species.

$$Q_k^g = [Q_k^{g,m}]^{n_k} = \frac{1}{[\{(1-f_k)N_k\}!]^{n_k}}. \tag{3.52}$$

Finally, the partition function Q_g of ground state segments of the complete system is the product of partition functions of ground state segments of individual species.

$$Q_g = \prod_k Q_k^g \tag{3.53}$$

$$= \prod_k \frac{1}{[\{(1-f_k)N_k\}!]^{n_k}}. \tag{3.54}$$

Note that the combined partition function $Q_{ex}Q_g$ is the partition function due to finite stiffness of molecules.

3.4.5 Overall Partition Function of System

Putting the partition functions of all four subsystems in Eq. 3.25,

$$Q = \prod_k \left(\frac{V^{n_k}}{n_k!\,\Lambda_k^{3n_k}} \right) e^{\frac{V}{v_r}\sum_{kk'} \frac{\phi_k \phi_{k'} \epsilon_{1,kk'}}{k_B T}} \cdot \frac{V^{n_0}}{n_0!\,\Lambda_0^{3n_0}} \cdot \prod_k \left(\frac{g_k^{f_k N_k n_k}}{\{(f_k N_k)!\,\}^{n_k}} \right) \times e^{-\frac{V}{v_r}\sum_k \frac{f_k \phi_k \epsilon_{2,k}}{k_B T}} \cdot \prod_k \frac{1}{[\{(1-f_k)N_k\}!\,]^{n_k}}. \tag{3.55}$$

Simplifying,

$$Q = \frac{V^{n_0}}{n_0!\,\Lambda_0^{3n_0}} \prod_k \left[\frac{V^{n_k}}{n_k!\,\Lambda_k^{3n_k}} \frac{g_k^{f_k N_k n_k}}{\{(f_k N_k)!\,\}^{n_k}} \frac{1}{[\{(1-f_k)N_k\}!\,]^{n_k}} \right] e^{\frac{V}{v_r}\sum_{kk'} \frac{\phi_k \phi_{k'} \epsilon_{1,kk'}}{k_B T} - \frac{V}{v_r}\sum_k \frac{f_k \phi_k \epsilon_{2,k}}{k_B T}}. \tag{3.56}$$

The above partition function can be written in more compact form if we abstractly assume $f_0 = 0$,

$$Q = \prod_k^0 \left[\frac{V^{n_k}}{n_k!\,\Lambda_k^{3n_k}} \frac{g_k^{f_k N_k n_k}}{[(f_k N_k)!\,\{(1-f_k)N_k\}!\,]^{n_k}} \right] \cdot e^{\frac{V}{v_r}\left(\frac{\sum_{kk'} \phi_k \phi_{k'} \epsilon_{1,kk'} - \sum_k f_k \phi_k \epsilon_{2,k}}{k_B T} \right)}. \tag{3.57}$$

3.5 Thermodynamics of Multicomponent Fluids

Thermodynamic properties of the canonical ensemble can be derived in a straight forward manner by using the partition function Eq. 3.56. In this section, we have derived equations of free energy, pressure (SL-EOS), entropy, glass transition temperature, internal energy, isochoric heat capacity, isobaric heat capacity and isobaric expansion coefficient. While deriving these quantities von Konigslow *et al.* procedure has been adapted in several instances.

3.5.1 Free Energy

Helmholtz's free energy F can be found by using $F = -k_B T \ln Q$. After applying Stirling's approximation and discarding terms which only consist of constants N_k and/or are linear

in n_k, as such terms only change reference zero of free energy, we have,

$$\frac{F}{k_BT} = -\frac{V}{v_r}\left[\sum_{kk'}\frac{\epsilon_{1,kk'}}{k_BT}\phi_k\phi_{k'} - \sum_k \frac{\epsilon_{2,k}}{k_BT}f_k\phi_k\right] + \left[n_0\ln\left(\frac{n_0\Lambda_0^3}{V}\right) - n_0\right] \tag{3.58}$$
$$+\sum_k\left[n_k\ln\left(\frac{n_k\Lambda_k^3}{V}\right) - n_k\right] + \sum_k N_k n_k\left[f_k\ln\left\{\frac{f_k}{g_k(1-f_k)}\right\} + \ln(1-f_k)\right].$$

The following term can be added to the above equation because it is linear in n_k,

$$\sum_k n_k\left[\ln\left(\frac{N_k v_k}{\Lambda_k^3}\right) + 1\right].$$

Therefore Eq. 3.58 becomes,

$$\frac{F}{k_BT} = -\frac{V}{v_r}\left[\sum_{kk'}\frac{\epsilon_{1,kk'}}{k_BT}\phi_k\phi_{k'} - \sum_k \frac{\epsilon_{2,k}}{k_BT}f_k\phi_k\right] + \left[n_0\ln\left(\frac{n_0\Lambda_0^3}{V}\right) - n_0\right] \tag{3.59}$$
$$+\sum_k\left[n_k\ln\left(\frac{N_k n_k v_k}{V}\right)\right] + \sum_k N_k n_k\left[f_k\ln\left\{\frac{f_k}{g_k(1-f_k)}\right\} + \ln(1-f_k)\right].$$

At equilibrium, fractions of excited segments f_k of all species adjust to minimize the free energy F of the system. Thus, we take the derivative of Eq. 3.59 of free energy F with respect to fraction $f_{k'}$ of a particular species k' and equate to zero. After replacing k' back to k, we have,

$$f_k = \frac{g_k e^{-V\phi_k\epsilon_{2,k}/N_k n_k v_r k_B T}}{1 + g_k e^{-V\phi_k\epsilon_{2,k}/N_k n_k v_r k_B T}}. \tag{3.60}$$

To verify the soundness of above expression lets consider two cases. Case(i): Take $\epsilon_{2,k} = 0 \implies f_k = \frac{g_k}{1+g_k}$, which is true because energy of excited states of species k is same as the energy ground state, thus, the system tends to equally occupy all states. Since there are g_k configurations of each excited state and only 1 configuration of ground state so fraction of excited states f_k of species k should be equal to $f_k = \frac{Total\ \ Configurations\ of\ Excited\ States}{Total\ Number\ of\ Configurations of\ All States}$. Case(ii): Take $\epsilon_{2,k} \to \infty \implies f_k = 0$, which is also true because the energy of the excited state is infinite, thus, it is very difficult for the system to occupy the excited state at finite temperatures. Consequently, the fraction of excited states f_k of species k is zero.

We will see later in section 3.5.2 that in order to satisfy condition $P \to 0$ as $\rho \to 0$, it is

necessary to have $\Lambda_0^3 = v_k e$ [197]. Thus, equation 3.59 becomes,

$$\frac{F}{k_B T} = -\frac{V}{v_r}\left[\sum_{kk'}\frac{\epsilon_{1,kk'}}{k_B T}\phi_k\phi_{k'} - \sum_k \frac{\epsilon_{2,k}}{k_B T} f_k \phi_k\right] + \left[n_0 \ln\left(\frac{n_0 v_0}{V}\right)\right] \tag{3.61}$$
$$+ \sum_k \left[n_k \ln\left(\frac{N_k n_k v_k}{V}\right)\right] + \sum_k N_k n_k \left[f_k \ln\left\{\frac{f_k}{g_k(1-f_k)}\right\} + \ln(1-f_k)\right].$$

Following von Konigslow *et al.* Ref. [197], we define a quantity α_k that is the ratio of volume of a molecule of species k to the reference volume v_r,

$$\alpha_k \equiv \frac{N_k v_k}{v_r}. \tag{3.62}$$

Thus, equation 3.61 becomes,

$$\frac{F}{k_B T} = -\frac{V}{v_r}\left[\sum_{kk'}\frac{\epsilon_{1,kk'}}{k_B T}\phi_k\phi_{k'} - \sum_k \frac{\epsilon_{2,k}}{k_B T} f_k \phi_k\right] + \frac{V}{v_0}\phi_0 \ln\phi_0 \tag{3.63}$$
$$+ \sum_k \frac{V}{v_r}\frac{\phi_k}{\alpha_k}\ln\phi_k + \sum_k \frac{V\phi_k}{v_k}\left[f_k \ln\left\{\frac{f_k}{g_k(1-f_k)}\right\} + \ln(1-f_k)\right].$$

To write the above expression Eqs. 3.17 and 3.16 have been used. Moreover, Eq. 3.60 becomes,

$$f_k = \frac{g_k e^{-v_k \epsilon_{2,k}/v_r k_B T}}{1 + g_k e^{-v_k \epsilon_{2,k}/v_r k_B T}}. \tag{3.64}$$

From Eq. 3.64 notice that fractions of excited segments f_k are independent of volume V of the system. From the definitions given in paper by von Konigslow *et al* [197] the scaled density is,

$$\tilde{\rho} \equiv \sum_k \phi_k. \tag{3.65}$$

Average interaction energy is,

$$\epsilon_1^* \equiv \frac{1}{\tilde{\rho}} \sum_{kk'} \epsilon_{1,kk'}\phi_k\phi_{k'}. \tag{3.66}$$

Scaled pressure is,

$$\tilde{P} \equiv \frac{v_r P}{\epsilon_1^*}. \tag{3.67}$$

Scaled temperature is,

$$\tilde{T} \equiv \frac{k_B T}{\epsilon_1^*}. \tag{3.68}$$

Average molecular size r is,

$$r \equiv \frac{1}{\tilde{\rho}} \sum_k \frac{\phi_k}{\alpha_k}. \tag{3.69}$$

From Sanchez and Lacombe paper Ref. [164] we know,

$$\tilde{P} = \frac{P}{P^*}, \tag{3.70}$$

$$\tilde{T} = \frac{T}{T^*}, \tag{3.71}$$

$$\tilde{\rho} = \frac{\rho}{\rho^*} = \frac{V^*}{V}. \tag{3.72}$$

Thus, from Eq. 3.65 implies,

$$V^* = \sum_k N_k n_k v_k. \tag{3.73}$$

Moreover, the characteristic volume V^* was related to the characteristic mass-density ρ^* as,

$$\rho^* = \frac{\sum_k n_k M_k}{V^*}, \tag{3.74}$$

where M_k is the molecular mass of molecules of species k with Boltzmann constant 8.3145 $J/mol.K$. The characteristic specific-volume v^* is,

$$v^* = \frac{1}{\rho^*} = \frac{V^*}{\sum_k n_k M_k}. \tag{3.75}$$

Number of moles of species k is,

$$n_k = \frac{m_k}{M_k}. \tag{3.76}$$

Following von Konigslow *et al.* [197] characteristic temperature T^* and pressure P^* can be written by using Eqs. 3.68 and 3.67 as,

$$P^* = \frac{\epsilon_1^*}{v_r}, \tag{3.77}$$

$$T^* = \frac{\epsilon_1^*}{k_B}. \tag{3.78}$$

Pure-component characteristic parameters were defined as,

$$V_k^* = N_k n_k v_k, \tag{3.79}$$

$$\rho_k^* = \frac{m_k}{V_k^*} = \frac{n_k M_k}{V_k^*} = \frac{M_k}{\alpha_k v_r}, \tag{3.80}$$

$$P_k^* = \frac{\epsilon_{1,kk}}{v_r}, \tag{3.81}$$

$$T_k^* = \frac{\epsilon_{1,kk}}{k_B}. \tag{3.82}$$

The above expression of P_k^* has been written by assuming that the reference volume of a pure system is the same as the reference volume of a mixed system *i.e.* $v_{r,k} = v_{r,m} = v_r$.

Cross-component interaction energies were defined as,

$$\epsilon_{1,kk'} \equiv \zeta_{kk'}(\epsilon_{1,kk}\epsilon_{1,k'k'})^{1/2}, \qquad k \neq k' \tag{3.83}$$

Thus, Eq. 3.66 was expanded,

$$\epsilon_1^* = \frac{1}{\tilde{\rho}} \left[\sum_{\substack{kk' \\ k \neq k'}} \epsilon_{1,kk'} \phi_k \phi_{k'} + \sum_k \epsilon_{1,kk} \phi_k^2 \right]. \tag{3.84}$$

By using these definitions α_k from Eq. 3.62 becomes,

$$\alpha_k = \frac{M_k P_k^*}{k_B \rho_k^* T_k^*}. \tag{3.85}$$

The reference volume for pure systems becomes,

$$v_{r,k} = \frac{k_B T_k^*}{P_k^*}. \tag{3.86}$$

Pure-component average interaction energy becomes,

$$\epsilon_{1,kk} = k_B T_k^*. \tag{3.87}$$

Thus, pure systems can be characterized either by using $\alpha_k, v_0, \epsilon_{1,kk}$ or, equivalently, by using P_k^*, T_k^*, ρ_k^*.

Finally, in this study the hole volume v_0 for mixtures is taken to be constant — independent of volume fractions of the components. This produces inconsistency by which the hole volume of mixed-phase does not approach to the pure component hole volume in the limit of vanishing volume fractions of all components of the system except one, as described by von Konigslow *at el.* [197].

Let's introduce some new parameters to characterize the flexing of molecules. Flexing of molecules is considered completely independent from all other molecules present in the system so there are no cross interactions. Define characteristic flexing temperatures of molecules as,

$$T_k^{**} \equiv \frac{\epsilon_{2,k}}{k_B}. \tag{3.88}$$

Define characteristic ratios as,

$$T_{r,k} \equiv \frac{T_k^{**}}{T_k^*} = \frac{\epsilon_{2,k}}{\epsilon_{1,kk}}, \tag{3.89}$$

$$V_{r,k} \equiv \frac{v_k}{v_r}, \tag{3.90}$$

$$N_k = \frac{\alpha_k}{V_{r,k}}. \tag{3.91}$$

Also note the following useful relations,

$$N_k n_k = \frac{V\phi_k}{v_k} = \frac{V}{v_r}\frac{N_k\phi_k}{\alpha_k}. \tag{3.92}$$

Alternatively,

$$N_k n_k = \frac{P_k^* V_k^*}{k_B T_k^*}\frac{1}{V_{r,k}} = \frac{m_k P_k^*}{k_B \rho_k^* T_k^*}\frac{1}{V_{r,k}} = \frac{m_k \alpha_k}{M_k V_{r,k}}. \tag{3.93}$$

Thus, fractions of excited segments from Eq. 3.64 become,

$$f_k = \frac{g_k e^{-T_{r,k}V_{r,k}/\tilde{T}_k}}{1 + g_k e^{-T_{r,k}V_{r,k}/\tilde{T}_k}}. \tag{3.94}$$

3.5.2 Equation of State

The equation of state can be obtained by using,

$$P = -\left(\frac{\partial F}{\partial V}\right)_{\{n_k\},T}. \tag{3.95}$$

We put the expression of free energy from Eq. 3.63 above and note that fraction of excited segments f_k is independent of volume V of the system, $\phi_k = N_k n_k v_k/V$, $\alpha_k = N_k v_k/v_r$ and $n_0 = n_0(V)$ because of incompressibility condition Eq. 3.15.

$$\frac{v_r P}{k_B T} = -\sum_k \left(\frac{1}{\alpha_0} - \frac{1}{\alpha_k}\right)\phi_k - \frac{1}{\alpha_0}\ln\phi_0 - \sum_{kk'}\frac{\epsilon_{1,kk'}}{k_B T}\phi_k\phi_{k'} + \frac{1}{\alpha_0}\left[1 - \ln\left(\frac{\Lambda_0^3}{v_0}\right)\right]. \quad (3.96)$$

The above equation of state of a finitely flexible system is the same as Eq.[15] of an infinitely flexible system in Ref. [197]. Therefore, following Ref. [197] the requirement that $\tilde{P} \to 0$ as $\tilde{\rho} \to 0$ requires $\Lambda_0^3 = v_0 e$. Thus,

$$\frac{v_r P}{k_B T} = -\sum_k \left(\frac{1}{\alpha_0} - \frac{1}{\alpha_k}\right)\phi_k - \frac{1}{\alpha_0}\ln\phi_0 - \sum_{kk'}\frac{\epsilon_{1,kk'}}{k_B T}\phi_k\phi_{k'}. \quad (3.97)$$

Moreover, SL-EOS can be obtained by following the same steps mentioned in Ref. [197]. That is, using the definitions described in section 3.5.1 Eq. 3.97 becomes,

$$\tilde{\rho}^2 + \tilde{P} + \tilde{T}\left[\left(\frac{1}{\alpha_0} - \frac{1}{r}\right)\tilde{\rho} + \frac{1}{\alpha_0}\ln(1-\tilde{\rho})\right] = 0. \quad (3.98)$$

Without loss of generality take $v_r = v_0$ so that Eq. 3.98 gives SL-EOS,

$$\tilde{\rho}^2 + \tilde{P} + \tilde{T}\left[\left(1 - \frac{1}{r}\right)\tilde{\rho} + \ln(1-\tilde{\rho})\right] = 0. \quad (3.99)$$

3.5.3 Entropy

To find an expression of entropy S of the system compare Eq. 3.63 with the standard definition of free energy $F = E - TS$,

$$\frac{S}{k_B} = -\frac{V}{v_0}\phi_0\ln\phi_0 - \sum_k \frac{V}{v_r}\frac{\phi_k}{\alpha_k}\ln\phi_k - \sum_k \frac{V\phi_k}{v_k}\left[f_k \ln\left\{\frac{f_k}{g_k(1-f_k)}\right\} + \ln(1-f_k)\right]. \quad (3.100)$$

Put the value of f from equation 3.64 we get,

$$\frac{S}{k_B} = -\frac{V\phi_0}{v_0}\ln\phi_0 - \sum_k \frac{V\phi_k}{v_r}\frac{\ln\phi_k}{\alpha_k} + \sum_k \frac{V\phi_k}{v_r}\frac{f_k\epsilon_{2,k}}{k_B T} - \sum_k \frac{V\phi_k}{v_k}\ln(1-f_k). \quad (3.101)$$

In the above expression, the first term is translational entropy of holes, the second term is the translational entropy of molecules. The last two terms represent the configurational

entropy of the system. Since ϕ_0, ϕ_k and f_k are always less than 1 so all terms in the above expression are positive. Thus the entropy of the system is always positive at all temperatures. However, this is contradictory to the Gibbs DiMarzio criterion for glass transitions Refs. [36,62] discussed in section 2.8.3. This means that in the Condo model [23] negative entropy is, in fact, a consequence of using an artificial lattice.

3.5.4 Glass Transition Temperature

As discussed in section 3.5.3, the Gibbs DiMarzio criterion for glass transitions Refs. [36,62] is incorrect thus an alternate criterion for glass transitions is required. However, the success of the Condo model [23] in predicting glass transition temperatures and retrograde vitrification is very reasonable. Thus, instead of completely discarding the Gibbs DiMarzio criterion, it can be generalized by proposing that the glass transition occurs at a temperature where entropy of a system becomes a fraction x of the entropy of that system at infinite temperature. Thus, put $S(T_g) \equiv xS_\infty = xS(T \to \infty)$ in Eq. 3.101 to get,

$$\frac{xS_\infty}{k_B} + \frac{V_g\phi_{0,g}}{v_0}\ln\phi_{0,g} + \sum_k \frac{V_g\phi_{k,g}}{v_r}\frac{\ln\phi_{k,g}}{\alpha_k} - \sum_k \frac{V_g\phi_{k,g}}{v_r}\frac{f_{k,g}\epsilon_{2,k}}{k_BT_g} + \sum_k \frac{V_g\phi_{k,g}}{v_k}\ln(1-f_{k,g}) = 0. \tag{3.102}$$

In the above expression, volume V depends on pressure and temperature of the system through equation of state 3.97. Thus, the above expression is a T_g versus P relation for multicomponent fluid systems.

3.5.5 Internal Energy

Again compare Eq. 3.63 with $F = E - TS$ to get,

$$\frac{E}{k_BT} = -\frac{V}{v_r}\left[\sum_{kk'}\frac{\epsilon_{1,kk'}}{k_BT}\phi_k\phi_{k'} - \sum_k \frac{\epsilon_{2,k}}{k_BT}f_k\phi_k\right]. \tag{3.103}$$

3.5.6 Isochoric Heat Capacity

Isochoric heat capacity is given by,

$$C_V = \left.\frac{\partial E}{\partial T}\right|_{\{n_k\},V}. \tag{3.104}$$

Putting equation 3.103 in the above definition,

$$\frac{C_V}{k_B} = \sum_k \frac{V\phi_k}{v_k} \left(\frac{v_k}{v_r} \frac{\epsilon_{2,k}}{k_B T} \right)^2 f_k(1 - f_k). \tag{3.105}$$

3.5.7 Isobaric Heat Capacity

Using the definition,

$$C_P = T \frac{\partial S}{\partial T}\bigg|_{\{n_k\},P}. \tag{3.106}$$

Putting entropy from Eq. 3.101,

$$\frac{C_P}{k_B} = \frac{V}{v_r} \frac{\left(\frac{v_r P}{k_B T} + \sum_{kk'} \frac{\epsilon_{1,kk'}}{k_B T} \phi_k \phi_{k'} \right)^2}{\left[\left(\sum_k \phi_k \right) \left(\frac{\sum_k \phi_k}{\alpha_0 \phi_0} + \frac{1}{r} \right) - 2 \sum_{kk'} \frac{\epsilon_{1,kk'}}{k_B T} \phi_k \phi_{k'} \right]} + \sum_k \frac{V\phi_k}{v_k} \left(\frac{v_k}{v_r} \frac{\epsilon_{2,k}}{k_B T} \right)^2 f_k(1 - f_k). \tag{3.107}$$

Note, second term in above expression is C_V/k_B, therefore,

$$\frac{C_P - C_V}{k_B} = \frac{V}{v_r} \frac{\left(\frac{v_r P}{k_B T} + \sum_{kk'} \frac{\epsilon_{1,kk'}}{k_B T} \phi_k \phi_{k'} \right)^2}{\left[\left(\sum_k \phi_k \right) \left(\frac{\sum_k \phi_k}{\alpha_0 \phi_0} + \frac{1}{r} \right) - 2 \sum_{kk'} \frac{\epsilon_{1,kk'}}{k_B T} \phi_k \phi_{k'} \right]}. \tag{3.108}$$

Moreover, in Eq. 3.107 first term is the heat capacity of a system with infinitely flexible molecules whereas second term is due to the introduction of finite flexibility in molecules. At sufficiently low temperatures there will be negligible segments in flexed/excited states. So, for the low temperature limit the second term vanishes. Thus, the second term can be regarded as the incremental change in heat capacity ΔC_P due to flexing of segments,

$$\frac{\Delta C_P}{k_B} = \sum_k \frac{V\phi_k}{v_k} \left(\frac{v_k}{v_r} \frac{\epsilon_{2,k}}{k_B T} \right)^2 f_k(1 - f_k). \tag{3.109}$$

In this study only two energy levels have been considered to account for flexing of molecules. However, real systems may have multiple energy levels. If a more realistic system were considered in the present study the incremental change in heat capacity ΔC_P would sharply

drops to zero below glass transition temperatures, as observed in quasi-statically cooling systems [156, 173]. Thus, isobaric heat capacity below glass transition temperatures becomes,

$$\frac{C_P}{k_B} = \frac{V}{v_r} \frac{\left(\frac{v_r P}{k_B T} + \sum_{kk'} \frac{\epsilon_{1,kk'}}{k_B T} \phi_k \phi_{k'}\right)^2}{\left[\left(\sum_k \phi_k\right)\left(\frac{\sum_k \phi_k}{\alpha_0 \phi_0} + \frac{1}{r}\right) - 2\sum_{kk'} \frac{\epsilon_{1,kk'}}{k_B T} \phi_k \phi_{k'}\right]}. \tag{3.110}$$

3.5.8 Isobaric Expansion Coefficient

The isobaric expansion coefficient $\alpha_{P,k}$ is defined as,

$$\alpha_{P,k} = \frac{1}{V} \frac{\partial V}{\partial T}\bigg|_{P,n_k}. \tag{3.111}$$

Using equation of state Eq. 3.97 to get,

$$\alpha_{P,k} = \frac{1}{T} \frac{\left(\frac{v_r P}{k_B T} + \sum_{kk'} \frac{\epsilon_{1,kk'}}{k_B T} \phi_k \phi_{k'}\right)}{\left[\left(\sum_k \phi_k\right)\left(\frac{\sum_k \phi_k}{\alpha_0 \phi_0} + \frac{1}{r}\right) - 2\sum_{kk'} \frac{\epsilon_{1,kk'}}{k_B T} \phi_k \phi_{k'}\right]}. \tag{3.112}$$

3.5.9 Chemical Potential

Chemical potential of species k is,

$$\mu_k = \frac{\partial F}{\partial n_k}\bigg|_{T,V,n_{k'\neq k}}. \tag{3.113}$$

Using the Eq. 3.63 of free energy to have,

$$\frac{\mu_k}{\alpha_k k_B T} = -\frac{1}{\alpha_0}(1 + \ln \phi_0) + \frac{1}{\alpha_k}(1 + \ln \phi_k) - 2\sum_{k'} \frac{\epsilon_{1,kk'}}{k_B T} \phi_{k'} - \frac{1}{\alpha_k} \frac{n_0}{v_0} \frac{\partial v_0}{\partial n_k} \ln \phi_0 + \frac{v_r}{v_k} \ln(1 - f_k). \tag{3.114}$$

Following von Konigslow *et al.* [197], the hole volume is assumed constant so the second last term becomes zero,

$$\frac{\mu_k}{\alpha_k k_B T} = -\frac{1}{\alpha_0}(1 + \ln \phi_0) + \frac{1}{\alpha_k}(1 + \ln \phi_k) - 2\sum_{k'} \frac{\epsilon_{1,kk'}}{k_B T} \phi_{k'} + \frac{v_r}{v_k} \ln(1 - f_k). \tag{3.115}$$

3.6 Thermodynamics of Pure Fluids

For pure fluid systems, that is systems having only one species, equations of thermodynamic properties condense as follows.

3.6.1 Free Energy

$$\frac{F}{k_BT} = -\frac{V}{v_r}\left[\frac{\phi^2\epsilon_1}{k_BT} - \frac{\phi f\epsilon_2}{k_BT}\right] + \frac{V}{v_0}\phi_0 \ln\phi_0 + \frac{V}{v_r}\frac{\phi}{\alpha}\ln\phi + \frac{V\phi}{v}\left[f\ln\left\{\frac{f}{g(1-f)}\right\} + \ln(1-f)\right], \tag{3.116}$$

where, the fraction f of excited segments becomes,

$$f = \frac{ge^{-v\epsilon_2/v_rk_BT}}{1 + ge^{-v\epsilon_2/v_rk_BT}}. \tag{3.117}$$

Putting Eq. 3.117 in Eq. 3.116,

$$\frac{F}{k_BT} = -\frac{V}{v_r}\frac{\phi^2\epsilon_1}{k_BT} + \frac{V}{v_0}\phi_0\ln\phi_0 + \frac{V}{v_r}\frac{\phi}{\alpha}\ln\phi + \frac{V\phi}{v}\ln(1-f). \tag{3.118}$$

Scaled density as mentioned in section 3.5.2 simplified to,

$$\tilde{\rho} \equiv \phi. \tag{3.119}$$

Average interaction energy becomes,

$$\epsilon^* = \epsilon_1. \tag{3.120}$$

Scaled pressure for pure system becomes,

$$\tilde{P} \equiv \frac{v_rP}{\epsilon_1}. \tag{3.121}$$

Scaled temperature becomes,

$$\tilde{T} \equiv \frac{k_BT}{\epsilon_1}. \tag{3.122}$$

Average molecular size r reduced to,

$$r \equiv \alpha. \tag{3.123}$$

Characteristic volume becomes,

$$V^* = nNv. \tag{3.124}$$

Pure-component characteristic mass-density is,

$$\rho^* = \frac{nM}{V^*} = \frac{m}{V^*} = \frac{M}{Nv}, \tag{3.125}$$

where M is the molecular mass and n is the number of moles. Characteristic specific-volume becomes,

$$v^* = \frac{1}{\rho^*} = \frac{V^*}{nM}. \tag{3.126}$$

Number of moles in the system is,

$$n = \frac{m}{M}. \tag{3.127}$$

Pure-component characteristic temperature T^* and pressure P^* are,

$$P^* = \frac{\epsilon_1}{v_r}, \tag{3.128}$$

$$T^* = \frac{\epsilon_1}{k_B}. \tag{3.129}$$

Pure-component characteristic density is,

$$\rho^* = \frac{M}{\alpha v_r}. \tag{3.130}$$

Parameters α, v_r, ϵ_1 are equivalent to parameters P^*, T^*, ρ^* as,

$$v_r = \frac{k_B T^*}{P^*}, \tag{3.131}$$

$$\epsilon_1 = k_B T^*, \tag{3.132}$$

$$\alpha = \frac{MP^*}{k_B \rho^* T^*}. \tag{3.133}$$

For a given system, the above characteristic parameters are fixed except α that depends on the molecular mass of molecules in the system *i.e.* $\alpha = \alpha(M)$. Pure component characteristic flexing temperature becomes,

$$T^{**} = \frac{\epsilon_2}{k_B}. \tag{3.134}$$

Moreover, characteristic ratios become,

$$T_r = \frac{T^{**}}{T^*} = \frac{\epsilon_2}{\epsilon_1}, \tag{3.135}$$

$$V_r = \frac{v}{v_r}. \tag{3.136}$$

By using these definitions, write Eq. 3.118 of free energy as,

$$\frac{\rho^* F}{mP^*} = -\tilde{\rho} + \frac{\tilde{T}}{\alpha_0 \tilde{\rho}} (1-\tilde{\rho}) \ln (1-\tilde{\rho}) + \frac{\tilde{T}}{\alpha} \ln \tilde{\rho} + \frac{\tilde{T}}{V_r} \ln (1-f). \tag{3.137}$$

Also, rewrite fraction of excited segments as,

$$f = \frac{g e^{-V_r T_r/\tilde{T}}}{1 + g e^{-V_r T_r/\tilde{T}}}. \tag{3.138}$$

Also note the following useful relations,

$$Nn = \frac{V\phi}{v} = \frac{V}{v_r}\frac{N\phi}{\alpha}. \tag{3.139}$$

Alternatively,

$$Nn = \frac{P^* V^*}{k_B T^*}\frac{1}{V_r} = \frac{mP^*}{k_B \rho^* T^*}\frac{1}{V_r} = \frac{m\alpha}{MV_r}. \tag{3.140}$$

3.6.2 Equation of State

The equation of state will be modified to,

$$\frac{v_r P}{k_B T} = -\left(\frac{1}{\alpha_0} - \frac{1}{\alpha}\right)\phi - \frac{1}{\alpha_0}\ln \phi_0 - \frac{\phi^2 \epsilon_1}{k_B T}, \tag{3.141}$$

or,

$$\tilde{\rho}^2 + \tilde{P} + \tilde{T}\left[\left(\frac{1}{\alpha_0} - \frac{1}{r}\right)\tilde{\rho} + \frac{1}{\alpha_0}\ln(1-\tilde{\rho})\right] = 0. \tag{3.142}$$

3.6.3 Entropy

Equation of entropy condensed to,

$$\frac{S}{k_B} = -\frac{V}{v_0}\phi_0 \ln \phi_0 - \frac{V}{v_r}\frac{\phi}{\alpha}\ln\phi - \frac{V\phi}{v}\left[f \ln\left\{\frac{f}{g(1-f)}\right\} + \ln(1-f)\right]. \tag{3.143}$$

Put f from Eq. 3.117 to get,

$$\frac{S}{k_B} = -\frac{V\phi_0}{v_0}\ln\phi_0 - \frac{V\phi}{v_r}\frac{\ln\phi}{\alpha} + \frac{V\phi}{v_r}\frac{f\epsilon_2}{k_BT} - \frac{V\phi}{v}\ln(1-f). \tag{3.144}$$

Alternatively,

$$\frac{\rho^*T^*}{mP^*}S = -\frac{1}{\alpha_0\tilde{\rho}}(1-\tilde{\rho})\ln(1-\tilde{\rho}) - \frac{1}{\alpha}\ln\tilde{\rho} + \frac{fT_r}{\tilde{T}} - \frac{1}{V_r}\ln(1-f). \tag{3.145}$$

As highlighted in section 3.5.3 since $\tilde{\rho}$ and f are always less than 1 so all terms in the above expression will be positive. Thus entropy of the system is always positive at all temperatures.

3.6.4 Glass Transition Temperature

In section 3.5.3 it was shown that the Gibbs DiMarzio criterion for the glass transition is incorrect and an alternate criterion for the glass transition temperature calculations has been proposed. That is the glass transition occurs at a temperature where entropy of the system becomes fraction x of entropy S_∞ at $T \to \infty$. For pure systems, entropy S_∞ at infinite temperature is also the maximum entropy S_{max} of the system. Moreover, for pure systems, $\rho \to 0$ at $T \to \infty$. Thus, from Eq. 3.145, for long molecules we have,

$$\frac{\rho^*T^*}{mP^*}S_\infty = \frac{1}{\alpha_0}\left[1 + \frac{\alpha_0}{V_r}\ln(1+g)\right]. \tag{3.146}$$

Put $S(T_g) = xS_\infty$ in Eq. 3.145 and note that $r = \alpha$ to get,

$$\frac{x}{\alpha_0}\left[1 + \frac{\alpha_0}{V_r}\ln(1+g)\right] + \frac{1}{\alpha_0\tilde{\rho}_g}(1-\tilde{\rho}_g)\ln(1-\tilde{\rho}_g) + \frac{1}{\alpha}\ln\tilde{\rho}_g - \frac{f_gT_r}{\tilde{T}_g} + \frac{1}{V_r}\ln(1-f_g) = 0. \tag{3.147}$$

Again, in the above expression, density of the system depends on the pressure through equation of state Eq. 3.142. Thus, the above expression is a T_g versus P relation for pure systems.

3.6.5 Internal Energy

Internal energy is simplified to,

$$\frac{E}{k_BT} = -\frac{V}{v_r}\left(\frac{\phi^2\epsilon_1}{k_BT} - \frac{f\phi\epsilon_2}{k_BT}\right). \tag{3.148}$$

Alternatively,

$$\frac{\rho^*E}{mP^*} = -\tilde{\rho} + fT_r. \tag{3.149}$$

3.6.6 Isochoric Heat Capacity

Isochoric heat capacity becomes,

$$\frac{C_V}{k_B} = \frac{V\phi}{v}\left(\frac{v}{v_r}\frac{\epsilon_2}{k_BT}\right)^2 f(1-f). \tag{3.150}$$

Alternatively,

$$\frac{\rho^* T^*}{mP^*}C_V = \frac{1}{V_r}\left(\frac{V_r T_r}{\tilde{T}}\right)^2 f(1-f). \tag{3.151}$$

3.6.7 Isobaric Heat Capacity

Isobaric heat capacity reduced to,

$$\frac{C_P}{k_B} = \frac{V\phi}{v_r}\frac{\left(1+\frac{v_rP}{\phi^2\epsilon_1}\right)^2}{\frac{k_BT}{\phi\epsilon_1}\left[\frac{k_BT}{\phi\epsilon_1}\left(\frac{\phi}{\alpha_0\phi_0}+\frac{1}{r}\right)-2\right]} + \frac{V\phi}{v}\left(\frac{v}{v_r}\frac{\epsilon_2}{k_BT}\right)^2 f(1-f). \tag{3.152}$$

Again, the second term in above expression is C_V/k_B, therefore,

$$\frac{C_P - C_V}{k_B} = \frac{V\phi}{v_r}\frac{\left(1+\frac{v_rP}{\phi^2\epsilon_1}\right)^2}{\frac{k_BT}{\phi\epsilon_1}\left[\frac{k_BT}{\phi\epsilon_1}\left(\frac{\phi}{\alpha_0\phi_0}+\frac{1}{r}\right)-2\right]}. \tag{3.153}$$

Isobaric heat capacity Eq. 3.152 can also be written as,

$$\frac{\rho^* T^*}{mP^*}C_P = \frac{\left(1+\frac{\tilde{P}}{\tilde{\rho}^2}\right)^2}{\frac{\tilde{T}}{\tilde{\rho}}\left[\frac{\tilde{T}}{\tilde{\rho}}\left(\frac{1}{\alpha_0}\cdot\frac{\tilde{\rho}}{1-\tilde{\rho}}+\frac{1}{r}\right)-2\right]} + \frac{1}{V_r}\left(\frac{V_rT_r}{\tilde{T}}\right)^2 f(1-f). \tag{3.154}$$

As discussed in section 3.5.7, the second term in Eq. 3.152 is the incremental change in heat capacity ΔC_P due to flexing of segments. Thus,

$$\frac{\Delta C_P}{k_B} = \frac{V\phi}{v}\left(\frac{v}{v_r}\frac{\epsilon_2}{k_BT}\right)^2 f(1-f), \tag{3.155}$$

whereas, isobaric heat capacity below the glass transition is,

$$\frac{C_P}{k_B} = \frac{V\phi}{v_r}\frac{\left(1+\frac{v_rP}{\phi^2\epsilon_1}\right)^2}{\frac{k_BT}{\phi\epsilon_1}\left[\frac{k_BT}{\phi\epsilon_1}\left(\frac{\phi}{\alpha_0\phi_0}+\frac{1}{r}\right)-2\right]}. \tag{3.156}$$

3.6.8 Isobaric Expansion Coefficient

Isobaric expansion coefficient is modified to,

$$\alpha_P = \frac{1}{T} \frac{\left(1 + \frac{v_r P}{\phi^2 \epsilon_1}\right)}{\left[\frac{k_B T}{\phi \epsilon_1}\left(\frac{\phi}{\alpha_0 \phi_0} + \frac{1}{r}\right) - 2\right]}. \tag{3.157}$$

Alternately,

$$T^* \alpha_P = \frac{1}{\tilde{T}} \frac{\left(1 + \frac{\tilde{P}}{\tilde{\rho}^2}\right)}{\left[\frac{\tilde{T}}{\tilde{\rho}}\left(\frac{1}{\alpha_0} \cdot \frac{\tilde{\rho}}{1-\tilde{\rho}} + \frac{1}{r}\right) - 2\right]}. \tag{3.158}$$

3.6.9 Chemical Potential

Chemical potential for constant hole volume becomes,

$$\frac{\mu}{\alpha k_B T} = -\frac{1}{\alpha_0}(1 + \ln \phi_0) + \frac{1}{\alpha}(1 + \ln \phi) - 2\frac{\phi \epsilon_1}{k_B T}, \tag{3.159}$$

or,

$$\frac{\mu}{\alpha k_B T^*} = -\frac{\tilde{T}}{\alpha_0}[1 + \ln(1 - \tilde{\rho})] + \frac{\tilde{T}}{\alpha}(1 + \ln \tilde{\rho}) - 2\tilde{\rho}. \tag{3.160}$$

3.7 Thermodynamics of Binary Fluid Mixtures

3.7.1 Free Energy

Consider a binary mixture having one polymer species, denoted by p, and one solvent species (small molecules), denoted by s. Solvent molecules are considered to be infinitely rigid so f_s is zero at all temperatures. Thus, there will be no term involving f_s in thermodynamic equations. However, the fraction f_p of excited segments of the polymer species is,

$$f_p = \frac{g_p e^{-v_p \epsilon_{2,p}/v_r k_B T}}{1 + g_p e^{-v_p \epsilon_{2,p}/v_r k_B T}}. \tag{3.161}$$

For this system, free energy Eq. 3.63 is expanded as,

$$\frac{F}{k_BT} = -\frac{V}{v_r}\frac{\epsilon_{1,pp}}{k_BT}\phi_p^2 - \frac{V}{v_r}\frac{\epsilon_{1,ss}}{k_BT}\phi_s^2 - \frac{V}{v_r}\frac{2\epsilon_{1,sp}}{k_BT}\phi_s\phi_p + \frac{V}{v_r}\frac{\epsilon_{2,p}}{k_BT}f_p\phi_p + \frac{V}{v_0}\phi_0\ln\phi_0 \\ + \frac{V}{v_r}\frac{\phi_p}{\alpha_p}\ln\phi_p + \frac{V}{v_r}\frac{\phi_s}{\alpha_s}\ln\phi_s + \frac{V\phi_p}{v_p}\left[f_p\ln\left\{\frac{f_p}{g_p(1-f_p)}\right\} + \ln(1-f_p)\right]. \tag{3.162}$$

Put f_p from Eq. 3.60,

$$\frac{F}{k_BT} = -\frac{V}{v_r}\frac{\epsilon_{1,pp}}{k_BT}\phi_p^2 - \frac{V}{v_r}\frac{\epsilon_{1,ss}}{k_BT}\phi_s^2 - \frac{V}{v_r}\frac{2\epsilon_{1,sp}}{k_BT}\phi_s\phi_p + \frac{V}{v_r}\frac{\epsilon_{2,p}}{k_BT}f_p\phi_p + \frac{V}{v_0}\phi_0\ln\phi_0 \\ + \frac{V}{v_r}\frac{\phi_p}{\alpha_p}\ln\phi_p + \frac{V}{v_r}\frac{\phi_s}{\alpha_s}\ln\phi_s - \frac{V\phi_p}{v_p}\left[f_p\frac{v_p}{v_r}\frac{\epsilon_{2,p}}{k_BT} - \ln(1-f_p)\right]. \tag{3.163}$$

Scaled density expands as,

$$\tilde{\rho} = \phi_p + \phi_s. \tag{3.164}$$

Average interaction energy becomes,

$$\epsilon_1^* = \frac{1}{\tilde{\rho}}\left[\epsilon_{1,pp}\phi_p^2 + \epsilon_{1,ss}\phi_s^2 + \epsilon_{1,sp}\phi_s\phi_p\right]. \tag{3.165}$$

where, cross-component interaction energy becomes,

$$\epsilon_{1,sp} = \zeta_{sp}(\epsilon_{1,pp}\epsilon_{1,ss})^{1/2}. \tag{3.166}$$

Scaled pressure is the same,

$$\tilde{P} \equiv \frac{v_r P}{\epsilon_1^*}. \tag{3.167}$$

Scaled temperature is the same,

$$\tilde{T} \equiv \frac{k_BT}{\epsilon_1^*}. \tag{3.168}$$

Average molecular size r expands to,

$$r \equiv \frac{1}{\tilde{\rho}}\left[\frac{\phi_p}{\alpha_p} + \frac{\phi_s}{\alpha_s}\right]. \tag{3.169}$$

Number of moles is,

$$n_p = \frac{m_p}{M_p} \quad , \quad n_s = \frac{m_s}{M_s}. \tag{3.170}$$

Other binary characteristic parameters shall be expanded in similar fashion as,

$$V^* = N_p n_p v_p + N_s n_s v_s, \tag{3.171}$$

$$\rho^* = \frac{n_p M_p + n_s M_s}{V^*} = \frac{m_{total}}{V^*}, \tag{3.172}$$

$$v^* = \frac{1}{\rho^*} = \frac{V^*}{m_{total}}. \tag{3.173}$$

Characteristic temperature T^* and pressure P^* are the same,

$$P^* = \frac{\epsilon_1^*}{v_r} \qquad , \qquad T^* = \frac{\epsilon_1^*}{k_B}. \tag{3.174}$$

Similarly, pure-component characteristic parameters become,

$$V_p^* = N_p n_p v_p \qquad , \qquad V_s^* = N_s n_s v_s, \tag{3.175}$$

$$\rho_p^* = \frac{m_p}{V_p^*} = \frac{n_p M_p}{V_p^*} = \frac{M_p}{\alpha_p v_r}, \tag{3.176}$$

$$\rho_s^* = \frac{m_s}{V_s^*} = \frac{n_s M_s}{V_s^*} = \frac{M_s}{\alpha_s v_r}, \tag{3.177}$$

$$P_p^* = \frac{\epsilon_{1,pp}}{v_r} \qquad , \qquad P_s^* = \frac{\epsilon_{1,ss}}{v_r}, \tag{3.178}$$

$$T_p^* = \frac{\epsilon_{1,pp}}{k_B} \qquad , \qquad T_s^* = \frac{\epsilon_{1,ss}}{k_B}. \tag{3.179}$$

By using above definitions α_k become,

$$\alpha_p = \frac{M_p P_p^*}{k_B \rho_p^* T_p^*} \qquad , \qquad \alpha_s = \frac{M_s P_s^*}{k_B \rho_s^* T_s^*}. \tag{3.180}$$

Reference volume for individual pure systems are,

$$v_{r,p} = \frac{k_B T_p^*}{P_p^*} \qquad or \qquad v_{r,s} = \frac{k_B T_s^*}{P_s^*}. \tag{3.181}$$

whereas, reference volume of the mixed system should be,

$$v_r = \frac{k_B T^*}{P^*}. \tag{3.182}$$

However, in this work it is assumed that reference volumes of pure and mixed systems are close to each other and thus they are assumed equal *i.e.* $v_r = v_{r,p} = v_{r,s}$. However, in general, not all reference volumes need to be equal. This is a discrepancy in the SL-EOS that need to be reconciled [197]. Binary-component average interaction energies are,

$$\epsilon_{1,pp} = k_B T_p^* \qquad , \qquad \epsilon_{1,ss} = k_B T_s^*. \tag{3.183}$$

Since solvent molecules are small and rigid so there will be no flexing parameters for solvent molecules. However, for polymer molecules flexing parameters become,

$$T_p^{**} \equiv \frac{\epsilon_{2,p}}{k_B}. \tag{3.184}$$

Characteristic ratios are,

$$T_{r,p} \equiv \frac{T_p^{**}}{T_p^*} = \frac{\epsilon_{2,p}}{\epsilon_{1,pp}}, \tag{3.185}$$

$$V_{r,p} \equiv \frac{v_p}{v_r}, \tag{3.186}$$

$$N_p = \frac{\alpha_p}{V_{r,p}}. \tag{3.187}$$

Also, note following useful relations,

$$N_p n_p = \frac{V\phi_p}{v_p} = \frac{V}{v_r}\frac{N_p\phi_p}{\alpha_p}. \tag{3.188}$$

Alternatively,

$$N_p n_p = \frac{P_p^* V_p^*}{k_B T_p^*}\frac{1}{V_{r,p}} = \frac{m_p P_p^*}{k_B \rho_p^* T_p^*}\frac{1}{V_{r,p}} = \frac{m_p \alpha_p}{M_p V_{r,p}}. \tag{3.189}$$

So, fraction f_p becomes,

$$f_p = \frac{g_p e^{-T_{r,p}V_{r,p}/\tilde{T}_p}}{1 + g_p e^{-T_{r,p}V_{r,p}/\tilde{T}_p}}. \tag{3.190}$$

Rewrite free energy as,

$$\frac{\rho_p^* F}{m_p P_p^*} = -\phi_p - \frac{T_s^*}{T_p^*}\frac{\phi_s^2}{\phi_p} - 2\frac{T_{sp}^*}{T_p^*}\phi_s + \frac{\tilde{T}_p}{\alpha_0\phi_p}(1-\tilde{\rho})\ln(1-\tilde{\rho}) + \frac{\tilde{T}_p}{\alpha_p}\ln\phi_p \\ + \tilde{T}_p\frac{\phi_s \ln\phi_s}{\alpha_s\phi_p} + \frac{\tilde{T}_p}{V_r}\ln(1-f_p). \tag{3.191}$$

3.7.2 Equation of State

Expansion of equation of state Eq. 3.97 is,

$$\frac{v_r P}{k_B T} = -\left(\frac{1}{\alpha_0} - \frac{1}{\alpha_p}\right)\phi_p - \left(\frac{1}{\alpha_0} - \frac{1}{\alpha_s}\right)\phi_s - \frac{1}{\alpha_0}\ln\phi_0 - \frac{\epsilon_{1,pp}}{k_B T}\phi_p^2 - \frac{\epsilon_{1,ss}}{k_B T}\phi_s^2 - \frac{\epsilon_{1,sp}}{k_B T}\phi_s\phi_p \tag{3.192}$$

or,

$$\frac{P}{P_p^*} + \left(\frac{1}{\alpha_0} - \frac{1}{\alpha_p}\right)\tilde{T}_p\phi_p + \left(\frac{1}{\alpha_0} - \frac{1}{\alpha_s}\right)\tilde{T}_p\phi_s + \frac{\tilde{T}_p\ln(1-\tilde{\rho})}{\alpha_0} + \phi_p^2 + \frac{T_s^*}{T_p^*}\phi_s^2 + \frac{T_{sp}^*}{T_p^*}\phi_s\phi_p = 0. \tag{3.193}$$

3.7.3 Entropy

Entropy of binary system expands as,

$$\frac{S}{k_B} = -\frac{V\phi_0}{v_0}\ln\phi_0 - \frac{V\phi_p}{v_r}\frac{\ln\phi_p}{\alpha_p} - \frac{V\phi_s}{v_r}\frac{\ln\phi_s}{\alpha_s} + \frac{V\phi_p}{v_r}\frac{f_p\epsilon_{2,p}}{k_B T} - \frac{V\phi_p}{v_p}\ln(1-f_p). \tag{3.194}$$

Alternatively,

$$\frac{\rho_p^* T_p^*}{m_p P_p^*} S = -\frac{(1-\tilde{\rho})\ln(1-\tilde{\rho})}{\alpha_0\phi_p} - \frac{\ln\phi_p}{\alpha_p} - \frac{\phi_s\ln\phi_s}{\alpha_s\phi_p} + \frac{f_p T_{r,p}}{\tilde{T}_p} - \frac{\ln(1-f_p)}{V_{r,p}}. \tag{3.195}$$

Since $\tilde{\rho}$, ϕ_s, ϕ_p and f_p are always less than 1 so all terms in the above expression will be positive at all temperatures. Thus entropy of the binary system is always positive. Moreover, for $v = v_0 = v_r$, Eq. 3.194 is near-equivalent of equation 2.48 of the Condo model Ref. [23] except terms that are constants or linear in n. Additional terms in equation 2.48 are causing the Condo entropy to be negative at low temperatures. Besides, the last term of Eq. 3.194 is proportional to N whereas in Eq. 2.48 the corresponding term is proportional to $N-2$. This difference is because of the use of the artificial lattice in the Condo model. Moreover, because of the artificial lattice $f_s \neq 0$ for the Condo model so terms involving f_s are also present in Eq. 2.48.

3.7.4 Glass Transition Temperature

As discussed in section 3.5.3 that the Gibbs DiMarzio criterion for the glass transition is incorrect. According to the alternate criterion for the glass transition, put $S(T_g) = xS_\infty$

in Eq. 3.195 to get,

$$\frac{\rho_p^* T_p^*}{m_p P_p^*} x S_\infty + \frac{(1-\tilde{\rho_g})\ln(1-\tilde{\rho_g})}{\alpha_0 \phi_{p,g}} + \frac{\ln \phi_{p,g}}{\alpha_p} + \frac{\phi_{s,g} \ln \phi_{s,g}}{\alpha_s \phi_{p,g}} - \frac{f_{p,g} T_{r,p}}{\tilde{T}_{p,g}} + \frac{\ln(1-f_{p,g})}{V_{r,p}} = 0. \tag{3.196}$$

3.7.5 Internal Energy

Internal energy expands as,

$$\frac{E}{k_B T} = -\frac{V}{v_r}\left[\frac{\epsilon_{1,pp}}{k_B T}\phi_p^2 + \frac{\epsilon_{1,ss}}{k_B T}\phi_s^2 + \frac{\epsilon_{1,sp}}{k_B T}\phi_p\phi_s - \frac{\epsilon_{2,p}}{k_B T} f_p \phi_p\right]. \tag{3.197}$$

Alternatively,

$$\frac{\rho_p^* E}{m_p P_p^*} = -\left[\phi_p + \frac{T_s^*}{T_p^*}\frac{\phi_s^2}{\phi_p} + \frac{T_{sp}^*}{T_P^*}\phi_s - f_p T_{r,p}\right]. \tag{3.198}$$

Eq. 3.197 is near-equivalent to Eq. (6) of the Condo *et al.* Ref. [23] if we assume $v = v_0 = v_r$.

3.7.6 Isochoric Heat Capacity

Isochoric heat capacity becomes,

$$\frac{C_V}{k_B} = \frac{V\phi_p}{v_p}\left(\frac{v_p}{v_r}\frac{\epsilon_{2,p}}{k_B T}\right)^2 f_p(1-f_p). \tag{3.199}$$

Alternatively,

$$\frac{\rho_p^* T_p^*}{m_p P^*} C_V = \frac{1}{V_{r,p}}\left(\frac{V_{r,p} T_{r,p}}{\tilde{T}_p}\right)^2 f_p(1-f_p). \tag{3.200}$$

3.7.7 Isobaric Heat Capacity

Isobaric heat capacity expands as,

$$\frac{C_P}{k_B} = \frac{V}{v_r}\frac{\left(\frac{v_r P}{k_B T} + \frac{\epsilon_{1,pp}}{k_B T}\phi_p^2 + \frac{\epsilon_{1,ss}}{k_B T}\phi_s^2 + \frac{\epsilon_{1,sp}}{k_B T}\phi_p\phi_s\right)^2}{\left[(\phi_p+\phi_s)\left(\frac{\phi_p+\phi_s}{\alpha_0\phi_0} + \frac{1}{r}\right) - 2\left(\frac{\epsilon_{1,pp}}{k_B T}\phi_p^2 + \frac{\epsilon_{1,ss}}{k_B T}\phi_s^2 + \frac{\epsilon_{1,sp}}{k_B T}\phi_p\phi_s\right)\right]} + \frac{V\phi_p}{v_p}\left(\frac{v_p}{v_r}\frac{\epsilon_{2,p}}{k_B T}\right)^2 f_p(1-f_p), \tag{3.201}$$

or,

$$\frac{C_P - C_V}{k_B} = \frac{V}{v_r} \frac{\left(\frac{v_r P}{k_B T} + \frac{\epsilon_{1,pp}}{k_B T}\phi_p^2 + \frac{\epsilon_{1,ss}}{k_B T}\phi_s^2 + \frac{\epsilon_{1,sp}}{k_B T}\phi_p\phi_s\right)^2}{\left[(\phi_p + \phi_s)\left(\frac{\phi_p+\phi_s}{\alpha_0\phi_0} + \frac{1}{r}\right) - 2\left(\frac{\epsilon_{1,pp}}{k_B T}\phi_p^2 + \frac{\epsilon_{1,ss}}{k_B T}\phi_s^2 + \frac{\epsilon_{1,sp}}{k_B T}\phi_p\phi_s\right)\right]}. \tag{3.202}$$

Alternatively,

$$\frac{\rho_p^* T_p^*}{m_p P_p^*} C_P = \frac{\tilde{\rho}}{\phi_p} \cdot \frac{\left(1 + \frac{\tilde{P}}{\tilde{\rho}^2}\right)^2}{\frac{\tilde{T}}{\tilde{\rho}}\left[\frac{\tilde{T}}{\tilde{\rho}}\left(\frac{1}{\alpha_0} \cdot \frac{\tilde{\rho}}{1-\tilde{\rho}} + \frac{1}{r}\right) - 2\right]} + \frac{1}{V_{r,p}}\left(\frac{V_{r,p} T_{r,p}}{\tilde{T}_p}\right)^2 f_p(1 - f_p), \tag{3.203}$$

where,

$$\tilde{T} = \frac{\tilde{\rho}^2}{\frac{\phi_p^2}{\tilde{T}_p} + \frac{\phi_s^2}{\tilde{T}_s} + \frac{\phi_p\phi_s}{\tilde{T}_{sp}}}. \tag{3.204}$$

Incremental change in heat capacity ΔC_P due to flexing of segments is,

$$\frac{\Delta C_P}{k_B} = \frac{V\phi_p}{v_p}\left(\frac{v_p}{v_r}\frac{\epsilon_{2,p}}{k_B T}\right)^2 f_p(1 - f_p), \tag{3.205}$$

whereas, isobaric heat capacity below the glass transition is,

$$\frac{C_P}{k_B} = \frac{V}{v_r} \frac{\left(\frac{v_r P}{k_B T} + \frac{\epsilon_{1,pp}}{k_B T}\phi_p^2 + \frac{\epsilon_{1,ss}}{k_B T}\phi_s^2 + \frac{\epsilon_{1,sp}}{k_B T}\phi_p\phi_s\right)^2}{\left[(\phi_p + \phi_s)\left(\frac{\phi_p+\phi_s}{\alpha_0\phi_0} + \frac{1}{r}\right) - 2\left(\frac{\epsilon_{1,pp}}{k_B T}\phi_p^2 + \frac{\epsilon_{1,ss}}{k_B T}\phi_s^2 + \frac{\epsilon_{1,sp}}{k_B T}\phi_p\phi_s\right)\right]}. \tag{3.206}$$

3.7.8 Isobaric Expansion Coefficient

Isobaric expansion coefficient becomes,

$$\alpha_{P,k} = \frac{1}{T} \frac{\left(\frac{v_r P}{k_B T} + \frac{\epsilon_{1,pp}}{k_B T}\phi_p^2 + \frac{\epsilon_{1,ss}}{k_B T}\phi_s^2 + \frac{\epsilon_{1,sp}}{k_B T}\phi_p\phi_s\right)}{\left[(\phi_p + \phi_s)\left(\frac{\phi_p+\phi_s}{\alpha_0\phi_0} + \frac{1}{r}\right) - 2\left(\frac{\epsilon_{1,pp}}{k_B T}\phi_p^2 + \frac{\epsilon_{1,ss}}{k_B T}\phi_s^2 + \frac{\epsilon_{1,sp}}{k_B T}\phi_p\phi_s\right)\right]}. \tag{3.207}$$

Alternately,

$$T_p^* \alpha_P = \frac{1}{\tilde{T}_p} \frac{\left(1 + \frac{\tilde{P}}{\tilde{\rho}^2}\right)}{\left[\frac{\tilde{T}}{\tilde{\rho}}\left(\frac{1}{\alpha_0} \cdot \frac{\tilde{\rho}}{1-\tilde{\rho}} + \frac{1}{r}\right) - 2\right]}, \tag{3.208}$$

where,

$$\tilde{T} = \frac{\tilde{\rho}^2}{\frac{\phi_p^2}{\tilde{T}_p} + \frac{\phi_s^2}{\tilde{T}_s} + \frac{\phi_p \phi_s}{\tilde{T}_{sp}}}. \tag{3.209}$$

3.7.9 Chemical Potential

Chemical potential of solvent 's' for constant hole volume is,

$$\frac{\mu_s}{\alpha_s k_B T} = -\frac{1}{\alpha_0}(1 + \ln \phi_0) + \frac{1}{\alpha_s}(1 + \ln \phi_s) - 2\left(\frac{\epsilon_{1,ss}}{k_B T}\phi_s + \frac{\epsilon_{1,sp}}{k_B T}\phi_p\right), \tag{3.210}$$

or,

$$\frac{\mu}{\alpha_s k_B T_s^*} = -\frac{\tilde{T}_s}{\alpha_0}[1 + \ln(1 - \tilde{\rho})] + \frac{\tilde{T}_s}{\alpha_s}(1 + \ln \phi_s) - 2\left(\phi_s + \frac{T_{sp}^*}{T_s^*}\phi_p\right). \tag{3.211}$$

3.8 Unaccounted Degrees of Freedom

3.8.1 Rotational and Vibrational Degrees of Freedom

To fit isobaric heat capacity equation 3.154 on experimental data of pure polymeric systems it is necessary to consider rotational and vibrational degrees of freedom that are ignored in the model since significant heat energy stores in these degrees of freedom. Linear vibration includes kinetic energy and potential energy of vibrating molecular bonds whereas rotational vibration includes the kinetic energy of flexing segments. The potential energy of flexing segments is already considered in the model through flexing energy ϵ_2. Fortunately, the free energy from these degrees of freedom only depends on temperature of the system. Thus, SL-EOS is insensitive to these degrees of freedom because of equation 3.95. However, for heat capacity equations, the effect of these degrees of freedom should be taken into account by adding the first two terms of Taylor's expansion in heat capacity equations, *i.e.*,

$$C_{rot.,vib.}(T) = A + BT. \tag{3.212}$$

Thus, the final expression that should be fitted on heat capacity data above glass transition region is,

$$\frac{C_P}{m} = \frac{P^*}{\rho^* T^*}\left[\frac{\left(1 + \frac{\tilde{P}}{\tilde{\rho}^2}\right)^2}{\frac{\tilde{T}}{\tilde{\rho}}\left[\frac{\tilde{T}}{\tilde{\rho}}\left(\frac{1}{\alpha_0}\cdot\frac{\tilde{\rho}}{1-\tilde{\rho}} + \frac{1}{r}\right) - 2\right]} + \frac{1}{V_r}\left(\frac{V_r T_r}{\tilde{T}}\right)^2 f(1-f)\right] + A + BT. \tag{3.213}$$

3.8.2 Higher Energy Levels for Bending

In this model, only one flexed state has been assumed to account for the finite flexibility of molecules. However, the model can be improved by considering several excited states of different energies. For instance, for a system having two flexed states, the free energy equation will be modified to,

$$\frac{F}{k_BT} = -\frac{V}{v_0}\left[\frac{\phi^2\epsilon_1 - f_1\phi\epsilon_2 - f_2\phi\epsilon_3}{k_BT}\right] + \frac{V}{v_0}\phi_0\ln\phi_0 + \frac{V}{v_0}\frac{\phi}{\alpha}\ln\phi + \frac{V\phi}{v}\left[f_1\ln\left(\frac{f_1}{1-f_1-f_2}\right) + f_2\ln\left(\frac{f_2}{1-f_1-f_2}\right) + \ln\left(1-f_1-f_2\right) - f_1\ln\left(g_1\right) - f_2\ln\left(g_2\right)\right]. \tag{3.214}$$

While writing the above expression it is assumed $v_r = v_0$. At equilibrium, the fraction of excited segments in each flexed state becomes,

$$f_1 = \frac{g_1 e^{-\frac{v\epsilon_2}{v_0 k_B T}}}{1 + g_1 e^{-\frac{v\epsilon_2}{v_0 k_B T}} + g_2 e^{-\frac{v\epsilon_3}{v_0 k_B T}}}, \tag{3.215}$$

$$f_2 = \frac{g_2 e^{-\frac{v\epsilon_3}{v_0 k_B T}}}{1 + g_1 e^{-\frac{v\epsilon_2}{v_0 k_B T}} + g_2 e^{-\frac{v\epsilon_3}{v_0 k_B T}}}. \tag{3.216}$$

Internal energy and entropy become,

$$E = -\frac{V}{v_0}\left[\phi^2\epsilon_1 - f_1\phi\epsilon_2 - f_2\phi\epsilon_3\right]. \tag{3.217}$$

$$\frac{S}{k_B} = -\frac{V}{v_0}\phi_0\ln\phi_0 - \frac{V}{v_0}\frac{\phi}{\alpha}\ln\phi - \frac{V\phi}{v}\left[f_1\ln\left(\frac{f_1}{1-f_1-f_2}\right) + f_2\ln\left(\frac{f_2}{1-f_1-f_2}\right) + \ln\left(1-f_1-f_2\right) - f_1\ln\left(g_1\right) - f_2\ln\left(g_2\right)\right]. \tag{3.218}$$

Isochoric heat capacity becomes,

$$\frac{C_V}{Nnk_B} = \frac{c_1^2 g_1 e^{-\frac{c_1}{T}} + c_2^2 g_2 e^{-\frac{c_2}{T}} + (c_1-c_2)^2 g_1 g_2 e^{-\frac{c_1+c_2}{T}}}{T^2(1 + g_1 e^{-\frac{c_1}{T}} + g_2 e^{-\frac{c_2}{T}})^2}, \tag{3.219}$$

where,

$$c_1 \equiv \frac{V\phi\epsilon_2}{Nnv_0k_B} = \frac{v\epsilon_2}{v_0k_B}, \tag{3.220}$$

$$c_2 \equiv \frac{V\phi\epsilon_3}{Nnv_0k_B} = \frac{v\epsilon_2}{v_0k_B}. \tag{3.221}$$

$$\tag{3.222}$$

Isobaric heat capacity becomes,

$$\frac{C_P}{k_B} = \frac{V\phi}{v_0}\frac{\left(1+\frac{v_0P}{\phi^2\epsilon_1}\right)^2}{\frac{k_BT}{\phi\epsilon_1}\left[\frac{k_BT}{\phi\epsilon_1}\left(\frac{\phi}{\phi_0}+\frac{1}{r}\right)-2\right]} + \frac{V\phi}{v}\left[\frac{c_1^2g_1e^{-\frac{c_1}{T}}+c_2^2g_2e^{-\frac{c_2}{T}}+(c_1-c_2)^2g_1g_2e^{-\frac{c_1+c_2}{T}}}{T^2(1+g_1e^{-\frac{c_1}{T}}+g_2e^{-\frac{c_2}{T}})^2}\right]. \tag{3.223}$$

However, such extensions make the model very complex involving many fitting parameters.

Chapter 4

Regression, Analysis and Comparison

The model requires experimental data to regress characteristic parameters. These characteristic parameters can be divided into three sets. First set of characteristic parameters includes pure-component parameters P_k^*, T_k^* and ρ_k^*. These parameters can be obtained, in a conventional way, by fitting SL-EOS Eq. 3.142 on PVT data of pure systems [95, 164]. Second set of parameters includes binary interaction parameters $\zeta_{kk'}$ and mixture hole volume v_0. These parameters can be obtained from experimental data of solubility and/or swelling [197]. Third set consists of flexing parameters of pure systems: $g_k, \epsilon_{2,k}$ and x_k. These parameters can be obtained by using glass transition temperature versus pressure data [23] and/or by using isobaric heat capacity data. In this research, we are only dealing with pure fluids and binary solvent-polymer mixtures. Thus, mentioning explicitly, the required pure-component characteristic parameters are P_p^*, T_p^* and ρ_p^* for pure polymers and P_s^*, T_s^* and ρ_s^* for pure solvents. Whereas, for binary mixtures, the required parameters are ζ_{sp} and v_0. Since solvent molecules are too small to flex thus $g_s = 0$ and consequently all terms involving $\epsilon_{2,s}$ vanish in all equations. Moreover, solvent molecules do not undergo glass transition thus we cannot define parameter x_s for solvent. Thus, the required flexing parameters for pure polymers as well as for binary mixtures are g_p and $\epsilon_{2,p}$. However, note that x_p is not an independent parameter, specific reasons are discussed later in the thesis. Apart from that, following von Konigslow *et al.* [197] we have chosen $v_r = v_0$ for all systems without losing generality.

Since the extension proposed in this model is similar to the extension proposed by Condo *et al.* [23] thus flexing parameters of the proposed model have a direct correspondence with flexing parameters of Condo model. Flexing parameters of the Condo model are lattice number z (instead of g_p and g_s), energy of flexed segments of polymer $\epsilon_{2,p}$ and energy of flexed segments of solvent $\epsilon_{2,s}$ that is zero. Contrary to the present model, in Condo

model terms involving f_s do not vanish because Condo model assumes the same lattice number $z \neq 0$ for polymer and solvent in a binary mixture however in the present model the corresponding parameter $g_s = 0$. In addition, the Condo model is based on the Gibbs DiMarzio criterion [36,62] that asserts entropy $S(T_g) = 0$ so we can say that for the Condo model $x_p = 0$. In short, x_p is the only additional parameter in the present model that is not present in the Condo model. Once we have a procedure for finding x_p we may follow Condo's method to regress g_p and $\epsilon_{2,p}$. Moreover, in the present model, we have assumed that $v = v_0$ (or $V_r = 1$) without loss of generality. The same is true for the lattice-based Condo model because the artificial lattice imposes the requirement that $v = v_0$.

4.1 Method # 1

As discussed in the previous section, the Condo method could be used to regress flexing parameters g_p and $\epsilon_{2,p}$ by assuming an arbitrary value of x_p. The Condo method requires two experimental values, the glass transition temperature T_g of the pure polymeric system at atmospheric pressure and the slope dT_g/dP of glass transition temperature versus pressure curve. By using these two experimental values one can plot a straight line in $T_g - P$ plane and regress g_p and $\epsilon_{2,p}$ by fitting Eq. 3.147 on that straight line against an assumed value of x_p with a constraint that the regressed curve must pass through T_g. Finally, the same procedure can be repeated for different values of x_p to get multiple sets $(x_p, g_p, \epsilon_{2,p})$.

Figure 4.1 shows the $T_g(P)$ plots obtained by fitting Eq. 3.147 on the straight line against $x = 0.3, 0.6$ and 0.8 for pure poly(methyl-methacrylate) (PMMA). It can be noticed that all resulting $T_g(P)$ curves are close to the experimental data [128] because the values of $(g_p, \epsilon_{2,p})$ adjusts accordingly as the value of x_p changes (see table 4.1). This means that the choice of x_p does not have significant effect on $T_g(P)$ curves. Thus there is a redundancy in this method. However, corresponding $C_P(T)$ theoretical curves [1] shifts due to changing x values as shown in figure 4.2. This redundancy gives an opportunity to simultaneously fit Eq. 3.152 on isobaric heat capacity data. In other words, both $T_g(P)$ and $C_P(T)$ experimental data are required to lock all unknown parameters.

Since fitting Eq. 3.147 on $T_g(P)$ experimental data alone cannot lock the model parameters this enabled the Condo model to work for Gibbs DiMarzio criterion ($x_p = 0$). To further substantiate this argument we have plotted Eq. 2.48 of the Condo model in figure 4.3 by regressing z and $\epsilon_{2,p}$ against several arbitrary non-zero values of entropy $S(T_g) \neq 0$ and found that all curves obey the experimental data. The values of flexing parameters

[1] Isobaric heat capacity equation for the Condo model is found to be exactly the same as Eq. 3.152 of the present model for long polymer chains.

Flexing Parameters by Condo Method		
x_p	g_p	$\epsilon_{2,p}$ (J/mol)
0.3	2.16	9182
0.6	5.73	5859
0.8	63.68	8063

Table 4.1: Values of flexing parameters for pure PMMA regressed by using Condo *et al.* method against different values of x_p. Experimental data is taken from [128].

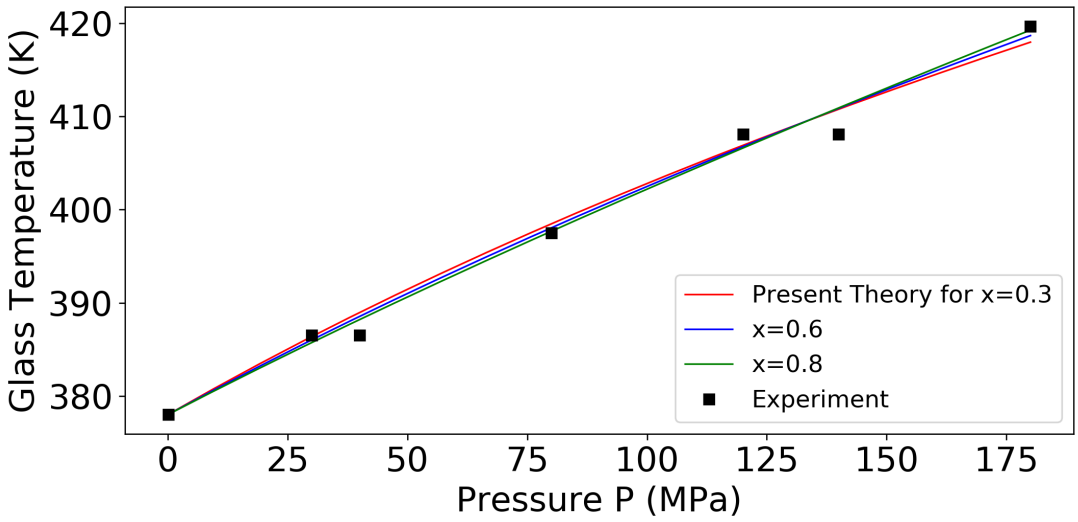

Figure 4.1: Glass transition temperature versus pressure curves for pure PMMA obtained by following Condo *et al.* method for different values of x_p. Experimental data [128] are shown by black points.

regressed by using arbitrary values of $S(T_g)$ are shown in the table 4.2. This proves that the Gibbs DiMarzio criterion worked because of a redundancy that can be removed by simultaneously fitting $T_g(P)$ and $C_P(T)$ equations on experimental data.

4.1.1 Limitations

This method has the following limitations:

1. The slope of $T_g(P)$ curve is assumed to be constant so this method can only be used for the polymeric systems that have linear $T_g(P)$ behaviour over a given pressure range.

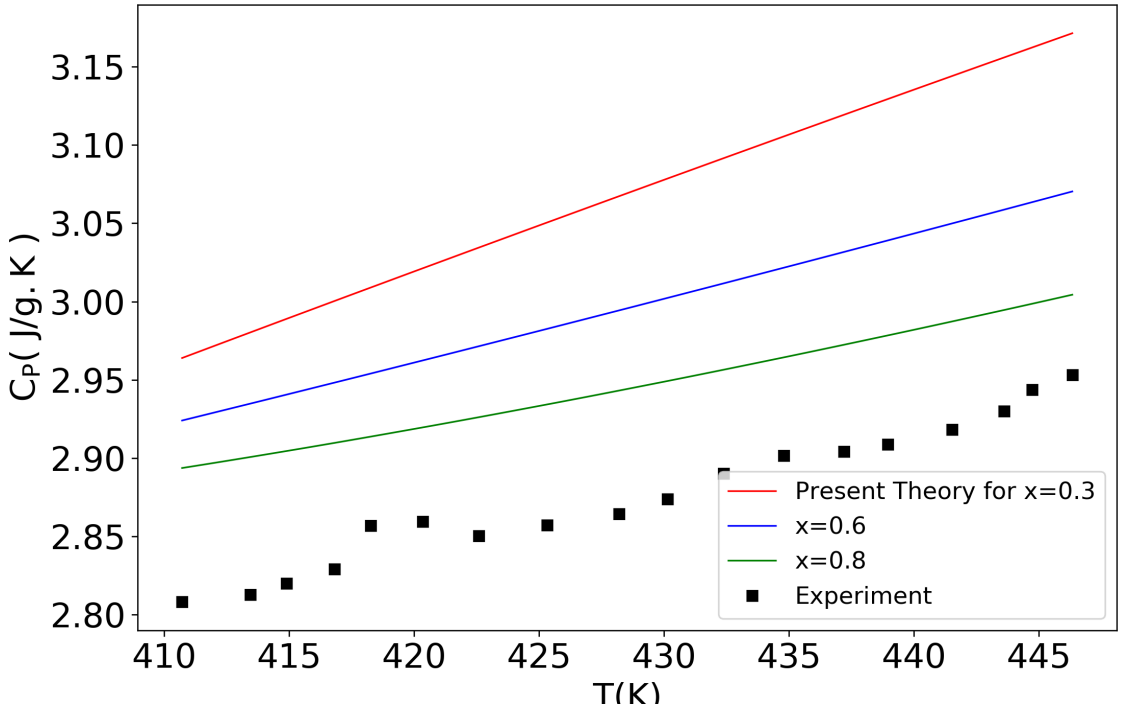

Figure 4.2: Isobaric heat capacity C_p versus temperature T curves from pure PMMA obtained for Condo *et al.* method against different values of x. Experimental data [45] are shown by black points.

2. Extensive experimental $T_g(P)$ data is required to find the reliable value of slope dT_g/dP. This limits the predictive power of this method.
3. With the finding that Gibbs DiMarzio criterion is incorrect, now isobaric specific heat capacity data is also required to regress flexing parameters.

4.2 Method # 2

To overcome the limitations of the previous method and thus to increase the predictive power of the model it is inevitable to have an alternate method. The root-cause of the limitations is the use of experimental value dT_g/dP. To find an equation of dT_g/dP one needs to take the derivative of Eq. 3.147 of T_g with respect to pressure. However, Eq. 3.147 follows from Eq. 3.145 of entropy. Thus, one should be able to use dS/dT instead dT_g/dP

Flexing Parameters of Condo Model		
$S@Tg$ (J/g.K)	z	$\epsilon_{2,p}$ (J/mol)
-0.2	4.0	8807
0.0	5.0	7428
0.2	6.0	6388

Table 4.2: Values of flexing parameters for pure PMMA regressed for Condo *et al.* model against different values of $S(T_g)$. Experimental data is taken from [128].

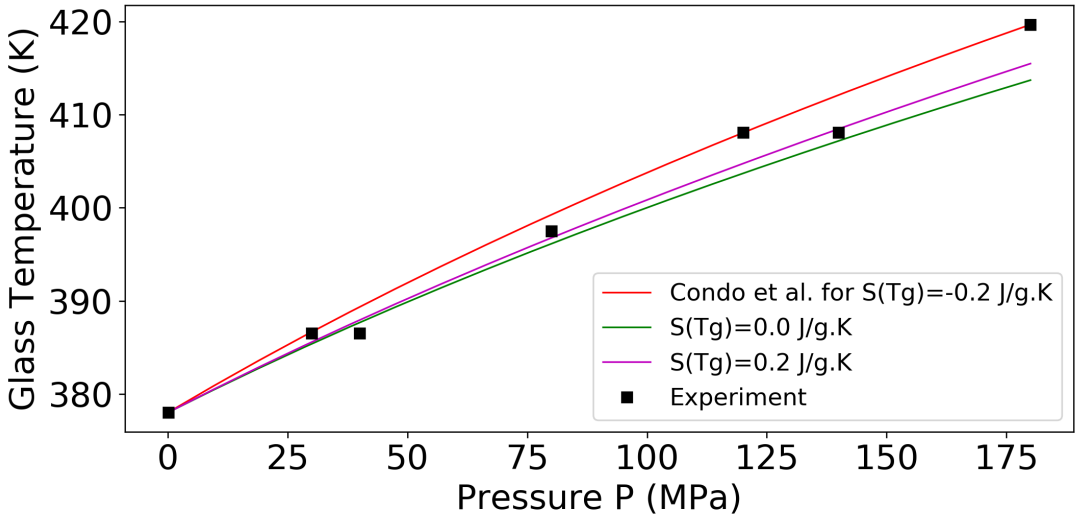

Figure 4.3: Glass transition temperature versus pressure curves for pure PMMA obtained for Condo *et al.* model against different values of $S(T_g)$. Experimental data [128] are shown by black points.

to regress flexing parameters. In addition, Eq. 3.106 implies that isobaric heat capacity corresponds to dS/dT. This provides an inspiration to replace dT_g/dP experimental value with some appropriate value of isobaric heat capacity. Since many authors have mentioned $\Delta C_P(T_g)$ across T_g in their research papers so it is best to choose $\Delta C_P(T_g)$ value as a replacement of dT_g/dP. In a nutshell, we can simultaneously solve Eq. 3.155 and Eq. 3.147 at $T = T_g$ and $P = P_{atm}$ to find the values of g_p and $\epsilon_{2,p}$ against a series of assumed values of x_p. Finally, a value of x_p that gives the best C_p data fit should be the correct value. So, for pure PMMA, figures 4.4 and 4.5 of predicted $T_g(P)$ and $C_p(T)$ curves have been plotted by using this technique. Experimental data of T_g is taken from Ref. [128]

whereas $\Delta C_p(T_g)$ is calculated by using C_p data from Ref. [45]. It is clear from the figures that increasing values of x_p shifts heat capacity curve downward while opposite is true for the glass transition temperature curve. Thus, a trade-off should be hypothesized to get simultaneous fits on heat capacity and glass transition temperature data.

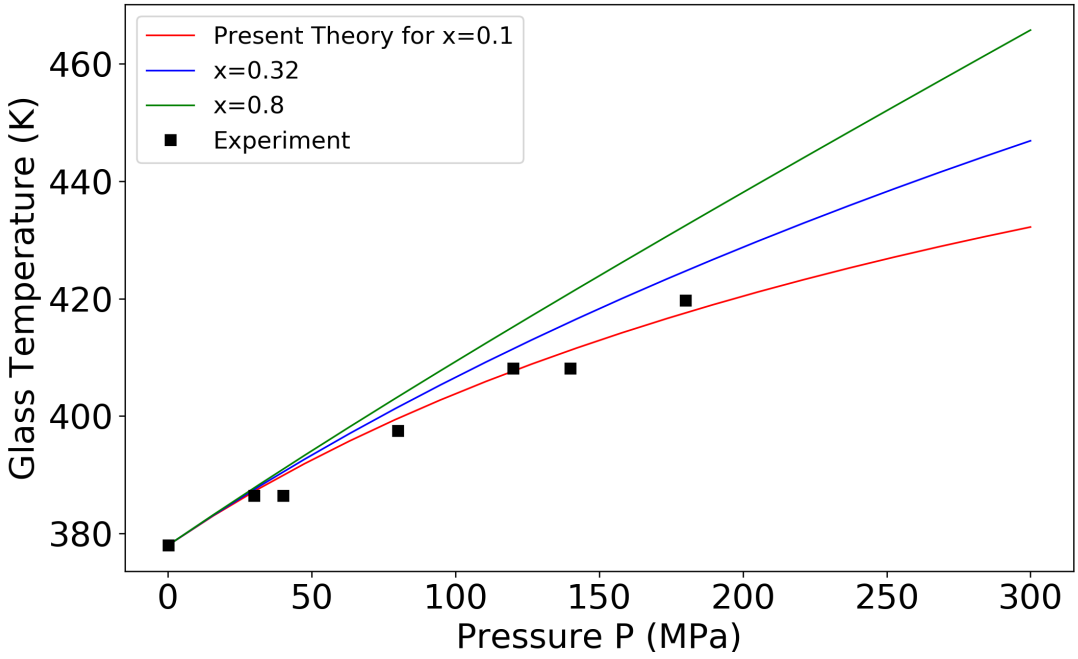

Figure 4.4: Glass transition temperature versus pressure curves for pure PMMA against different values of x_p. Experimental data [128] are shown by black points.

Figure 4.6 shows a plot of g_p versus x_p for pure PMMA obtained by solving Eqs. 3.147 and 3.155 simultaneously at $T = T_g$ and $P = P_{atm}$. The plot has a minimum $g_p(x) = 1.66$ at $x_p = 0.32$ and corresponding $\epsilon_{2,p} = 8094$ J/mol. From figures 4.4 and 4.5 it can be noticed that at this minimum ($x_p = 0.323$) both $T_g(P)$ and $C_p(T)$ predictions are reasonable. This offers a hope to hypothesize that:

"The value of x_p at g_{min} is the correct value that simultaneously describes the $T_g(P)$ and $C_P(T)$ behaviour of pure polymeric systems".

In this work we have used this method for calculating values of flexibility parameters.

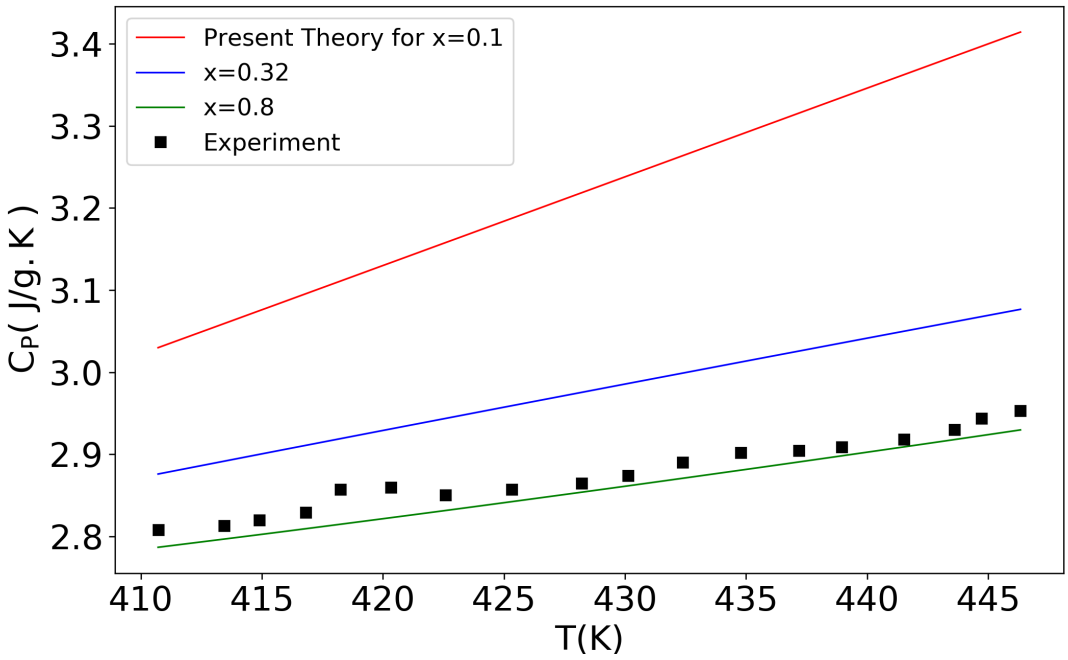

Figure 4.5: Isobaric heat capacity C_p versus temperature T curves of pure PMMA against different values of x_p. Experimental data [45] are shown by black points.

4.2.1 Justification of Hypothesis

In the present model, it is assumed that pure polymeric systems consist of two energy levels, unflexed and flexed, to account for the finite flexibility of polymer molecules. However, this assumption is very crude and real systems can have many intermediate flexed states having energies between the energies of unflexed and flexed states. Consequently, these intermediate states manifest their presence by changing the values of multiplicity g_p of the flexed state in the model. In other words, by assuming two energy levels for flexing we are assigning equal energy $\epsilon_{2,p}$ to all intermediate states and the highest flexed state. Thus to make predictions of the model accurate above glass transition temperature it is necessary to purge these intermediate states out from the highest flexed state by minimizing the multiplicity g_p.

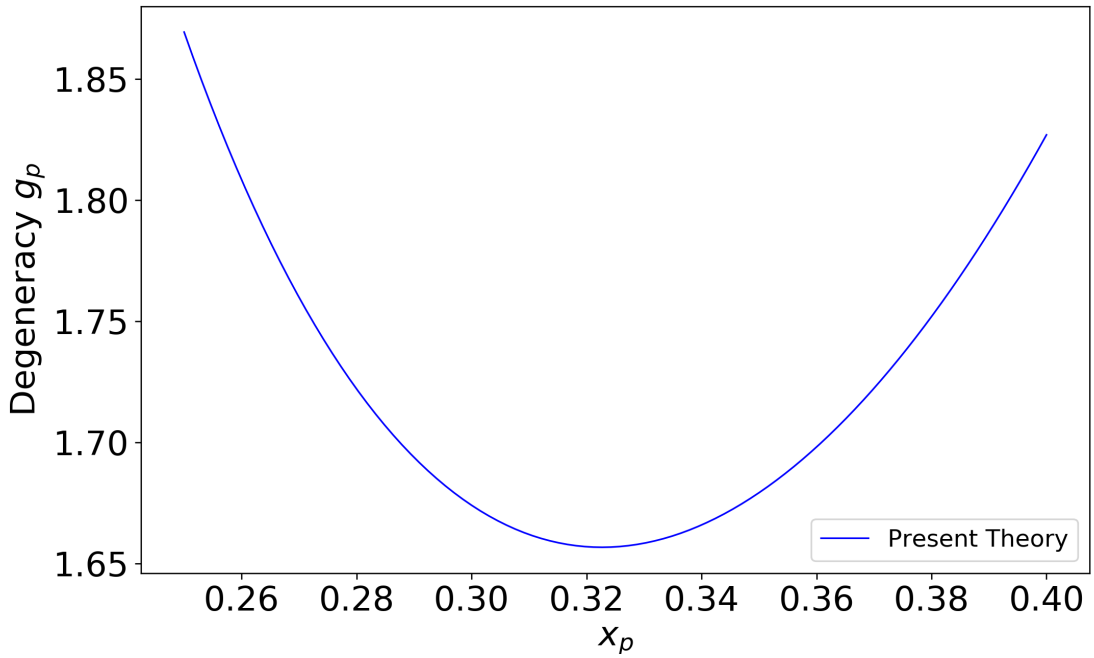

Figure 4.6: Plot of degeneracy g_p versus x_p for pure PMMA obtained by solving Eq. 3.147 and Eq. 3.155 simultaneously. To obtain the above plot the T_g data is used from [128] whereas C_p data is used from [45].

4.3 Calculated Flexibility Parameters for Present Model by using Method #2

In this section comparisons of $T_g(P)$ and $C_P(T)$ predictions from the present model and the Condo model [23] have been presented. SL-EOS characteristic parameters and references of experimental data used in this study are mentioned in tables 4.3 and 4.4, respectively.

The values of glass transition temperatures at atmospheric pressure are mentioned explicitly in the references of T_g data. However, values of $\Delta C_P(T_g)$ have been found by fitting two straight lines on experimental $C_P(T)$ data. One straight line $[C_P(T) = A + BT]$ is fitted on the data below T_g while the other straight line $[C'_P(T) = A' + B'T]$ is fitted on the data above T_g. Then, $\Delta C_P(T_g)$ is determined by subtracting both straight line equations at $T = T_g$ *i.e.* $\Delta C_P(T_g) = C'_P(T_g) - C_P(T_g)$. The calculated values of $\Delta C_p(T_g)$ are given in table 4.5.

Polymer Type	SL-EOS Parameters			
	Ref.	P^* (MPa)	T^* (K)	ρ^* (g/cm^3)
PMMA	[128]	503.0	696	1.269
PS	[151]	357.0	735	1.105
PVAc	[157]	504.2	592	1.282
PVME	[157]	463.0	567	1.120
PC	[157]	574.4	728	1.293

Table 4.3: SL-EOS parameters of polymers.

Experimental Data References			
Polymer Name	**Abbreviation**	$T_g(P)$**-Data**	$C_P(T)$**-Data**
Polymethyl-methacrylate	PMMA$^{(a)}$	[65]	[45]
Polymethyl-methacrylate	PMMA$^{(b)}$	[128]	[2]
Polystyrene	PS	[151]	[156]
Polyvinyl-acetate	PVAc	[160]	[169]
Polyvinyl-methylether	PVME	[14]	[150]
Polycarbonate	PC	[214]	[208]

Table 4.4: References of experimental data of polymers used in this study.

.

Polymers	Isobaric Specific Heat Capacity (J/g.K)					
	Ref.	A	B	A′	B′	$\Delta C_P(T_g)$
PMMA (1981)	[45]	0.000	0.0039	0.349	0.0037	0.266
PMMA (1997)	[2]	0.000	0.0055	1.214	0.0033	0.376
PS	[156]	0.000	0.0037	0.515	0.0031	0.291
PVAc	[169]	0.000	0.0035	1.096	0.0016	0.488
PVME	[150]	0.358	0.0028	1.134	0.0018	0.520
PC	[208]	0.114	0.0031	0.902	0.0017	0.231

Table 4.5: Values of A and B are regressed by fitting equation $C_P = C_{P\infty} + A + BT$ on experimental heat capacity data below glass transition temperature. Values of A' and B' are similarly regressed by fitting equation $C'_P = C_{P\infty} + A' + B'T$ on heat capacity data above glass transition temperature. $\Delta C_P(T_g)$ is estimated by $\Delta C_P(T_g) = C'_P(T_g) - C_P(T_g)$. Note, $C_{P\infty}$ is the heat capacity of infinitely flexible molecules *i.e.* Eq. 3.156.

Polymer Type	Glass Transition Data			
	Ref.	T_g (K)	dT_g/dP (K/MPa)	Linear Pr. Range (MPa)
PMMA (2011)	[65]	352.00	0.300	150.00
PMMA (1975)	[128]	378.00	0.236	180.00
PS	[151]	374.00	0.316	160.00
PVAc	[160]	311.00	**0.216**	**150.00**
PVME	[14]	247.60	**0.149**	**177.70**
PC	[214]	423.40	0.530	59.30

Table 4.6: Experimental data of glass transition temperatures at atmospheric pressure of different polymers with corresponding references. For PVAc and PVME dT_g/dP values have been self-regressed in this study by performing linear fits on the experimental glass transition temperature data over the mentioned linear pressure range.

Moreover, table 4.7 shows calculated values of flexibility parameters found by simultaneously solving Eq. 3.147 and Eq. 3.155 against different values of x for the point T_g and then choosing the values that have given g_{min}.

4.4 Calculated Flexibility Parameters for the Condo Model by using Method #1

To plot $T_g(P)$ and $C_P(T)$ graphs from the Condo theory [23] we need to calculate flexibility parameters by using the Condo procedure and Gibbs DiMarzio criterion (Method # 1). In general, $T_g(P)$ behaviour of polymers is not linear so to calculate dT_g/dP we have only considered $T_g(P)$ experimental data within a pressure range over which $T_g(P)$ behaviour of polymers is reasonably linear. Then, dT_g/dP values have been regressed by fitting straight lines over the linear part of $T_g(P)$ data. Regressions have been carried out with a constraint that straight lines must pass through point $T_g(P_{atm})$. For most polymers that are used in this study, dT_g/dP values are explicitly mentioned in the corresponding references (see table 4.6). However, for PVAc and PVME, dT_g/dP values have been self-regressed. Regressed values of dT_g/dP and the corresponding pressure range used for the regression are mentioned in table 4.6.

Thus, by using dT_g/dP and T_g straight lines have been plotted over the linear pressure range for each polymeric system and the Condo flexibility parameters, z and $\epsilon_{2,p}$, have been regressed by fitting Eq. 2.48 of the Condo paper [23] on corresponding $T_g(P)$ straight lines within the mentioned linear pressure range. Regressed values of these flexibility parameters

Polymer Type	Present Theory Parameters			Condo Theory Parameters	
	g	ϵ_2 (J/mol)	x	z	ϵ_2 (J/mol)
PMMA (a)	1.08	7094	0.293	4	4714
PMMA (b)	1.66	8094	0.323	5	7428
PS	1.67	8013	0.311	5	7160
PVAc	1.91	6815	0.321	5	6029
PVME	1.83	5387	0.288	5	4480
PC	0.84	8273	0.317	4	6247

Table 4.7: Estimated values of flexing parameters of the present model and the Condo model [23].

are mentioned in table 4.7.

4.5 Comparison of Predictions from Present Theory and Condo Theory

In sections 4.3 and 4.4 characteristic parameters of the present model and the Condo model have been evaluated and mentioned in table 4.7. Thus, the final step is to compare corresponding $T_g(P)$ and $C_p(T)$ plots of both models.

It is clear from figure 4.7 that $T_g(P)$ predictions from the present theory are better than the corresponding predictions from the Condo theory for all polymers. Besides, the present theory made predictions by using only two experimental values, namely, the glass transition temperature at atmospheric pressure and the change in isobaric heat capacity across glass transition. On the other hand, the Condo model requires extensive $T_g(P)$ data for regression of flexibility parameters. Thus, the present model is more powerful as well as more accurate as compared to the Condo model in predicting $T_g(P)$ behaviour of polymers.

Figure 4.8 shows predicted $C_p(T)$ behaviour of polymers at atmospheric pressure and above glass transition temperatures of corresponding polymers. Flexibility parameters are mentioned in table 4.7. Again, for all pure polymers, predictions from the present model are superior compared to the Condo model. As discussed in section 3.8, these isobaric heat capacity plots have been obtained by using Eq. 3.213 to account for the degrees of freedom that are ignored in both models. Values of A and B are taken from table 4.5 against corresponding polymers.

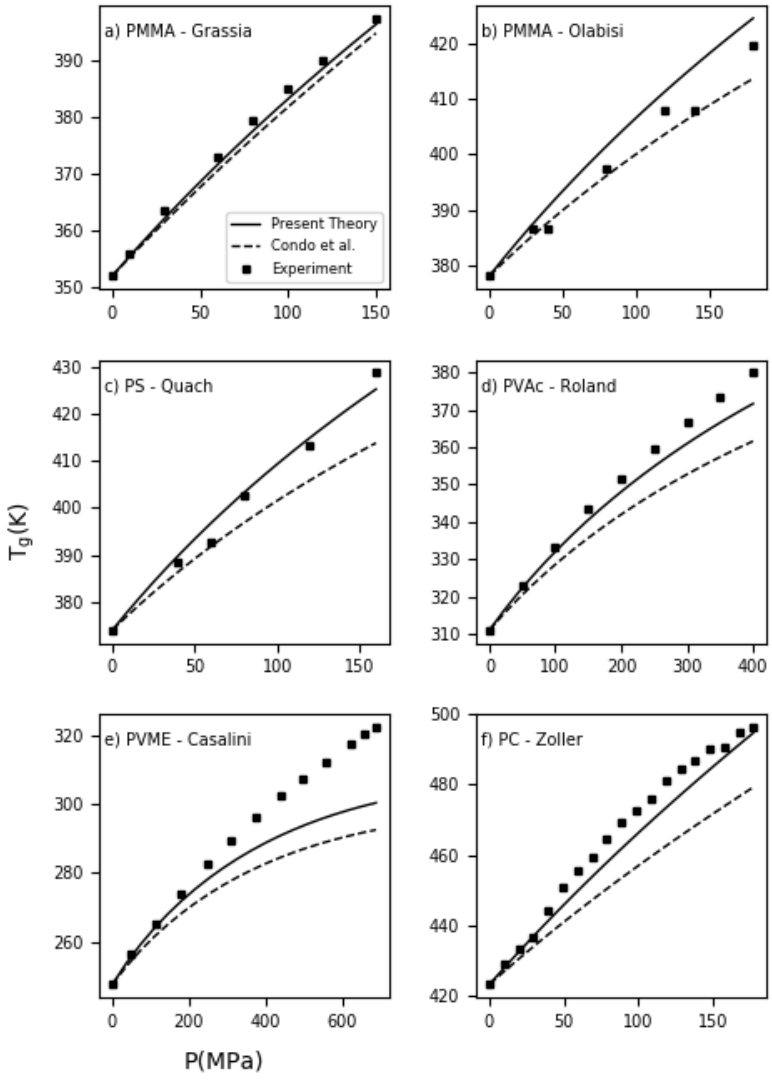

Figure 4.7: Glass transition temperature as a function of pressure for pure polymers. (a) PMMA (2011), (b) PMMA (1975), (c) PS, (d) PVAc, (e) PVME, and (f) PC. Experimental data are shown by black squares taken from references [14,65,128,151,160,214], respectively. Solid curves show theoretical predictions from the present theory and dashed curves show predictions from the Condo theory.

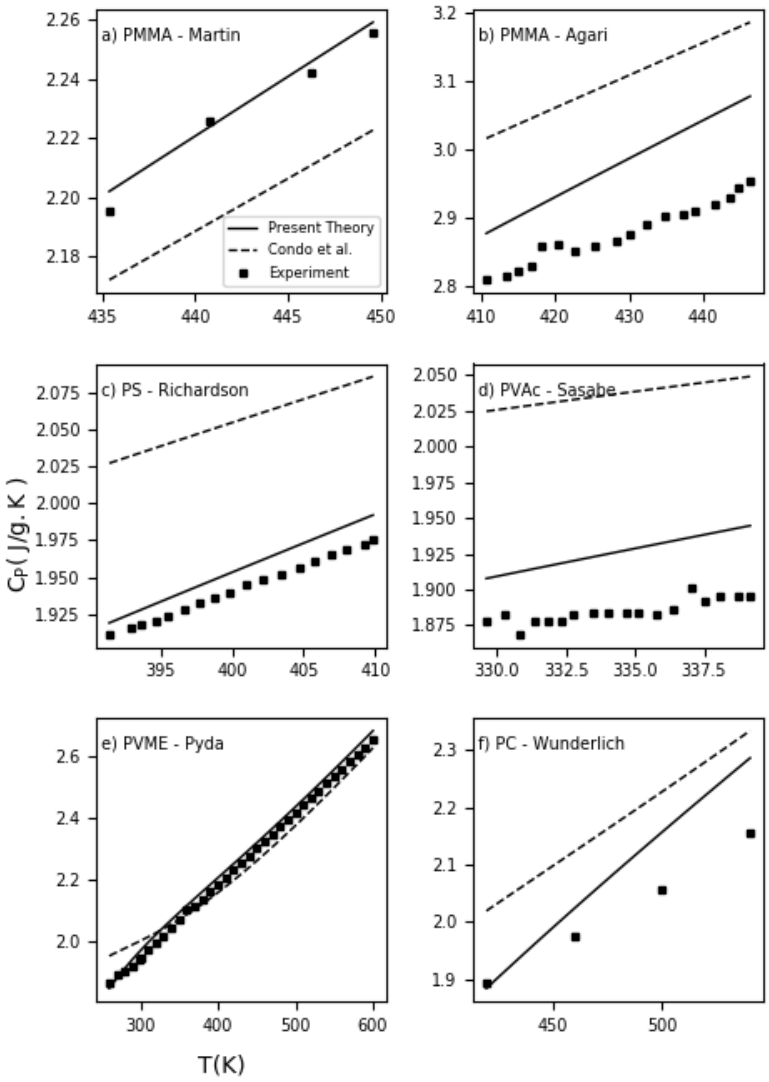

Figure 4.8: Isobaric heat capacity as a function of temperature for pure polymers above glass transition temperatures of corresponding polymers. (a) PMMA (1981), (b) PMMA (1997), (c) PS, (d) PVAc, (e) PVME, and (f) PC. Experimental data are shown by black squares taken from references [2, 45, 150, 156, 169, 208], respectively. Solid curves show theoretical predictions from the present theory and dashed curves show predictions from the Condo theory.

Chapter 5

Binary Solvent-Polymer Mixtures

In chapter 4 a detailed method has been outlined to evaluate flexibility parameters of the present model for pure polymeric systems. Later in the chapter, a comparison of glass transition temperature versus pressure predictions from the present model and the Condo model has been presented. Thus, we are now in a position to move ahead and discuss binary solvent-polymer mixtures. As discussed at the beginning of chapter 4 that for binary mixtures there are two more characteristic parameters, namely, the binary interaction parameter ζ_{sp} and the mixture hole volume v_0, however, there are no binary flexing parameters as each segment is assumed to be independent of neighbouring segments. It is fortuitous that SL-EOS of mixtures (Eq. 3.192) and Eq. 3.210 of the chemical potential of solvent in mixed-phase do not contain any term involving flexing parameters. Consequently, we can use the method highlighted by von Konigslow *et al.* [197] without any adaption to regress ζ_{sp} and v_0. Thus, after regression, Eq. 3.196 can be used to predict glass transition temperature versus pressure behaviour of binary mixtures. However, before indulging into details, first, a summary of von Konigslow *et al.* [197] method for regression of ζ_{sp} and v_0 is highlighted in next section.

5.1 Summary of Regression Method

The von Konigslow *et al.* method is based on a constant mixture hole volume to keep a consistent zero of chemical potential, however, because of this assumption the mixture hole volume does not limit correctly to pure-component hole volumes [197]. Consider a binary mixture consisting of a solvent s and a polymer p. Steps to regress ζ_{sp} and v_0 for this solvent-polymer mixture are enumerated below,

1. Independently regress pure-component characteristic parameters of solvent s and polymer p by using PVT data of corresponding pure systems and EOS 3.142. For this regression, assume that the reference volume of an individual species is equal to hole volume of that species *i.e.* $v_{r,s} = v_{0,s}$ for pure solvent and $v_{r,p} = v_{0,p}$ for pure polymeric system.
2. Take experimental solubility χ_s data and/or swelling S_w data at different temperatures and pressures, preferably, above critical point of solvent s.
3. Assume a value of ζ_{sp} and v_0. Then, for temperatures and pressures over which experimental solubility and/or swelling data is given, calculate the chemical potential of solvent in pure solvent phase by using Eq. 3.160 and EOS 3.142. Notice that EOS 3.142 is used to calculate volume fraction ϕ_s^{pure} of solvent in the pure solvent phase.
4. Thus, the chemical potential of solvent in mixed-phase is now known because of the condition of chemical equilibrium *i.e.* the chemical potential of solvent in the pure solvent phase should be equal to the chemical potential of solvent in the mixed-phase.
5. Simultaneously solve Eq. 3.210 of the chemical potential of solvent in mixed-phase and EOS of mixed-phase Eq. 3.192 to get volume fraction of solvent ϕ_s and polymer ϕ_p in mixed-phase at all temperatures and pressure over which solubility and/or swelling data is given.
6. Once ϕ_s^{pure}, ϕ_s and ϕ_p is known, theoretical values of solubility χ_s and/or swelling S_w can be evaluated at given temperatures and pressures by using,

$$\chi_s = \frac{M_s\phi_s/\alpha_s}{M_s\phi_s/\alpha_s + M_p\phi_p/\alpha_p}, \tag{5.1}$$

$$S_w = \frac{\phi_s^{pure}}{\phi_s}. \tag{5.2}$$

7. Predicted solubility and/or swelling data can be compared with the corresponding experimental data and thus iteration for ζ_{sp} and v_0 can be performed to the minimize residual mean square error.

Note that α_k of mixed-phase is different from α_k of pure phases. α_k of pure phases can be evaluated by using Eq. 3.85. However, to evaluate α_k for mixed-phase the following transformation has to be used,

$$\alpha_k = \alpha_k^{pure}\frac{v_{0,k}}{v_0}, \tag{5.3}$$

where, $v_{0,k}$ is the hole volume of pure system of species k and v_0 is the hole volume of mixture. In addition, von Konigslow *et al.* [197] also assumed that the mixture hole volume is close to the solvent hole volume. Based on this assumption, α_s in denominators on the left hand side of Eqs. 3.159 and 3.210 are assumed to be equal. Moreover, $'1'$ present inside the bracket of second term on the right hand side of both equations has been canceled while equating both equations for chemical equilibrium.

5.2 Prediction of Glass Transition Temperatures of Binary Mixture

To evaluate the success of the model let's focus on polystyrene - carbon dioxide (PS/CO_2) binary mixture. By using the method highlighted in section 5.1 iteration has been performed to get ζ_{sp} and v_0 using the experimental solubility data from Ref. [74]. Pure-component characteristic parameters and flexing parameters are used from tables 4.3 and 4.7, respectively. Thus, regressed values are $\zeta_{sp} = 1.088$, $v_0 = 4.355\ cm^3/mol$ and the corresponding solubility plot is shown in figure 5.1. Finally, $T_g(P)$ prediction from Eq. 3.196 is shown in figure 5.2. It is clear that $T_g(P)$ prediction from the present model is in good agreement with the experimental data taken from [22]. Increasing pressure results in the depression of glass transition temperature. This prediction is superior to the prediction of the Condo model [22].

Recall that to determine volume fractions ϕ_s and ϕ_p, the mixture hole volume is assumed to be close to the pure solvent hole volume. However, figure 5.2 has been obtained by assuming that the mixture hole volume is equal to the pure polymer hole volume $v_0 = v_{0,p}$ because this assumption ensures that at low pressures $T_g(P)$ predictions limit properly to pure PS $T_g(P)$ values. So, this assumption tends to minimize errors arising due to different hole volumes. In short, to calculate ϕ_s and ϕ_p it is assumed that $v_0 \approx v_{0,s}$, however, to calculate $T_g(P)$ behaviour it is assumed that $v_0 \approx v_{0,p}$.

5.3 Limitations

Although the theory is successful in predicting glass transition behaviour of PS/CO_2 mixtures, however, when the theory is applied on PC/CO_2 and $PMMA/CO_2$ binary mixtures that undergo retrograde vitrification the predictions from the present theory do not turn out to be correct.

Figures 5.3 and 5.4 show solubility and $T_g(P)$ plot of PC/CO_2 mixture from the present

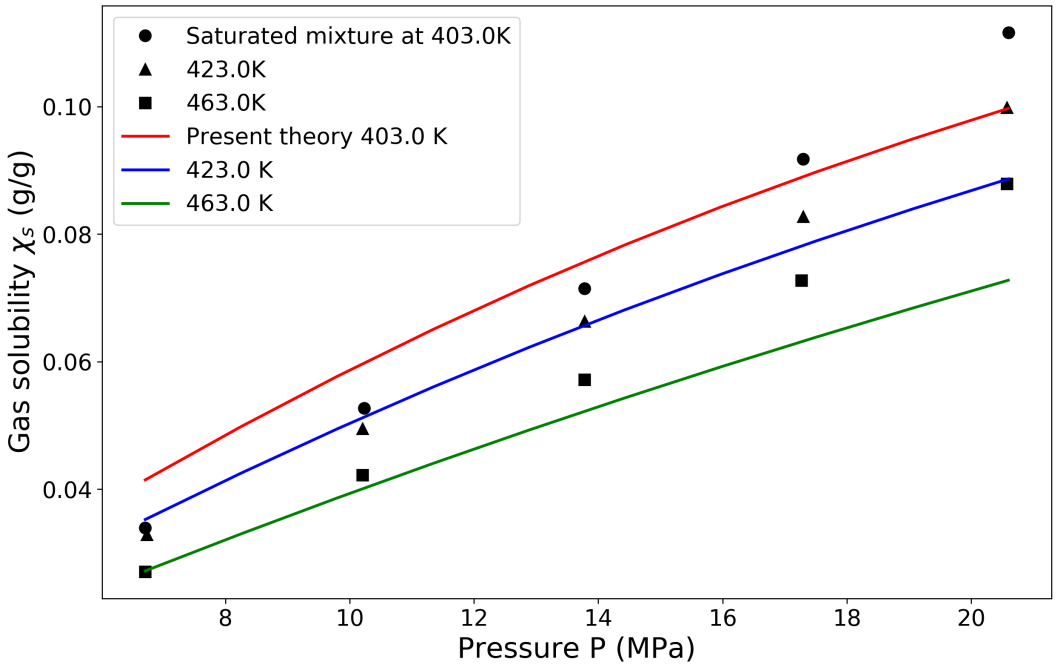

Figure 5.1: Solubility data with theoretical fits for binary PS/CO_2 mixture at $\zeta_{sp} = 1.088$ and $v_0 = 4.355\ cm^3/mol$. Theoretical fits from the von Konigslow model [197] are shown by solid curves while the experimental data [74] is shown by solid points.

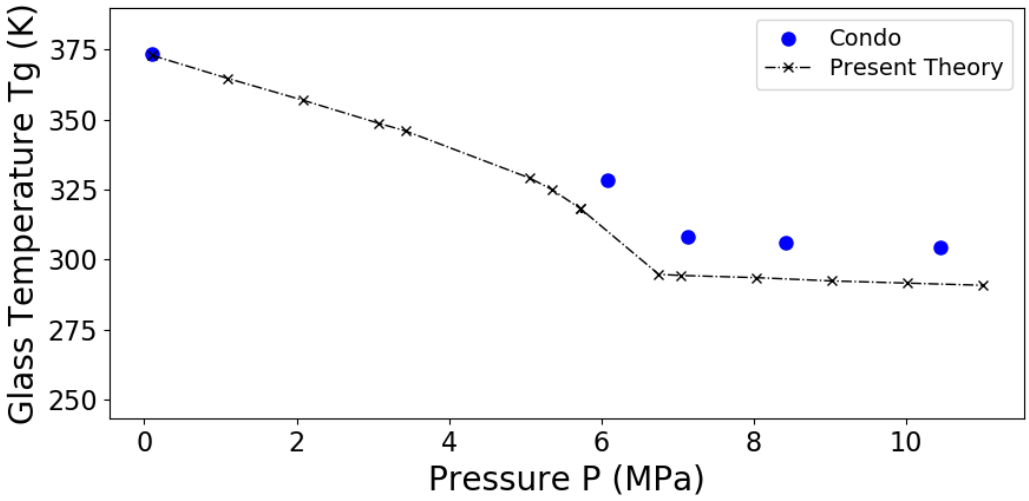

Figure 5.2: Glass transition temperature versus pressure plot of binary PS/CO_2 mixture for $\zeta_{sp} = 1.088$ and $v_0 = 4.355\ cm^3/mol$. The black cross points are from the present theory while blue circles show experimental data taken from reference [22]. The dotted-black curve is a guide to the eye.

theory against regressed values of $\zeta_{sp} = 1.0667$ and $v_0 = 4.470\ cm^3/mol$. The experimental data of solubility is taken from [180, 182] whereas experimental data of glass transition temperature is taken from [5, 167, 212]. It is clear that the PC/CO_2 undergoes retrograde vitrification, however, the present theory does not show a retrograde vitrification trend.

A similar contradiction between the present theory and experiment has been observed in PMMA/CO_2 mixture. Figures 5.5 and 5.6 show solubility and $T_g(P)$ plot of PMMA/CO_2 mixture from the present theory against regressed values of $\zeta_{sp} = 1.1188$ and $v_0 = 3.427\ cm^3/mol$. The experimental data of solubility is taken from [153, 205] whereas experimental data of glass transition temperature is taken from [21]. Again, the present theory does not show the retrograde vitrification trend. On the other hand, the Condo model reasonably predicts the retrograde vitrification behaviour in PMMA/CO_2 system [21, 22].

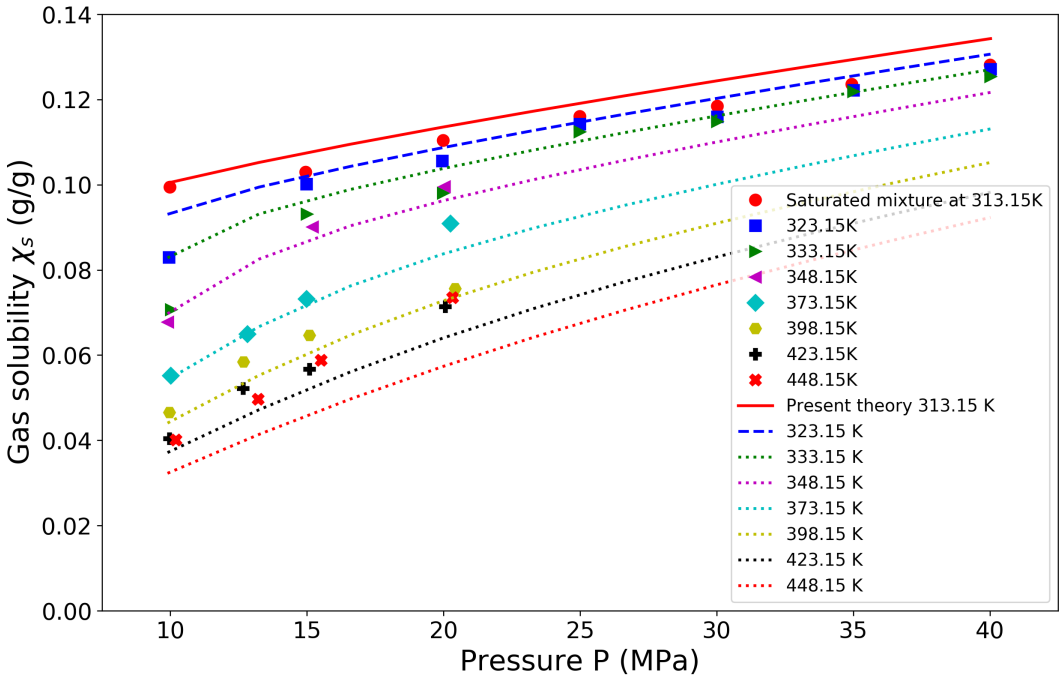

Figure 5.3: Solubility data with theoretical fits for binary PC/CO_2 mixture at $\zeta_{sp} = 1.0667$ and $v_0 = 4.470\ cm^3/mol$. Theoretical fits from the von Konigslow model [197] are shown by curves while the experimental data [180, 182] is shown by solid points.

However, it should be noted that the present theory in itself is capable of predicting retrograde vitrification if one hand-picked a value of ζ_{sp}. For instance, figures 5.7 and

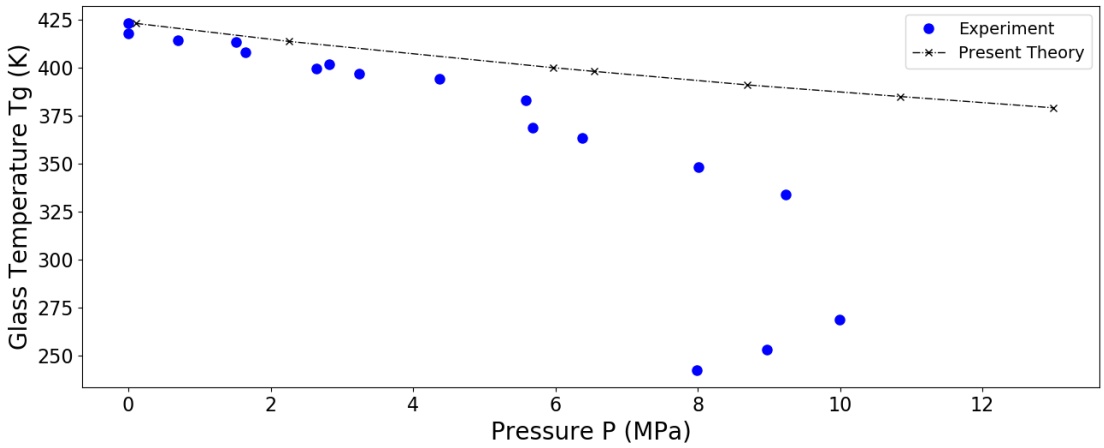

Figure 5.4: Glass transition temperature versus pressure plot of binary PC/CO_2 mixture for $\zeta_{sp} = 1.0667$ and $v_0 = 4.470\ cm^3/mol$. The black cross points are from the present theory while blue circles show experimental data taken from reference [5, 167, 212]. The dotted-black curve is a guide to the eye.

5.8 show two more $T_g(P)$ curves of PS/CO_2 mixture from the present theory against $\zeta_{sp} = 1.100$ and 1.124, respectively. Similar, $T_g(P)$ behaviours were identified by the Condo model [22]. Especially, figure 5.8 shows retrograde vitrification behaviour at the hand-picked values: $\zeta_{sp} = 1.124$ and $v_0 = 4.355\ cm^3/mol$. It is clear from the figures that $T_g(P)$ behaviour of binary mixtures is very sensitive to the value of ζ_{sp}. This means that it is essential to have accurate solubility data. Moreover, the model should be free from inconsistencies and crude assumptions. However, as discussed earlier, the present model involves inevitable inconsistencies. It should be noted discrepancies in the regressed values of ζ_{sp} and thus $T_g(P)$ predictions of the Condo model and the present model are arising due to two reasons. First, contrary to the present model, the Condo model assumes that the mixture hole volume is not constant (see Eq. 2.45). Second, the Condo model assumes that $\alpha_k^{mix} = \alpha_k^{pure}$, again contrary to the present model (see Eq. 5.3). These two differences are changing the regressed values of ζ_{sp}. Thus $T_g(P)$ prediction from the present model is different from the Condo model.

Attempts to Resolve Issues:

There are two basic issues in the model. First, the model assumes different reference volumes for pure solvent, pure polymer and binary mixture. Because of different reference volumes the values of T_s^*, T_p^*, α_s and α_p should be different in pure and mixed systems.

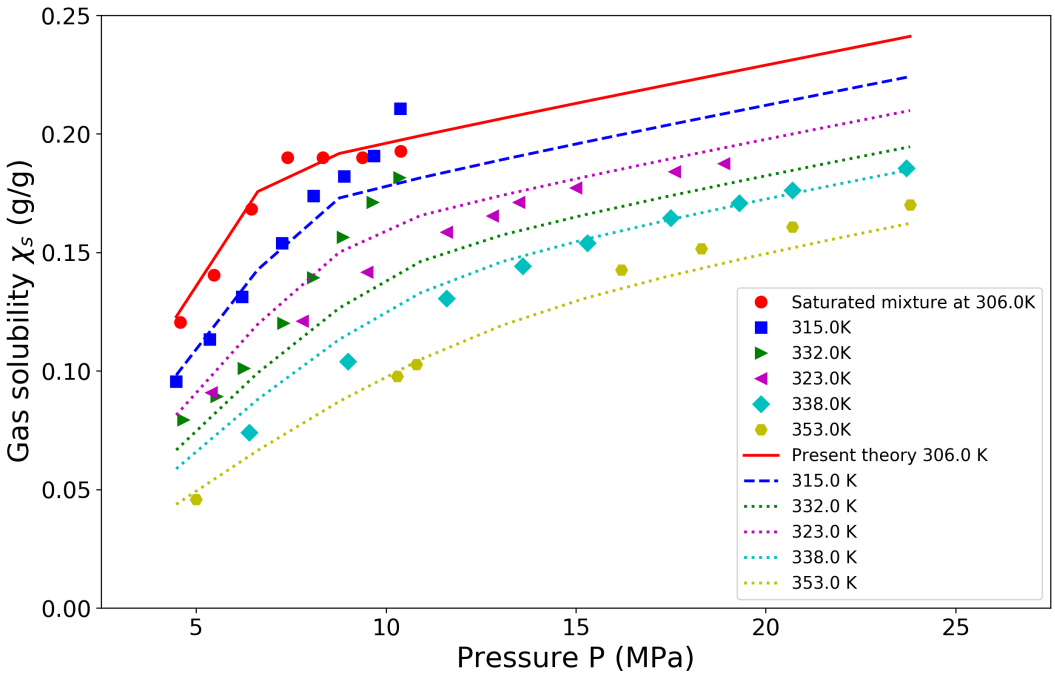

Figure 5.5: Solubility data with theoretical fits for binary PMMA/CO_2 mixture at $\zeta_{sp} = 1.1188$ and $v_0 = 3.427\ cm^3/mol$. Theoretical fits from the von Konigslow model [197] are shown by curves while the experimental data [153, 205] is shown by solid points.

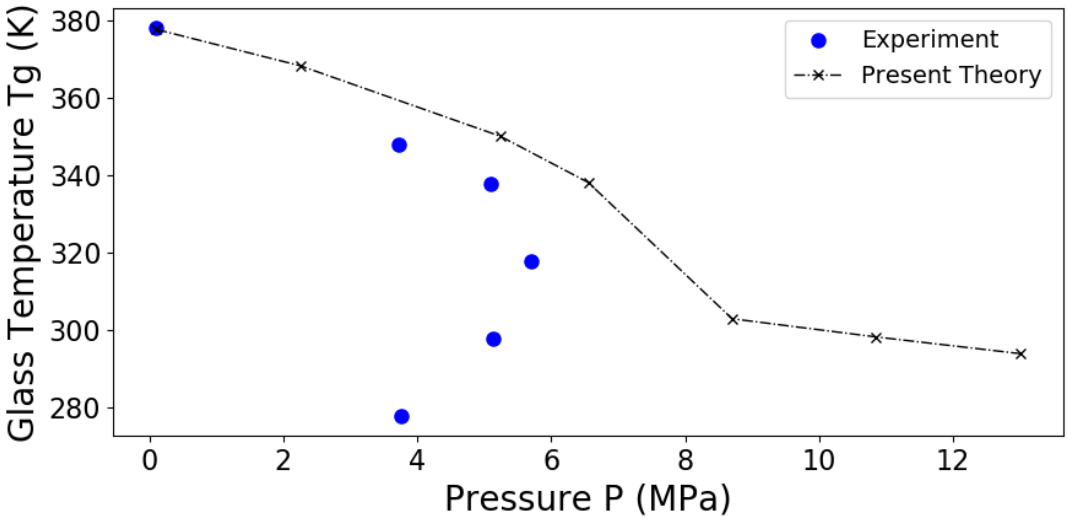

Figure 5.6: Glass transition temperature versus pressure plot of binary PMMA/CO_2 mixture for $\zeta_{sp} = 1.1188$ and $v_0 = 3.427\ cm^3/mol$. The black cross points are from the present theory while blue circles show experimental data taken from references [21]. The dotted-black curve is a guide to the eye.

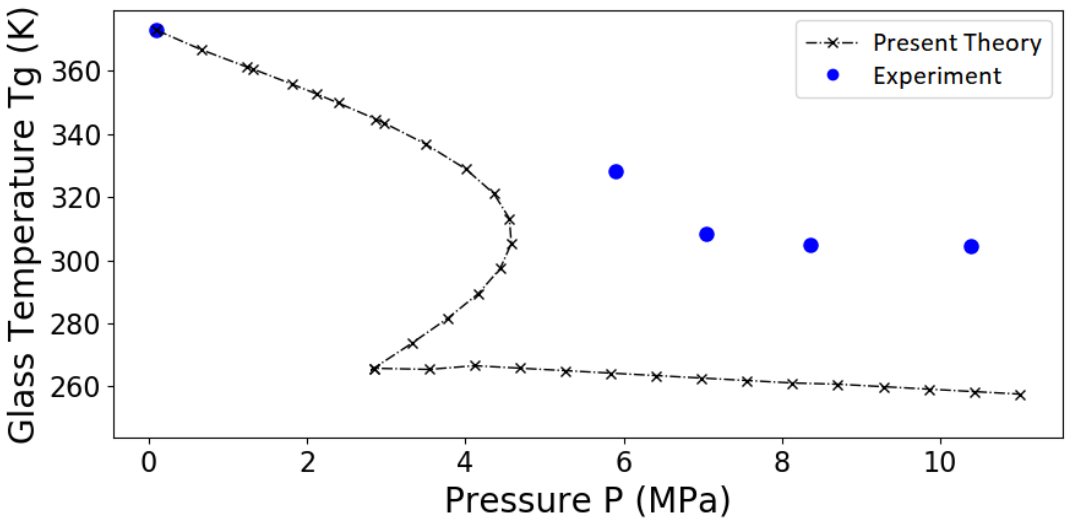

Figure 5.7: Glass transition temperature versus pressure plot of binary PS/CO_2 mixture for $\zeta_{sp} = 1.100$ and $v_0 = 4.355\ cm^3/mol$. The black cross points are from the present theory while blue circles show experimental data taken from reference [22]. The dotted-black curve is a guide to the eye.

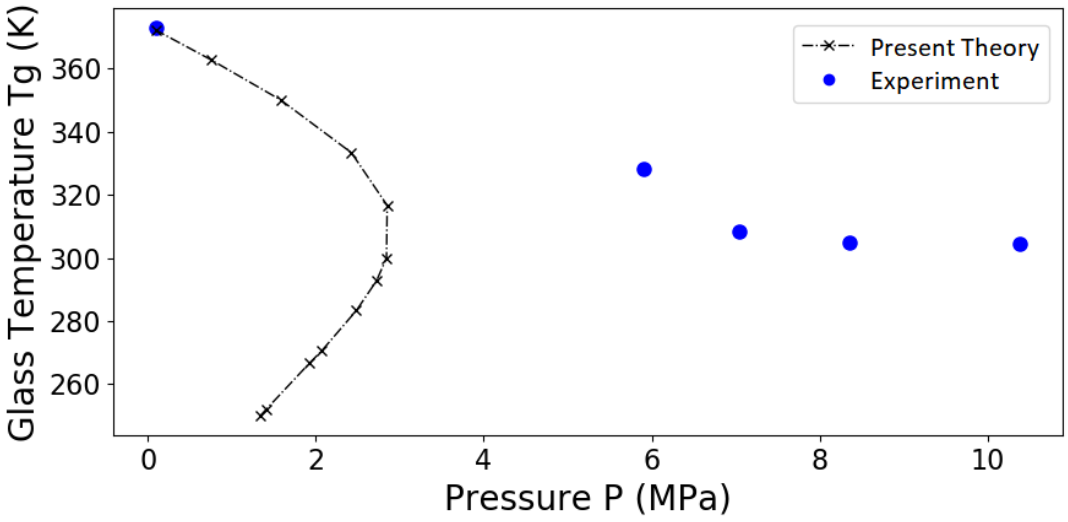

Figure 5.8: Glass transition temperature versus pressure plot of binary PS/CO_2 mixture for $\zeta_{sp} = 1.124$ and $v_0 = 4.355\ cm^3/mol$. The black cross points are from the present theory while blue circles show experimental data taken from reference [22]. The dotted-black curve is a guide to the eye.

This introduces an arbitrariness in the formula of solubility 5.1 that involves α_s and α_p. For instance, the Condo method assumes same values of α_s and α_p in pure and binary systems, whereas, the von Konigslow method re-scales α_s and α_p but does not re-scale T_s^* and T_p^*. Thus, both methods are not accurate.

The second issue is that the von Konigslow method assumes a constant hole volume while the Condo method assumes an arbitrary mixing rule (Eq. 2.45) to calculate hole volumes of mixed systems. Both of these approaches are arbitrary.

The first issue can be resolved easily by re-scaling pure component parameter T_s^* and T_p^* with respect to a fixed reference volume *i.e.* keep a same reference volume in the pure solvent, pure polymer and binary system (for instance, take reference volume equal to hole volume of pure polymer in the pure solvent, pure polymer and binary system). This automatically re-scales α_k's in the solubility formula because of Eq. 3.85. After doing this the model has only the second inaccuracy *i.e.* the approach towards mixture hole volume. To study the effect of this arbitrariness we had regressed values of ζ_{sp} of the present model for PS/CO_2, PC/CO_2 and PMMA/CO_2 by using both constant mixture hole volume approach (with and without von Konigslow's approximation) and the arbitrary mixing rule (Eq. 2.45) approach (without von Konigslow's approximation). We found that for these three binary mixtures the constant hole volume approach is underestimating the values of ζ_{sp} is not predicting retrograde vitrification. Whereas, the arbitrary mixing rule approach is overestimating the values of ζ_{sp} and is always predicting retrograde vitrification (even in PS/CO_2 mixture that does not undergo retrograde vitrification).

Chapter 6

Conclusions

In this work, the off-lattice SL-EOS model [197] is generalized to the case of finite flexible molecules by allowing molecules to have two energy levels of flexing. The flexing states are treated as internal degrees of freedom thus they depend only on the temperature of the system. The proposed extension is inspired by the lattice-based Condo *et al.* model [23]. Thus the off-lattice model and Condo model have been compared in detail for several pure polymeric materials and binary polymer-solvent mixtures.

For pure polymeric systems, the glass transition versus pressure and the isobaric heat capacity versus temperature predictions were utilized to make the comparison of the present model and Condo model. The present model predicted the experimental data more accurately than the Condo model. Furthermore, the present model is superior to the Condo model in some other aspects. In the Condo model, two experimental values, T_g at atmospheric pressure and dT_g/dP, are required to regress model parameters ϵ_p and z. However, since dT_g/dP is a constant thus the model can only be used for polymers having a fairly linear $T_g(P)$ behaviour. Moreover, to obtain an accurate value of dT_g/dP significant $T_g(P)$ data is usually required that ruins the purpose of the model *i.e.* to make $T_g(P)$ predictions. On the other hand, the present model is free from these two limitations. Instead of dT_g/dP value, the present model uses the value $\Delta C_P(T_g)$ at atmospheric pressure. Thus the present model can be applied to polymers having non-linear $T_g(P)$ behaviour. Moreover, since this approach requires $C_P(T)$ data to calculate the value of $\Delta C_P(T_g)$ thus the approach does not compromise the purpose of the model *i.e.* $T_g(P)$ predictions.

The worse performance of the Condo model is due to the fact that the Condo model is a lattice-fluid model that only allows coordination number z to be an integer. However, in the present model, the hypothetical parameter z is replaced by the degeneracy g which

is a real parameter that can take non-integer values. Indeed, when the Condo model is allowed to take non-integer coordination numbers performance of the model improves. However, this was expected because the Condo model requires significant $T_g(P)$ data. So, it is essentially a verification of the experimental inputs.

Equations of the present model and the Condo model are very similar. Comparing equations 3.64 and 2.44 of the fraction of excited segments from the present model and Condo model, respectively, one can notice that the factor $z-2$ of Condo model is replaced by the degeneracy g in the present model. In addition, equations of entropy 3.194 and 2.48 from the present model and Condo model are also very similar.

The present model also revealed that the entropy of polymers cannot become negative thus the Gibbs DiMarzio criterion is incorrect. This prediction is in agreement with other authors [6,206,207] who argued that the criterion is a lattice-based effect and, in reality, the entropy of polymers should not become negative. However, several authors [41] including Condo *et al.* decided to further explore the thermodynamics of glass transition based on the Gibbs DiMarzio criterion.

The present model is also applied to binary polystyrene/CO_2 mixture and found to be successful in predicting the depression of the glass transition temperature of polystyrene with increasing CO_2 pressure. The predictions are in excellent agreement with experimental data. However, predictions of the model for polycarbonate/CO_2 and PMMA/CO_2 are not correct because of inconsistencies in the theory that are making regressed values of ζ_{sp} less accurate. But, the model in itself can show retrograde vitrification behaviour against hand-picked values of ζ_{sp}.

In a nutshell, the present model is more powerful than the lattice-based Condo model and the off-lattice SL model [197]. It generalizes the off-lattice SL model which is not capable of predicting glass transition in polymers. It is free from the criticism of artificial lattice and Gibbs DiMarzio criterion. It requires significantly less experimental data to regress model parameters than the Condo model. The model has replaced integer coordination number z with non-integer degeneracy g. It is capable of predicting the depression of the glass transition temperature due to increasing gas pressure in binary polymer-solvent mixtures. The model is based on the *ab initio* approach of statistical mechanics and can be used to optimize industrial processes related to the manufacturing of polymers.

References

[1] A Abe and PJ Flory. The thermodynamic properties of mixtures of small, nonpolar molecules. *Journal of the American Chemical Society*, 87(9):1838–1846, 1965.

[2] Y Agari, A Ueda, Y Omura, and S Nagai. Thermal diffusivity and conductivity of PMMA/PC blends. *Polymer*, 38(4):801–807, 1997.

[3] Roza M Aseeva. *Handbook of polymeric foams and foam technology*. Hanser, 2004.

[4] Roger A Assink. Plasticization of poly (dimethyl siloxane) by high-pressure gases as studied by NMR relaxation. *Journal of Polymer Science: Polymer Physics Edition*, 12(11):2281–2290, 1974.

[5] Tapan Banerjee and G Glenn Lipscomb. Direct measurement of the carbon dioxide-induced glass transition depression in a family of substituted polycarbonates. *Journal of Applied Polymer Science*, 68(9):1441–1449, 1998.

[6] J Baschnagel, M Wolfgardt, W Paul, and K Binder. Entropy theory and glass transition: A test by Monte Carlo simulation. *Journal of Research of the National Institute of Standards and Technology*, 102(2):159, 1997.

[7] Muhammad Ahsan Bashir, Mohammad Al-Haj Ali, Vasileios Kanellopoulos, Jukka Seppälä, Esa Kokko, and Sameer Vijay. The effect of pure component characteristic parameters on Sanchez–Lacombe equation of state predictive capabilities. *Macromolecular Reaction Engineering*, 7(5):193–204, 2013.

[8] AJ Batschinski. Investigations of the internal friction of fluids. *Z Phys Chem*, 84:643–706, 1913.

[9] Rene J Bender. *Handbook of foamed plastics*. Lake Publishing Corporation, 1965.

[10] Enrico Bernardo, Laura Fiocco, Giulio Parcianello, Enrico Storti, and Paolo Colombo. Advanced ceramics from preceramic polymers modified at the nano-scale: A review. *Materials*, 7(3):1927–1956, 2014.

[11] GC Berry. Remarks on the energy parameters in lattice treatments of the glassy state. *Macromolecules*, 13(3):550–553, 1980.

[12] James J Binney, Nigel J Dowrick, Andrew J Fisher, and Mark EJ Newman. *The theory of critical phenomena: An introduction to the renormalization group*. Oxford University Press, 1992.

[13] John Cardy. *Scaling and renormalization in statistical physics*, volume 5. Cambridge University Press, 1996.

[14] R Casalini and CM Roland. Dynamic properties of polyvinylmethylether near the glass transition. *The Journal of Chemical Physics*, 119(7):4052–4059, 2003.

[15] David Chandler. Introduction to modern statistical mechanics. *Oxford University Press, Oxford, UK*, 1987.

[16] Dae Han Chang, Hoon Kwack Tae, and Luo Hong-Lie. Effects of coupling agent on the rheological behavior and processability of polypropylene. *J Appl Polym Sci*, 29(8):2599–2615, 1984.

[17] Walter G Chapman, George Jackson, and Keith E Gubbins. Phase equilibria of associating fluids: chain molecules with multiple bonding sites. *Molecular Physics*, 65(5):1057–1079, 1988.

[18] WG Chapman, KE Gubbins, G Jackson, and M Radosz. I&EC Res. 29, 1709 (1990). *Google Scholar CAS*, 1989.

[19] Junhan Cho and Isaac C Sanchez. An analytical free energy and the temperature-pressure superposition principle for pure polymeric liquids. *Macromolecules*, 31(19):6650–6661, 1998.

[20] Morrel H Cohen and David Turnbull. Molecular transport in liquids and glasses. *The Journal of Chemical Physics*, 31(5):1164–1169, 1959.

[21] PD Condo and Keith P Johnston. Retrograde vitrification of polymers with compressed fluid diluents: Experimental confirmation. *Macromolecules*, 25(24):6730–6732, 1992.

[22] PD Condo, Donald R Paul, and Keith P Johnston. Glass transitions of polymers with compressed fluid diluents: Type II and III behavior. *Macromolecules*, 27(2):365–371, 1994.

[23] PD Condo, Isaac C Sanchez, CG Panayiotou, and Keith P Johnston. Glass transition behavior including retrograde vitrification of polymers with compressed fluid diluents. *Macromolecules*, 25(23):6119–6127, 1992.

[24] RM Conforti, TA Barbari, P Vimalchand, and MD Donohue. A lattice-based activity coefficient model for gas sorption in glassy polymers. *Macromolecules*, 24(11):3388–3394, 1991.

[25] M Costas, HI Epstein, BC Sanctuary, D Richon, and H Renon. Equilibrium theory of r-mer fluids. *The Journal of Physical Chemistry*, 85(9):1264–1266, 1981.

[26] M Costas and BC Sanctuary. Theory of pure r-mers in the Guggenheim approximation. *The Journal of Physical Chemistry*, 85(21):3153–3160, 1981.

[27] Miguel Costas and BC Sanctuary. Equation of state molecular parameters for a theory of pure r-mer fluids in the liquid phase. *Fluid Phase Equilibria*, 18(1):47–60, 1984.

[28] GT Dee and DJ Walsh. Equations of state for polymer liquids. *Macromolecules*, 21(3):811–815, 1988.

[29] R Defay and I Prigogine. Thermodynamique chimique. *Éditions Desoer, Liège, Éditions Dunod, Paris,*, 1950.

[30] Brahatheeswaran Dhandayuthapani, Yasuhiko Yoshida, Toru Maekawa, and D Sakthi Kumar. Polymeric scaffolds in tissue engineering application: A review. *International Journal of Polymer Science*, 2011, 2011.

[31] Ernesto Di Maio, Salvatore Iannace, Giuseppe Mensitieri, and Luigi Nicolais. A predictive approach based on the Simha–Somcynsky free-volume theory for the effect of dissolved gas on viscosity and glass transition temperature of polymeric mixtures. *Journal of Polymer Science Part B: Polymer Physics*, 44(13):1863–1873, 2006.

[32] AT DiBenedetto. Molecular properties of amorphous high polymers. A cell theory for amorphous high polymers. *Journal of Polymer Science Part A: General Papers*, 1(11):3459–3476, 1963.

[33] EA DiMarzio. Structure and mobility in molecular and atomic glasses. In *Annals of the New York Academy of Sciences*, volume 371, page 1. 1981.

[34] EA DiMarzio and F Dowell. Theoretical prediction of the specific heat of polymer glasses. *Journal of Applied Physics*, 50(10):6061–6066, 1979.

[35] EA DiMarzio and JH Gibbs. Chain stiffness and the lattice theory of polymer phases. *The Journal of Chemical Physics*, 28(5):807–813, 1958.

[36] Edmund A Dimarzio and Julian H Gibbs. Molecular interpretation of glass temperature depression by plasticizers. *Journal of Polymer Science Part A: General Papers*, 1(4):1417–1428, 1963.

[37] Edmund A DiMarzio, Julian H Gibbs, Paul D Fleming III, and Isaac C Sanchez. Effects of pressure on the equilibrium properties of glass-forming polymers. *Macromolecules*, 9(5):763–771, 1976.

[38] Arthur K Doolittle. Studies in Newtonian flow. II. The dependence of the viscosity of liquids on free-space. *Journal of Applied Physics*, 22(12):1471–1475, 1951.

[39] Arthur K Doolittle. Studies in Newtonian flow. III. The dependence of the viscosity of liquids on molecular weight and free space (in homologous series). *Journal of Applied Physics*, 23(2):236–239, 1952.

[40] Arthur K Doolittle and Dortha B Doolittle. Studies in Newtonian flow. V. Further verification of the free-space viscosity equation. *Journal of Applied Physics*, 28(8):901–905, 1957.

[41] Jacek Dudowicz, Karl F Freed, and Jack F Douglas. Entropy theory of polymer glass formation revisited. I. General formulation. *The Journal of Chemical Physics*, 124(6):064901, 2006.

[42] Paul Ehrenfest. Phase changes in the ordinary and extended sense classified according to the corresponding singularities of the thermodynamic potential. In *Proceedings of the Academy of Sciences Amsterdam*, volume 36, pages 153–157, 1933.

[43] Shalom Eliezer, Ajoy K Ghatak, and Heinrich Hora. *Fundamentals of equations of state*. World Scientific, 2002.

[44] J Richard Elliott Jr, S Jayaraman Suresh, and Marc D Donohue. A simple equation of state for non-spherical and associating molecules. *Industrial & Engineering Chemistry Research*, 29(7):1476–1485, 1990.

[45] Fernando Fernandez-Martin, I Fernandez-Pierola, and Arturo Horta. Glass transition temperature and heat capacity of heterotacticlike PMMA. *Journal of Polymer Science: Polymer Physics Edition*, 19(9):1353–1363, 1981.

[46] RW Fillers and NW Tschoegl. The effect of pressure on the mechanical properties of polymers. *Transactions of the Society of Rheology*, 21(1):51–100, 1977.

[47] Paul J Flory. Thermodynamics of heterogeneous polymers and their solutions. *The Journal of Chemical Physics*, 12(11):425–438, 1944.

[48] Paul J Flory. *Principles of Polymer Chemistry*. Cornell University Press, 1953.

[49] Paul J Flory, RA Orwoll, and A Vrij. Statistical thermodynamics of chain molecule liquids. II. Liquid mixtures of normal paraffin hydrocarbons. *Journal of the American Chemical Society*, 86(17):3515–3520, 1964.

[50] PJ Flory. Statistical thermodynamics of semi-flexible chain molecules. *Proceedings of the Royal Society of London. Series A. Mathematical and Physical Sciences*, 234(1196):60–73, 1956.

[51] PJ Flory and A Abe. Thermodynamic properties of nonpolar mixtures of small molecules. *Journal of the American Chemical Society*, 86(17):3563–3565, 1964.

[52] PJ Flory, RA Orwoll, and A Vrij. Statistical thermodynamics of chain molecule liquids. I. An equation of state for normal paraffin hydrocarbons. *Journal of the American Chemical Society*, 86(17):3507–3514, 1964.

[53] RH Fowler and EA Guggenheim. Statistical thermodynamics. *Cambridge University Press*, 1949.

[54] Thomas G Fox and Paul J Flory. The glass temperature and related properties of polystyrene. Influence of molecular weight. *Journal of Polymer Science*, 14(75):315–319, 1954.

[55] Thomas G Fox Jr and Paul J Flory. Viscosity-molecular weight and viscosity-temperature relationships for polystyrene and polyisobutylene1,2. *Journal of the American Chemical Society*, 70(7):2384–2395, 1948.

[56] Thomas G Fox Jr and Paul J Flory. Second-order transition temperatures and related properties of polystyrene. I. Influence of molecular weight. *Journal of Applied Physics*, 21(6):581–591, 1950.

[57] Thomas G Fox Jr and Paul J Flory. Further studies on the melt viscosity of polyisobutylene. *The Journal of Physical Chemistry*, 55(2):221–234, 1951.

[58] Hiroshi Fujita. Free diffusion in a two-component system in which there is a volume change on mixing. *Journal of the American Chemical Society*, 83(13):2862–2865, 1961.

[59] Hiroshi Fujita. Notes on free volume theories. *Polymer Journal*, 23(12):1499–1506, 1991.

[60] G Gee. The thermodynamic analysis of the effect of pressure on the glass temperature of polystyrene. *Polymer*, 7(4):177–191, 1966.

[61] Julian H Gibbs. Nature of the glass transition in polymers. *The Journal of Chemical Physics*, 25(1):185–186, 1956.

[62] Julian H Gibbs and Edmund A DiMarzio. Nature of the glass transition and the glassy state. *The Journal of Chemical Physics*, 28(3):373–383, 1958.

[63] L Glicksman. Notes from MIT summer program 4.10S foams and cellular materials: Thermal and mechanical properties. *Cambridge, MA, June*, 29, 1992.

[64] Martin Goldstein and Robert Simha. *The glass transition and the nature of the glassy state*, volume 279. New York Academy of Sciences, 1976.

[65] Luigi Grassia and Alberto D'Amore. Isobaric and isothermal glass transition of PMMA: Pressure-volume-temperature experiments and modelling predictions. *Journal of Non-Crystalline Solids*, 357(2):414–418, 2011.

[66] Joachim Gross and Gabriele Sadowski. Application of perturbation theory to a hard-chain reference fluid: An equation of state for square-well chains. *Fluid Phase Equilibria*, 168(2):183–199, 2000.

[67] Joachim Gross and Gabriele Sadowski. Perturbed-chain SAFT: An equation of state based on a perturbation theory for chain molecules. *Industrial & Engineering Chemistry Research*, 40(4):1244–1260, 2001.

[68] Joachim Gross and Gabriele Sadowski. Application of the perturbed-chain SAFT equation of state to associating systems. *Industrial & Engineering Chemistry Research*, 41(22):5510–5515, 2002.

[69] Yuri Guerrieri, Karen Valverde Pontes, Gloria Meyberg Nunes Costa, and Marcelo Embiruçu. *A survey of equations of state for polymers*. InTech: Rijeka, Croatia, 2012.

[70] EA Guggenheim. Mixtures. Oxford University Press, 1952.

[71] Edward Armand Guggenheim. Statistical thermodynamics of mixtures with non-zero energies of mixing. *Proceedings of the Royal Society of London. Series A. Mathematical and Physical Sciences*, 183(993):213–227, 1944.

[72] Mourad Hamedi, Ronald P Danner, and J Larry Duda. A lattice-fluid, group-contribution treatment of the glass transition of homopolymers, copolymers, and polymer solutions. *Journal of Applied Polymer Science*, 89(3):697–705, 2003.

[73] Bruce Hartmann and Mustafa A Haque. Equation of state for polymer liquids. *Journal of Applied Polymer Science*, 30(4):1553–1563, 1985.

[74] Mohammad Hasan. *A systematic study of solubility of physical blowing agents and their blends in polymers and their nanocomposites*. PhD thesis, University of Toronto, 2013.

[75] Mohammad M Hasan, Yao G Li, Guangming Li, Chul B Park, and Pu Chen. Determination of solubilities of CO_2 in linear and branched polypropylene using a magnetic

suspension balance and a PVT apparatus. *Journal of Chemical & Engineering Data*, 55(11):4885–4895, 2010.

[76] Ivan Havlíček, Vladimír Vojta, Michal Ilavskỳ, and Jaroslav Hrouz. Molecular parameters of polymers obtained from the Gibbs-DiMarzio theory of glass formation. *Macromolecules*, 13(2):357–362, 1980.

[77] Robert Nobbs Haward. *The physics of glassy polymers*. Springer Science & Business Media, 2012.

[78] Terrell L Hill. *An introduction to statistical thermodynamics*. Courier Corporation, 1986.

[79] KM Hong and J Noolandi. Conformational entropy effects in a compressible lattice fluid theory of polymers. *Macromolecules*, 14(5):1229–1234, 1981.

[80] Kevin G Honnell and Carol K Hall. A new equation of state for athermal chains. *The Journal of Chemical Physics*, 90(3):1841–1855, 1989.

[81] Stanley H Huang and Maciej Radosz. Equation of state for small, large, polydisperse, and associating molecules. *Industrial & Engineering Chemistry Research*, 29(11):2284–2294, 1990.

[82] Maurice L Huggins. Theory of solutions of high polymers. *Journal of the American Chemical Society*, 64(7):1712–1719, 1942.

[83] Maurice L Huggins. Thermodynamic properties of solutions of long-chain compounds. *Annals of the New York Academy of Sciences*, 43(1):1–32, 1942.

[84] Gregg Jaeger. The Ehrenfest classification of phase transitions: Introduction and evolution. *Archive for history of exact sciences*, 53(1):51–81, 1998.

[85] RK Jain and Robert Simha. On the statistical thermodynamics of multicomponent fluids equation of state. *Macromolecules*, 13(6):1501–1508, 1980.

[86] K Kamide. Thermodynamics of polymer solution phase equilibria and critical phenomena. *Polymer Science Library 9*, 442, 1990.

[87] Mehran Kardar. *Statistical physics of particles*. Cambridge University Press, 2007.

[88] Walter Kauzmann. The nature of the glassy state and the behavior of liquids at low temperatures. *Chemical Reviews*, 43(2):219–256, 1948.

[89] Yeongyoon Kim, Chul B Park, P Chen, and Russell B Thompson. Origins of the failure of classical nucleation theory for nanocellular polymer foams. *Soft Matter*, 7(16):7351–7358, 2011.

[90] Yeongyoon Kim, Chul B Park, P Chen, and Russell B Thompson. Towards maximal cell density predictions for polymeric foams. *Polymer*, 52(24):5622–5629, 2011.

[91] Yeongyoon Kim, Chul B Park, P Chen, and Russell B Thompson. Maximal cell density predictions for compressible polymer foams. *Polymer*, 54(2):841–845, 2013.

[92] Daniel Klempner, Kurt Charles Frisch, et al. *Handbook of polymeric foams and foam technology*, volume 404. Hanser Munich etc., 1991.

[93] Vitaly J Klenin. *Thermodynamics of systems containing flexible-chain polymers*. Elsevier, 1999.

[94] J Koppelmann. Proceedings of the Fourth International Congress on Rheology. 1965.

[95] Robert H Lacombe and Isaac C Sanchez. Statistical thermodynamics of fluid mixtures. *The Journal of Physical Chemistry*, 80(23):2568–2580, 1976.

[96] Arthur H Landrock. *Handbook of plastic foams: Types, properties, manufacture and applications*. Elsevier, 1995.

[97] E Struik LC. *Physical aging in amorphous polymers and other materials*. Elsevier, 1978.

[98] Shau-Tarng Lee. Introduction: polymeric foams, mechanisms, and materials. In *Polymeric Foams*, pages 15–29. CRC press, 2004.

[99] Shau-Tarng Lee, Chul B Park, and Natarajan S Ramesh. *Polymeric foams: Science and Technology*. CRC press, 2006.

[100] John Edward Lennard-Jones and AF Devonshire. Critical phenomena in gases. *Proceedings of the Royal Society of London. Series A - Mathematical and Physical Sciences*, 163(912):53–70, 1937.

[101] G Li, F Gunkel, J Wang, CB Park, and V Altstädt. Solubility measurements of N_2 and CO_2 in polypropylene and ethene/octene copolymer. *Journal of Applied Polymer Science*, 103(5):2945–2953, 2007.

[102] G Li, H Li, J Wang, and CB Park. Investigating the solubility of CO_2 in polypropylene using various EOS models. *Cellular Polymers*, 25(4):237–248, 2006.

[103] G Li, J Wang, CB Park, P Moulinie, and R Simha. Comparison of SS-based and SL-based estimation of gas solubility. In *ANTEC conference proceedings*, volume 2, pages 2566–2575. Society of Plastics Engineers, 2004.

[104] Guangming Li. *Thermodynamic investigation of the solubility of physical blowing agents in polymer melts*. ProQuest, 2007.

[105] Yao Gai Gary Li. *Development of a novel visualization and measurement apparatus for the PVT behaviours of polymer/gas solutions*. University of Toronto, 2008.

[106] YG Li and CB Park. Effects of branching on the pressure-volume-temperature behaviors of PP/CO_2 solutions. *Industrial & Engineering Chemistry Research*, 48(14):6633–6640, 2009.

[107] YG Li, CB Park, HB Li, and J Wang. Measurement of the PVT property of PP/CO_2 solution. *Fluid Phase Equilibria*, 270(1-2):15–22, 2008.

[108] Zhan-Wei Li, Zhong-Yuan Lu, Zhao-Yan Sun, Ze-Sheng Li, and Li-Jia An. Calculating the equation of state parameters and predicting the spinodal curve of isotactic polypropylene/poly (ethylene-co-octene) blend by molecular dynamics simulations combined with Sanchez- Lacombe lattice fluid theory. *The Journal of Physical Chemistry B*, 111(21):5934–5940, 2007.

[109] Xia Liao, Yaogai G Li, Chul B Park, and P Chen. Interfacial tension of linear and branched PP in supercritical carbon dioxide. *The Journal of Supercritical Fluids*, 55(1):386–394, 2010.

[110] SH Mahmood, M Keshtkar, and CB Park. Determination of carbon dioxide solubility in polylactide acid with accurate PVT properties. *The Journal of Chemical Thermodynamics*, 70:13–23, 2014.

[111] SH Mahmood, CL Xin, JH Lee, and CB Park. Study of volume swelling and interfacial tension of the polystyrene–carbon dioxide–dimethyl ether system. *Journal of colloid and interface science*, 456:174–181, 2015.

[112] Norman Henry March and Mario P Tosi. *Introduction to liquid state physics*. World Scientific, 2002.

[113] Todd M Martin and Douglas M Young. Correlation of the glass transition temperature of plasticized PVC using a lattice fluid model. *Polymer*, 44(16):4747–4754, 2003.

[114] Monique Martina and Dietmar W Hutmacher. Biodegradable polymers applied in tissue engineering research: A review. *Polymer International*, 56(2):145–157, 2007.

[115] JE Mayer and M Goeppert. Statistical Mechanics. *John Wiley & Sons, New York*, 1940.

[116] Gregory Mckenna. Glass formation and glassy behavior. *Comprehensive Polymer Science*, 2:311–362, 12 1989.

[117] JE McKinney and M Goldstein. Journal of Research of the National Institute of Standards and Technology. *Sect. A*, 78:331, 1974.

[118] Alexander Renfrew Miller. Theory of solutions of high polymers. 1948.

[119] WK Moonan and NW Tschoegl. Effect of pressure on the mechanical properties of polymers. 2. Expansivity and compressibility measurements. *Macromolecules*, 16(1):55–59, 1983.

[120] WK Moonan and NW Tschoegl. Effect of pressure on the mechanical properties of polymers. 3. Substitution of the glassy parameters for those of the occupied volume. *International Journal of Polymeric Materials*, 10(3):199–211, 1984.

[121] WK Moonan and NW Tschoegl. The effect of pressure on the mechanical properties of polymers. IV. Measurements in torsion. *Journal of Polymer Science: Polymer Physics Edition*, 23(4):623–651, 1985.

[122] NF Mott and RW Gurney. Note on the theory of liquids. *Transactions of the Faraday Society*, 35:364–368, 1939.

[123] VS Nanda and Robert Simha. Equation of state of polymer liquids and glasses at elevated pressures. *The Journal of Chemical Physics*, 41(12):3870–3878, 1964.

[124] Evelyne Neau. A consistent method for phase equilibrium calculation using the Sanchez–Lacombe lattice–fluid equation of state. *Fluid Phase Equilibria*, 203(1-2):133–140, 2002.

[125] Erik Nies and Alexander Stroeks. A modified hole theory of polymeric fluids. 1. Equation of state of pure components. *Macromolecules*, 23(18):4088–4092, 1990.

[126] M Ohshima and ST Lee. Foam extrusion: Principles and practice, 2000.

[127] Michael I Ojovan. Ordering and structural changes at the glass–liquid transition. *Journal of Non-Crystalline Solids*, 382:79–86, 2013.

[128] Olagoke Olabisi and Robert Simha. Pressure-volume-temperature studies of amorphous and crystallizable polymers. I. Experimental. *Macromolecules*, 8(2):206–210, 1975.

[129] Hasan Orbey, Costas P Bokis, and Chau-Chyun Chen. Equation of state modeling of phase equilibrium in the low-density polyethylene process: The Sanchez-Lacombe, statistical associating fluid theory, and Polymer-Soave-Redlich-Kwong equations of state. *Industrial & Engineering Chemistry Research*, 37(11):4481–4491, 1998.

[130] C Panayiotou and JH Vera. The quasi-chemical approach for non-randomness in liquid mixtures. Expressions for local surfaces and local compositions with an application to polymer solutions. *Fluid Phase Equilibria*, 5(1-2):55–80, 1980.

[131] C Panayiotou and JH Vera. Local compositions and local surface area fractions: A theoretical discussion. *The Canadian Journal of Chemical Engineering*, 59(4):501–505, 1981.

[132] C Panayiotou and JH Vera. An improved lattice-fluid equation of state for pure component polymeric fluids. *Polymer Engineering & Science*, 22(6):345–348, 1982.

[133] C Panayiotou and JH Vera. On the fluid lattice and Gibbs-DiMarzio theories. *Journal of Polymer Science: Polymer Letters Edition*, 22(11):601–606, 1984.

[134] Constantinos G Panayiotou. Thermodynamics of gas solubility in polymeric liquids. *Die Makromolekulare Chemie: Macromolecular Chemistry and Physics*, 187(12):2867–2882, 1986.

[135] Constantinos G Panayiotou. Lattice-fluid theory of polymer solutions. *Macromolecules*, 20(4):861–871, 1987.

[136] H Park, CB Park, C Tzoganakis, KH Tan, and P Chen. Surface tension measurement of polystyrene melts in supercritical carbon dioxide. *Industrial & Engineering Chemistry Research*, 45(5):1650–1658, 2006.

[137] H Park, RB Thompson, N Lanson, C Tzoganakis, CB Park, and P Chen. Effect of temperature and pressure on surface tension of polystyrene in supercritical carbon dioxide. *The Journal of Physical Chemistry B*, 111(15):3859–3868, 2007.

[138] Elio Passaglia and Gordon M Martin. Variation of glass temperature with pressure in polypropylene. *Journal of Research of the National Bureau of Standards. Section A, Physics and Chemistry*, 68(3):273, 1964.

[139] RK Pathria. Statistical Mechanics, 1996.

[140] DR Paul and AT DiBenedetto. Thermodynamic and molecular properties of amorphous high polymers. In *Journal of Polymer Science Part C: Polymer Symposia*, volume 16, pages 1269–1288. Wiley Online Library, 1967.

[141] André Péneloux, Evelyne Rauzy, and Richard Fréze. A consistent correction for Redlich-Kwong-Soave volumes. *Fluid Phase Equilibria*, 8(1):7–23, 1982.

[142] Ding-Yu Peng and Donald B Robinson. A new two-constant equation of state. *Industrial & Engineering Chemistry Fundamentals*, 15(1):59–64, 1976.

[143] G Pezzin, F Zilio-Grandi, and P Sanmartin. The dependence of the glass transition temperature on molecular weight for polyvinylchloride. *European Polymer Journal*, 6(7):1053–1061, 1970.

[144] Claudia I Poser and Isaac C Sanchez. Interfacial tension theory of low and high molecular weight liquid mixtures. *Macromolecules*, 14(2):361–370, 1981.

[145] John M Prausnitz, FF Anderson, EA Grens, CA Eckert, R Hsieh, and JP O'connell. *Computer calculations for multicomponent vapor-liquid and liquid-liquid equilibria*. Prentice-Hall Englewood Cliffs, NJ, 1980.

[146] John M Prausnitz, Rudiger N Lichtenthaler, and Edmundo Gomes De Azevedo. *Molecular thermodynamics of fluid-phase equilibria*. Pearson Education, 1998.

[147] I. Prigogine. *The Molecular Theory of Solutions*. Series in physics. North-Holland Publishing Company, New York, 1957.

[148] Ilya Prigogine and André Bellemans. Application of the cell model to the statistical thermodynamics of solutions. Volume change of mixing in solutions of molecules slightly different in size. *The Journal of Chemical Physics*, 21(3):561–562, 1953.

[149] Ilya Prigogine, N Trappeniers, and Victor Mathot. Statistical thermodynamics of r-mers and r-mer solutions. *Discussions of the Faraday Society*, 15:93–107, 1953.

[150] Marek Pyda, K Van Durme, Bernhard Wunderlich, and B Van Mele. Heat capacity of poly (vinyl methyl ether). *Journal of Polymer Science Part B: Polymer Physics*, 43(16):2141–2153, 2005.

[151] A Quach and Robert Simha. Pressure-volume-temperature properties and transitions of amorphous polymers; polystyrene and poly (orthomethylstyrene). *Journal of Applied Physics*, 42(12):4592–4606, 1971.

[152] Swalin RA. Thermodynamics of Solids. *John Wiley and Sons*, p178, 1972.

[153] Arvind Rajendran, Barbara Bonavoglia, Nicola Forrer, Giuseppe Storti, Marco Mazzotti, and Massimo Morbidelli. Simultaneous measurement of swelling and sorption in a supercritical CO_2 - poly (methyl methacrylate) system. *Industrial & Engineering Chemistry Research*, 44(8):2549–2560, 2005.

[154] G Rehage and W Borchard. The physics of glassy polymers. *Wiley, New York, 1973) Ch*, 1:54–107, 1973.

[155] LE Reichl. A modern course in statistical physics. *John Wiley & Sons Inc., NY*, 1998.

[156] MJ Richardson and NG Savill. Derivation of accurate glass transition temperatures by differential scanning calorimetry. *Polymer*, 16(10):753–757, 1975.

[157] Patrick A Rodgers. Pressure–volume–temperature relationships for polymeric liquids: A review of equations of state and their characteristic parameters for 56 polymers. *Journal of Applied Polymer Science*, 48(6):1061–1080, 1993.

[158] Patrick A Rodgers and Isaac C Sanchez. Improvement to the lattice-fluid prediction of gas solubilities in polymer liquids. *Journal of Polymer Science Part B: Polymer Physics*, 31(3):273–277, 1993.

[159] Brian Roffel and Ben Betlem. *Process dynamics and control: Modeling for control and prediction*. John Wiley & Sons, 2007.

[160] CM Roland and R Casalini. Temperature and volume effects on local segmental relaxation in poly (vinyl acetate). *Macromolecules*, 36(4):1361–1367, 2003.

[161] Dominick V Rosato, Donald V Rosato, and Matthew v Rosato. *Plastic product material and process selection handbook*. Elsevier, 2004.

[162] Michael Rubinstein, Ralph H Colby, et al. *Polymer Physics*, volume 23. Oxford university press New York, 2003.

[163] Isaac C Sanchez and Robert H Lacombe. Theory of liquid–liquid and liquid–vapour equilibria. *Nature*, 252(5482):381–383, 1974.

[164] Isaac C Sanchez and Robert H Lacombe. An elementary molecular theory of classical fluids. Pure fluids. *The Journal of Physical Chemistry*, 80(21):2352–2362, 1976.

[165] Isaac C Sanchez and Robert H Lacombe. Statistical thermodynamics of polymer solutions. *Macromolecules*, 11(6):1145–1156, 1978.

[166] Isaac C Sanchez and Patrick A Rodgers. Solubility of gases in polymers. *Pure and Applied Chemistry*, 62(11):2107–2114, 1990.

[167] Mehdi Sanieisichani. *Nanocellular Foams with a Superior Thermal Insulation Property*. PhD thesis, University of Toronto, 2017.

[168] SM Sapuan, N Suddin, and MA Maleque. A critical review of polymer-based composite automotive bumper systems. *Polymers and Polymer Composites*, 10(8):627–636, 2002.

[169] Hiroyuki Sasabe and Cornelius T Moynihan. Structural relaxation in poly (vinyl acetate). *Journal of Polymer Science: Polymer Physics Edition*, 16(8):1447–1457, 1978.

[170] Paul G Shewmon. *Transformations in metals*. McGraw-Hill, 1969.

[171] Robert Simha. Configurational thermodynamics of the liquid and glassy polymeric states. *Macromolecules*, 10(5):1025–1030, 1977.

[172] Robert Simha and Thomas Somcynsky. On the statistical thermodynamics of spherical and chain molecule fluids. *Macromolecules*, 2(4):342–350, 1969.

[173] NN Smirnova, EV Kolyakina, TG Kulagina, and DF Grishin. Influence of the molecular weight of polystyrene on its thermodynamic properties. *Russian Chemical Bulletin*, 62(10):2251–2257, 2013.

[174] Giorgio Soave. Equilibrium constants from a modified Redlich-Kwong equation of state. *Chemical Engineering Science*, 27(6):1197–1203, 1972.

[175] Thomas Somcynsky and Robert Simha. Hole theory of liquids and glass transition. *Journal of Applied Physics*, 42(12):4545–4548, 1971.

[176] Yuhua Song, Stephen M Lambert, and John M Prausnitz. Equation of state for mixtures of hard-sphere chains including copolymers. *Macromolecules*, 27(2):441–448, 1994.

[177] RS Spencer and GD Gilmore. Equation of state for polystyrene. *Journal of Applied Physics*, 20(6):502–506, 1949.

[178] Simon Stephan, Jinlu Liu, Kai Langenbach, Walter G Chapman, and Hans Hasse. Vapor-liquid interface of the Lennard-Jones truncated and shifted fluid: Comparison of molecular simulation, density gradient theory, and density functional theory. *The Journal of Physical Chemistry C*, 122(43):24705–24715, 2018.

[179] R Stryjek and JH Vera. PRSV2: A cubic equation of state for accurate vapor-liquid equilibria calculations. *The Canadian Journal of Chemical Engineering*, 64(5):820–826, 1986.

[180] Ying Sun, Miki Matsumoto, Kota Kitashima, Masashi Haruki, Shin-ichi Kihara, and Shigeki Takishima. Solubility and diffusion coefficient of supercritical CO_2 in polycarbonate and CO_2 induced crystallization of polycarbonate. *The Journal of Supercritical Fluids*, 95:35–43, 2014.

[181] PG Tait. The voyage of HMS challenger, vol. 2. *Part*, 2:1–73, 1888.

[182] Muoi Tang, Tz-Bang Du, and Yan-Ping Chen. Sorption and diffusion of supercritical carbon dioxide in polycarbonate. *The Journal of Supercritical Fluids*, 28(2-3):207–218, 2004.

[183] MR Tant and GL Wilkes. An overview of the nonequilibrium behavior of polymer glasses. *Polymer Engineering & Science*, 21(14):874–895, 1981.

[184] RB Thompson, JR MacDonald, and P Chen. Origin of change in molecular-weight dependence for polymer surface tension. *Physical Review E*, 78(3):030801, 2008.

[185] Russell B Thompson, Chul B Park, and P Chen. Reduction of polymer surface tension by crystallized polymer nanoparticles. *The Journal of Chemical Physics*, 133(14):144913, 2010.

[186] Hans Tompa. *Polymer solutions*. Butterworths Scientific Publications, 1956.

[187] Hugo Touchette. Ensemble equivalence for general many-body systems. *EPL (Europhysics Letters)*, 96(5):50010, 2011.

[188] Hugo Touchette. Equivalence and nonequivalence of ensembles: Thermodynamic, macrostate, and measure levels. *Journal of Statistical Physics*, 159(5):987–1016, 2015.

[189] Hugo Touchette, Richard S Ellis, and Bruce Turkington. An introduction to the thermodynamic and macrostate levels of nonequivalent ensembles. *Physica A: Statistical Mechanics and its Applications*, 340(1-3):138–146, 2004.

[190] Feelly Tumakaka, Joachim Gross, and Gabriele Sadowski. Modeling of polymer phase equilibria using perturbed-chain SAFT. *Fluid Phase Equilibria*, 194:541–551, 2002.

[191] Feelly Tumakaka, Joachim Gross, and Gabriele Sadowski. Thermodynamic modeling of complex systems using PC-SAFT. *Fluid Phase Equilibria*, 228:89–98, 2005.

[192] David Turnbull and Morrel H Cohen. Free-volume model of the amorphous phase: glass transition. *The Journal of Chemical Physics*, 34(1):120–125, 1961.

[193] Faheem Ullah, Muhammad Bisyrul Hafi Othman, Fatima Javed, Zulkifli Ahmad, and Hazizan Md Akil. Classification, processing and application of hydrogels: A review. *Materials Science and Engineering: C*, 57:414–433, 2015.

[194] JD Van der Waals. On the continuity of the gaseous and liquid states (doctoral dissertation). *Universiteit Leiden*, 1873.

[195] Kier von Konigslow. *An off-lattice derivation and thermodynamic consistency consideration for the Sanchez-Lacombe equation of state*. PhD thesis, University of Waterloo, 2017.

[196] Kier von Konigslow, Chul B Park, and Russell B Thompson. Evaluating characteristic parameters for carbon dioxide in the Sanchez–Lacombe equation of state. *Journal of Chemical & Engineering Data*, 62(2):585–595, 2017.

[197] Kier von Konigslow, Chul B Park, and Russell B Thompson. Polymeric foaming predictions from the Sanchez-Lacombe equation of state: Application to polypropylene-carbon dioxide mixtures. *Physical Review Applied*, 8(4):044009, 2017.

[198] Kier von Konigslow, Chul B Park, and Russell B Thompson. Application of a constant hole volume Sanchez-Lacombe equation of state to mixtures relevant to polymeric foaming. *Soft Matter*, 14(22):4603–4614, 2018.

[199] JS Vrentas and JL Duda. Diffusion in polymer–solvent systems. II. A predictive theory for the dependence of diffusion coefficients on temperature, concentration, and molecular weight. *Journal of Polymer Science: Polymer Physics Edition*, 15(3):417–439, 1977.

[200] Mikhail Petrovich Vukalovich and Viktor Vladimirovich Altunin. *Thermophysical properties of carbon dioxide*. Wellingborough, Collets, 1968.

[201] Teri A Walker, Coray M Colina, Keith E Gubbins, and Richard J Spontak. Thermodynamics of poly (dimethylsiloxane)/poly (ethylmethylsiloxane)(PDMS/PEMS) blends in the presence of high-pressure CO_2. *Macromolecules*, 37(7):2588–2595, 2004.

[202] Wen-Chou V Wang, Edward J Kramer, and Wolfgang H Sachse. Effects of high-pressure CO_2 on the glass transition temperature and mechanical properties of polystyrene. *Journal of Polymer Science: Polymer Physics Edition*, 20(8):1371–1384, 1982.

[203] MS Wertheim. Thermodynamic perturbation theory of polymerization. *The Journal of Chemical Physics*, 87(12):7323–7331, 1987.

[204] Malcolm L Williams, Robert F Landel, and John D Ferry. The temperature dependence of relaxation mechanisms in amorphous polymers and other glass-forming liquids. *Journal of the American Chemical Society*, 77(14):3701–3707, 1955.

[205] RG Wissinger and ME Paulaitis. Swelling and sorption in polymer–CO_2 mixtures at elevated pressures. *Journal of Polymer Science Part B: Polymer Physics*, 25(12):2497–2510, 1987.

[206] Hans-Peter Wittmann. On the validity of the Gibbs–DiMarzio theory of the glass transition of lattice polymers. *The Journal of Chemical Physics*, 95(11):8449–8458, 1991.

[207] M Wolfgardt, J Baschnagel, W Paul, and K Binder. Entropy of glassy polymer melts: Comparison between Gibbs-DiMarzio theory and simulation. *Physical Review E*, 54(2):1535, 1996.

[208] Bernhard Wunderlich and Herbert Baur. Heat capacities of linear high polymers. In *Heat Capacities of Linear High Polymers*, pages 151–368. Springer, 1970.

[209] Hankun Xie, Erik Nies, Alexander Stroeks, and Robert Simha. Some considerations on equation of state and phase relations: Polymer solutions and blends. *Polymer Engineering & Science*, 32(22):1654–1664, 1992.

[210] Xiaofei Xu, Diego E Cristancho, Stéphane Costeux, and Zhen-Gang Wang. Density-functional theory for polymer-carbon dioxide mixtures: A perturbed-chain SAFT approach. *The Journal of Chemical Physics*, 137(5):054902, 2012.

[211] Hiromi Yamakawa. *Modern theory of polymer solutions*. Harper & Row, 1971.

[212] Zhiyi Zhang and Y Paul Handa. An in situ study of plasticization of polymers by high-pressure gases. *Journal of Polymer Science Part B: Polymer Physics*, 36(6):977–982, 1998.

[213] Chongli Zhong and Hongyu Yang. Representation of the solubility of solids in supercritical fluids using the SAFT equation of state. *Industrial & Engineering Chemistry Research*, 41(19):4899–4905, 2002.

[214] Paul Zoller. A study of the pressure-volume-temperature relationships of four related amorphous polymers: Polycarbonate, polyarylate, phenoxy, and polysulfone. *Journal of Polymer Science: Polymer Physics Edition*, 20(8):1453–1464, 1982.

Glossary

acentric factor a number that tells how much a molecule is non-spherical.

blowing agent a fluid that is used to create macroscopic voids in polymeric foams.

chemical blowing agent a blowing agent that uses chemical processes to create macroscopic voids in polymeric foams.

configurational partition function a partition function that only contains configurational information of the system with no kinetic portion.

critical point a point at which the distinction between gaseous phase and liquids phase ceases to exist.

equations of state equations that relate thermodynamic state variables of systems in thermodynamic equilibrium.

glass transition A process in which a polymer melt changes from polymer liquid to polymer glass on cooling and vise versa.

macrostate the thermodynamic state of system is called macrostate.

microstate a state of the system defined by using microscopic coordinates of constituting particles, for instance, position, velocities, internal state etc.

molar volume Molar volume is the volume occupied by one mole of a substance at given temperature and pressure.

physical blowing agent a blowing agent that produces thermodynamic instabilities to create macroscopic voids in polymeric foams.

polymer macromolecules that consists of large number of repeating units.

polymeric foam a polymeric material with macroscopic voids.

retrograde vitrification A phenomenon in which polymer liquid to polymer glass transition occurs on heating and vise versa.

solvent a substance consisting of small molecules in fluid state that is usually mixed with polymer.

statistical mechanics branch of physics that uses microscopic argument to describe the average thermodynamic response of the system.

thermal fluctuations spontaneous deviations of thermodynamic systems from their equilibrium conditions.

thermodynamic state variables or coordinates properties that define the state of system in thermodynamic equilibrium.

thermodynamics branch of physics that deals with the conversion of one form or energy into another form of energy.